

FINAL REPORT ~ FHWA-OK-17-03

OVERTURNING FORCES AT BRIDGE ABUTMENTS AND THE INTERACTION OF HORIZONTAL FORCES FROM ADJACENT ROADWAYS

K. K. “Muralee” Muraleetharan, Ph.D., P.E., G.E.
Gerald Miller, Ph.D., P.E.
Royce Floyd, Ph.D., P.E.
Bo Zhang, Ph.D.
Amirata Taghavi, Ph.D.
Tommy Bounds, M.S., Ph.D. Student, P.E.
Zachary Bright, M.S., P.E.
School of Civil Engineering and Environmental Science (CEES)

Gallogly College of Engineering
The University of Oklahoma
Norman, Oklahoma

January 2018



The Oklahoma Department of Transportation (ODOT) ensures that no person or groups of persons shall, on the grounds of race, color, sex, religion, national origin, age, disability, retaliation or genetic information, be excluded from participation in, be denied the benefits of, or be otherwise subjected to discrimination under any and all programs, services, or activities administered by ODOT, its recipients, sub-recipients, and contractors. To request an accommodation please contact the ADA Coordinator at 405-521-4140 or the Oklahoma Relay Service at 1-800-722-0353. If you have any ADA or Title VI questions email ODOT-ada-titlevi@odot.org.

The contents of this report reflect the views of the author(s) who is responsible for the facts and the accuracy of the data presented herein. The contents do not necessarily reflect the views of the Oklahoma Department of Transportation or the Federal Highway Administration. This report does not constitute a standard, specification, or regulation. While trade names may be used in this report, it is not intended as an endorsement of any machine, contractor, process, or product.

OVERTURNING FORCES AT BRIDGE ABUTMENTS AND THE INTERACTION OF HORIZONTAL FORCES FROM ADJACENT ROADWAYS

FINAL REPORT ~ FHWA-OK-17-03

ODOT SP&R ITEM NUMBER 2228

Submitted to:

Dawn R. Sullivan, P.E.
Director of Capital Programs
Oklahoma Department of Transportation

Submitted by:

K. K. "Muralee" Muraleetharan, Ph.D., P.E., G.E.
Gerald Miller, Ph.D., P.E.
Royce Floyd, Ph.D., P.E.
Bo Zhang, Ph.D.
Amirata Taghavi, Ph.D.
Tommy Bounds, Ph.D. Student, P.E.
Zachary Bright, M.S., P.E.
School of Civil Engineering and Environmental Science (CEES)
University of Oklahoma



January 2018

TECHNICAL REPORT DOCUMENTATION PAGE

1. REPORT NO. FHWA-OK-17-03	2. GOVERNMENT ACCESSION NO.	3. RECIPIENT'S CATALOG NO.	
4. TITLE AND SUBTITLE Overturning Forces at Bridge Abutments and the Interaction of Horizontal Forces from Adjacent Roadways		5. REPORT DATE Jan 2018	
		6. PERFORMING ORGANIZATION CODE	
7. AUTHOR(S) K. K. "Muralee" Muraleetharan, Gerald Miller, Royce Floyd, Bo Zhang, Amirata Taghavi, Tommy Bounds, Zachary Bright		8. PERFORMING ORGANIZATION REPORT	
9. PERFORMING ORGANIZATION NAME AND ADDRESS University of Oklahoma, School of Civil Engineering and Environmental Science, 202 West Boyd Street, Room 334 Norman, OK 73019		10. WORK UNIT NO.	
		11. CONTRACT OR GRANT NO. ODOT SPR Item Number 2228	
12. SPONSORING AGENCY NAME AND ADDRESS Oklahoma Department of Transportation Office of Research and Implementation 200 N.E. 21st Street, Room G18 Oklahoma City, OK 73105		13. TYPE OF REPORT AND PERIOD COVERED Final Report Oct 2010 - Sep 2017	
		14. SPONSORING AGENCY CODE	
15. SUPPLEMENTARY NOTES			
16. ABSTRACT ODOT is experiencing a number of problems related to the interactions between bridge abutments and adjacent roadways. These problems include expansion joints closing, roller support bearings tilting, and beams pushing against abutment backwalls. Design, construction, repair, and maintenance guidelines to alleviate adverse effects of interactions between ODOT bridge abutments (non-integral), bridge decks, and adjacent roadways are developed based on field observations, instrumentation of selected bridges, and computer simulations. Three bridges were selected for detailed instrumentation including measurements of strains at various locations of approach slabs, approach pavements, and bridge decks; relative displacements between approach slabs and approach pavements; relative tilt of the abutment backwalls and pier caps; and temperatures at various locations over a period of seven years. At two of these bridges, measurements were also made before and after repairs. In addition, strains near newly installed expansion joints on five other bridges were monitored. The observed distresses were classified into two main categories. One related to rigid approach pavements exerting pressures on the bridges and the other related to lateral displacements from tall approach embankments early in the life of the bridges. A 4-inch pressure relief joint installed on an approach pavement was found to relieve bridge stresses caused by a rigid approach pavement. Providing expansion joints on rigid approach pavements at regular intervals, maintaining expansion joints on bridges and pavements, and geotechnical analyses to calculate lateral displacements from tall approach embankments during the design phase are some of the recommendations made to prevent or remediate the observed distresses.			
17. KEY WORDS Bridge-roadway interaction, Expansion joint, Pavement pressure, Approach embankment, Lateral displacement, Pressure relief joint.		18. DISTRIBUTION STATEMENT No restrictions. This publication is available from the Office of Research and Implementation, Oklahoma DOT.	
19. SECURITY CLASSIF. (OF THIS REPORT) Unclassified	20. SECURITY CLASSIF. (OF THIS PAGE) Unclassified	21. NO. OF PAGES 134	22. PRICE N/A

Form DOT F 1700.7 (08/72)

SI* (MODERN METRIC) CONVERSION FACTORS

APPROXIMATE CONVERSIONS TO SI UNITS

SYMBOL	WHEN YOU KNOW	MULTIPLY BY	TO FIND	SYMBOL
LENGTH				
in	Inches	25.4	millimeters	mm
ft	Feet	0.305	meters	m
yd	yards	0.914	meters	m
mi	miles	1.61	kilometers	km
AREA				
in ²	square inches	645.2	square millimeters	mm ²
ft ²	square feet	0.093	square meters	m ²
yd ²	square yard	0.836	square meters	m ²
ac	acres	0.405	hectares	ha
mi ²	square miles	2.59	square kilometers	km ²
VOLUME				
fl oz	fluid ounces	29.57	milliliters	mL
gal	gallons	3.785	liters	L
ft ³	cubic feet	0.028	cubic meters	m ³
yd ³	cubic yards	0.765	cubic meters	m ³
NOTE: volumes greater than 1000 L shall be shown in m ³				
MASS				
oz	ounces	28.35	grams	g
lb	pounds	0.454	kilograms	kg
T	short tons (2000 lb)	0.907	megagrams (or "metric ton")	Mg (or "t")
TEMPERATURE (exact degrees)				
°F	Fahrenheit	5 (F-32)/9 or (F-32)/1.8	Celsius	°C
ILLUMINATION				
fc	foot-candles	10.76	lux	lx
fl	foot-Lamberts	3.426	candela/m ²	cd/m ²
FORCE and PRESSURE or STRESS				
lbf	poundforce	4.45	newtons	N
lbf/in ²	poundforce per square inch	6.89	kilopascals	kPa
APPROXIMATE CONVERSIONS FROM SI UNITS				
SYMBOL	WHEN YOU KNOW	MULTIPLY BY	TO FIND	SYMBOL
LENGTH				
mm	millimeters	0.039	inches	in
m	meters	3.28	feet	ft
m	meters	1.09	yards	yd
km	kilometers	0.621	miles	mi
AREA				
mm ²	square millimeters	0.0016	square inches	in ²
m ²	square meters	10.764	square feet	ft ²
m ²	square meters	1.195	square yards	yd ²
ha	hectares	2.47	acres	ac
km ²	square kilometers	0.386	square miles	mi ²
VOLUME				
mL	milliliters	0.034	fluid ounces	fl oz
L	liters	0.264	gallons	gal
m ³	cubic meters	35.314	cubic feet	ft ³
m ³	cubic meters	1.307	cubic yards	yd ³
MASS				
g	grams	0.035	ounces	oz
kg	kilograms	2.202	pounds	lb
Mg (or "t")	megagrams (or "metric ton")	1.103	short tons (2000 lb)	T
TEMPERATURE (exact degrees)				
°C	Celsius	1.8C+32	Fahrenheit	°F
ILLUMINATION				
lx	lux	0.0929	foot-candles	fc
cd/m ²	candela/m ²	0.2919	foot-Lamberts	fl
FORCE and PRESSURE or STRESS				
N	newtons	0.225	poundforce	lbf
kPa	kilopascals	0.145	poundforce per square inch	lbf/in ²

*SI is the symbol for the International System of Units. Appropriate rounding should be made to comply with Section 4 of ASTM E380.
(Revised March 2003)

TABLE OF CONTENTS

1.0	GENERAL	1
2.0	OVERVIEW OF WORK DONE	2
	2.1 INSTRUMENTATION USED	2
	2.1.1 Strain Gage	2
	2.1.2 Thermistors	4
	2.1.3 Tiltmeters	5
	2.1.4 Crackmeters	7
	2.1.5 Data Logging System	8
	2.2 DATA COLLECTION AND ANALYSIS	12
	2.2.1. <i>The US 64 Westbound over Shell Creek</i>	12
	2.2.1.1 Abutment Rotation.....	14
	2.2.1.2 Relative Displacement between the Bridge Deck and the Approach Slab	16
	2.2.1.3 Axial Strains	17
	2.2.2. <i>Monitoring of Expansion Joint Widths</i>	19
	2.2.2.1 I-244 Bridges.....	20
	2.2.2.2 SH 76 Bridge over Rush Creek	25
	2.2.3. <i>The SH-3 Bridges over BNSF Railroad</i>	27
	2.2.3.1 Rotations of East Abutments before Repairs	33
	2.2.3.2 Displacement of the Bridge Deck Relative to the Abutment Wing Wall before Repairs	36
	2.2.3.3 Axial Strains – East Side before Repairs.....	38
	2.2.3.4 Axial Strains – West Side before Repairs	41
	2.2.3.5 Eastern Approach Embankment Displacements before Repairs	43
	2.2.3.6 Western Approach Embankment Displacements before Repairs	45
	2.2.3.7 Tilting of Pier Caps before Repairs	49
	2.2.3.8 Movements around Expansion Joints before Repairs	53
	2.2.4. <i>The SH-3 North Bridge over BNSF Railroad after Repairs</i>	56
	2.2.4.1 Rotations of the East Abutment after Repairs.....	58
	2.2.4.2 Displacement of the Bridge Deck Relative to the Abutment Wing Wall after Repairs	59
	2.2.4.3 Axial Strains – Eastern Side after Repairs	61
	2.2.4.4 Axial Strains – Western Side after Repairs	63
	2.2.4.5 Tilting of Pier Caps after Repairs	67
	2.2.4.6 Movements around Expansion Joints after Repairs	69
	2.2.5. <i>The 19th Street/I-35 Bridge before Repairs</i>	71
	2.2.5.1 Abutment Backwall Rotation before Repairs	81
	2.2.5.2 Relative Displacement between the Approach Pavement and the Abutment Wing Wall before Repairs	86

2.2.5.3 Axial Strains before Repairs.....	90
2.2.5.4 Proposed Remedial Measures.....	96
2.2.6. <i>The 19th Street/I-35 Bridge after Repairs</i>	99
2.2.6.1 Displacement of the Pressure Relief Joint after Repairs.....	102
2.2.6.2 Abutment Backwall Rotation after Repairs.....	103
2.2.6.3 Relative Displacement between the Approach Pavement and the Abutment Wing Wall after Repairs.....	106
2.2.6.4 Axial Strains after Repairs.....	107
3.0 ANALYSES.....	112
4.0 SUMMARY.....	116
4.1 THE SHELL CREEK BRIDGE.....	116
4.2 I-244 BRIDGES AND SH 76 BRIDGE OVER RUSH CREEK.....	116
4.3 THE SH-3 BRIDGES OVER THE BNSF RAILWAY.....	116
4.4 THE 19 TH STREET/I-35 BRIDGE.....	117
5.0 RECOMMENDATIONS.....	118
6.0 ACKNOWLEDGEMENTS.....	120
7.0 REFERENCES.....	121

LIST OF FIGURES

FIGURE 1. GEOKON MODEL 4000 VIBRATING WIRE STRAIN GAGE (GEOKON INC., 2013A).....	3
FIGURE 2. STRAIN GAGE SCHEMATIC (GEOKON INC., 2013A).....	3
FIGURE 3. GEOKON MODEL 3800 THERMISTOR (GEOKON INC., 2013B).....	4
FIGURE 4. GEOKON MODEL 6350 VIBRATING WIRE TILTMETER (GEOKON INC., 2013C).....	5
FIGURE 5. DIFFERENT SECTIONS OF GEOKON MODEL 6350 TILTMETER (GEOKON INC., 2013C).....	6
FIGURE 6. TOP VIEW OF AN INSTALLED TILTMETER (GEOKON INC., 2013C).....	7
FIGURE 7. GEOKON MODEL 4420 VIBRATING WIRE CRACKMETER (GEOKON INC., 2013D).....	7
FIGURE 8. DIFFERENT SECTIONS OF GEOKON MODEL 4420 VIBRATING WIRE CRACKMETER (GEOKON INC., 2013D).....	8
FIGURE 9. GEOKON MODEL 8021 MICRO-1000 DATA LOGGER; LEFT PICTURE IS FRONT VIEW AND THE RIGHT PICTURE IS BOTTOM VIEW (GEOKON INC., 2013E).....	9
FIGURE 10. INSIDE OF THE GEOKON MODEL 8021 MICRO-1000 DATA LOGGER BOX.....	10
FIGURE 11. GEOKON MODEL 8032 MULTIPLEXER (LEFT) AND ITS DATA LOGGER (RIGHT) (GEOKON INC., 2013F).....	11
FIGURE 12. CHANNELS INSIDE THE MULTIPLEXER (GEOKON INC., 2013F).....	11
FIGURE 13. A CLOSED EXPANSION JOINT ON THE SHELL CREEK BRIDGE.....	12

FIGURE 14. NORTHERN MOST ROCKER BEARING (BEFORE AND AFTER STRAIGHTENING) AND GIRDER ON THE WEST ABUTMENT OF THE SHELL CREEK BRIDGE.....	13
FIGURE 15. A BEAM PUSHING AGAINST AN ABUTMENT BACKWALL ON THE SHELL CREEK BRIDGE	13
FIGURE 16. INSTRUMENT LOCATIONS FOR THE SHELL CREEK BRIDGE.....	14
FIGURE 17. US 64 OVER SHELL CREEK BRIDGE – SOUTHWEST TILTMETER DATA (SW_TM)	15
FIGURE 18. US 64 OVER SHELL CREEK BRIDGE – NORTHWEST TILTMETER DATA (NW_TM)	15
FIGURE 19. US 64 OVER SHELL CREEK BRIDGE – SOUTHWEST CRACKMETER DATA (SW_CM).....	16
FIGURE 20. US 64 OVER SHELL CREEK BRIDGE – NORTHWEST CRACKMETER DATA (NW_CM)	17
FIGURE 21. US 64 OVER SHELL CREEK BRIDGE – NORTHWEST STRAIN GAGE 1 (NW_SG1).....	18
FIGURE 22. US 64 OVER SHELL CREEK BRIDGE -NORTHWEST STRAIN GAGE 3 (NW_SG3)	18
FIGURE 23. I-244 BRIDGES.....	19
FIGURE 24. JOINTS ON I-244 EAST OVER MARTIN LUTHER KING JR. BLVD. (NBI NO. 18027).....	20
FIGURE 25. JOINTS ON I-244 EAST OVER N. DETROIT AVE. (NBI NO. 18029)	20
FIGURE 26. JOINTS ON I-244 WEST OVER MARTIN LUTHER KING JR. BLVD. (NBI NO. 18024)	21
FIGURE 27. JOINTS ON I-244 WEST OVER N. DETROIT AVE. NBI NO. 18028	21
FIGURE 28. VARIATION OF JOINT WIDTHS WITH TEMPERATURE FOR I-244 EAST OVER MARTIN LUTHER KING JR. BLVD. (NBI NO. 18027)	22
FIGURE 29. VARIATION OF JOINT WIDTHS WITH TEMPERATURE FOR I-244 EAST OVER N. DETROIT AVE. (NBI NO. 18029)	23
FIGURE 30. JOINT WIDTHS OF EXPANSION JOINTS FOR I-244 WEST OVER MARTIN LUTHER KING JR. BLVD. (NBI NO. 18024)	24
FIGURE 31. JOINT WIDTHS OF EXPANSION JOINTS FOR I-244 WEST OVER N. DETROIT AVE. (NBI NO. 18028).....	25
FIGURE 32. SH 76 OVER RUSH CREEK	26
FIGURE 33. JOINT WIDTHS OF EXPANSION JOINTS ON SH 76 OVER RUSH CREEK.....	27
FIGURE 34. SH-3 BRIDGES OVER BNSF RAILROAD	29
FIGURE 35. ELEVATION OF THE SH-3 NORTH BRIDGE OVER BNSF RAILROAD.....	29
FIGURE 36. BEAMS PUSHING AGAINST ABUTMENT BACKWALLS AND A BENT ANCHOR BOLT.....	30
FIGURE 37. CRACKS IN THE SLOPE-WALL	30
FIGURE 38. EASTERN SIDE OF SH-3 BRIDGES OVER BNSF RAILROAD – INSTRUMENTATION LOCATIONS:.....	31
FIGURE 39. SH-3 BRIDGES OVER BNSF RAILROAD – LOCATIONS OF THE INCLINOMETERS (GOOGLE INC., 2013A).....	31
FIGURE 40. SH-3 BRIDGES OVER BNSF RAILROAD – TILTMETER LOCATIONS WITHIN THE EASTERN AND WESTERN INCLINOMETERS (ALL DIMENSIONS ARE IN FEET)	32
FIGURE 41. EAST ABUTMENT OF SH-3 SOUTH BRIDGE OVER BNSF RAILROAD – TMA3 AND TMA4 TILTMETER DATA BEFORE REPAIRS ...	34
FIGURE 42. EAST ABUTMENT OF SH-3 NORTH BRIDGE OVER BNSF RAILROAD – TMA1 AND TMA2 TILTMETER DATA BEFORE REPAIRS ..	35
FIGURE 43. EAST ABUTMENT OF SH-3 NORTH BRIDGE OVER BNSF RAILROAD – CMA2 CRACKMETER	36
FIGURE 44. EAST ABUTMENT OF SH-3 NORTH BRIDGE OVER BNSF RAILROAD – CMA1 CRACKMETER DATA BEFORE REPAIRS	37
FIGURE 45. EAST ABUTMENT OF SH-3 NORTH BRIDGE OVER BNSF RAILROAD – CMA2 CRACKMETER DATA BEFORE REPAIRS	37

FIGURE 46. SH-3 BRIDGES OVER BNSF RAILROAD – STRAIN GAGE LOCATIONS	38
FIGURE 47. EASTERN SIDE OF SH-3 NORTH BRIDGE OVER BNSF RAILROAD – NE_SG1 AND NE_SG3 STRAIN GAGE DATA BEFORE REPAIRS	39
FIGURE 48. EASTERN SIDE OF SH-3 NORTH BRIDGE OVER BNSF RAILROAD – NE_SG2 AND NE_SG4 STRAIN GAGE DATA BEFORE REPAIRS	40
FIGURE 49. STRESSES IN THE BRIDGE DECK NEAR THE ABUTMENTS DURING HEATING AND COOLING DUE TO CLOSED EXPANSION JOINTS....	41
FIGURE 50. WESTERN SIDE OF SH-3 NORTH BRIDGE OVER BNSF RAILROAD – NW_SG1 DATA BEFORE REPAIRS.....	42
FIGURE 51. WESTERN SIDE OF SH-3 NORTH BRIDGE OVER BNSF RAILROAD – NW_SG2 DATA BEFORE REPAIRS	42
FIGURE 52. WESTERN SIDE OF SH-3 NORTH BRIDGE OVER BNSF RAILROAD – NW_SG3 DATA BEFORE REPAIRS.....	43
FIGURE 53. SH-3 BRIDGES OVER BNSF RAILROAD – EASTERN EMBANKMENT DEFLECTION AT LOCATION IM1.....	44
FIGURE 54. SH-3 BRIDGES OVER BNSF RAILROAD – EASTERN EMBANKMENT DEFLECTION AT LOCATION IM4.....	44
FIGURE 55. SH-3 BRIDGES OVER BNSF RAILROAD – EASTERN EMBANKMENT DEFLECTION PROFILE ON AUGUST 24, 2013	45
FIGURE 56. SH-3 BRIDGES OVER BNSF RAILROAD – WESTERN EMBANKMENT DEFLECTION AT LOCATION IM1.....	46
FIGURE 57. SH-3 BRIDGES OVER BNSF RAILROAD – WESTERN EMBANKMENT DEFLECTION AT LOCATION IM2.....	47
FIGURE 58. SH-3 BRIDGES OVER BNSF RAILROAD – WESTERN EMBANKMENT DEFLECTION AT LOCATION IM3.....	47
FIGURE 59. SH-3 BRIDGES OVER BNSF RAILROAD – WESTERN EMBANKMENT DEFLECTION AT LOCATION IM5.....	48
FIGURE 60. SH-3 BRIDGES OVER BNSF RAILROAD – WESTERN EMBANKMENT DEFLECTION AT LOCATION IM6.....	48
FIGURE 61. SH-3 BRIDGES OVER BNSF RAILROAD – WESTERN EMBANKMENT DEFLECTION AT LOCATION IM7.....	49
FIGURE 62. PIER CAP INSTRUMENTATION ON PIER No. 4 OF THE SH-3 NORTH BRIDGE	50
FIGURE 63. LOCATIONS OF PIER CAP AND ROAD SURFACE INSTRUMENTATION ON SH-3 NORTH BRIDGE	50
FIGURE 64. SH-3 NORTH BRIDGE OVER BNSF RAILROAD – PIER CAP TILTMETER TM1-4 DATA BEFORE REPAIRS.....	51
FIGURE 65. SH-3 NORTH BRIDGE OVER BNSF RAILROAD – PIER CAP TILTMETER TM5-8 DATA BEFORE REPAIRS.....	52
FIGURE 66. EXPANSION JOINTS OF SH-3 NORTH BRIDGE OVER BNSF RAILROAD - CMP1-4 CRACKMETER DATA BEFORE REPAIRS.....	54
FIGURE 67. EXPANSION JOINTS OF SH-3 NORTH BRIDGE OVER BNSF RAILROAD - CMP5-8 CRACKMETER DATA BEFORE REPAIRS	55
FIGURE 68. REPAIR DETAILS FOR SH-3 NORTH BRIDGE OVER BNSF RAILROAD	56
FIGURE 69. DETAILS OF THE NEW SEALED EXPANSION JOINTS AT PIER No. 1 AND PIER No. 4 FOR SH-3 NORTH BRIDGE OVER BNSF RAILROAD.....	57
FIGURE 70. DETAILS OF NEW CONSTRUCTION JOINTS AT PIER No. 2 AND PIER No. 3 FOR SH-3 NORTH BRIDGE OVER BNSF RAILROAD..	57
FIGURE 71. DETAILS OF REHABILITATED CONSTRUCTION JOINTS AT ABUTMENTS FOR SH-3 NORTH BRIDGE OVER BNSF RAILROAD	58
FIGURE 72. EAST ABUTMENT OF SH-3 NORTH BRIDGE OVER BNSF RAILROAD – COMPARISONS OF TMA1 AND TMA2 TILTMETER DATA BEFORE AND AFTER REPAIRS	59
FIGURE 73. EAST ABUTMENT OF SH-3 NORTH BRIDGE OVER BNSF RAILROAD – COMPARISON OF CMA1 CRACKMETER DATA BEFORE AND AFTER REPAIRS.....	60
FIGURE 74. EAST ABUTMENT OF SH-3 NORTH BRIDGE OVER BNSF RAILROAD – COMPARISON OF CMA2 CRACKMETER DATA BEFORE AND AFTER REPAIRS.....	61

FIGURE 75. EASTERN SIDE OF SH-3 NORTH BRIDGE OVER BNSF RAILROAD – COMPARISON OF NE_SG1 STRAIN GAGE DATA BEFORE AND AFTER REPAIRS.....	62
FIGURE 76. EASTERN SIDE OF SH-3 NORTH BRIDGE OVER BNSF RAILROAD – COMPARISON OF NE_SG2 STRAIN GAGE DATA BEFORE AND AFTER REPAIRS.....	63
FIGURE 77. WESTERN SIDE OF THE SH-3 NORTH BRIDGE OVER BNSF RAILROAD – COMPARISON OF NW_SG1 DATA BEFORE AND AFTER REPAIRS.....	64
FIGURE 78. WESTERN SIDE OF THE SH-3 NORTH BRIDGE OVER BNSF RAILROAD – COMPARISON OF NW_SG2 DATA BEFORE AND AFTER REPAIRS.....	65
FIGURE 79. WESTERN SIDE OF SH-3 NORTH BRIDGES OVER BNSF RAILROAD – COMPARISON OF NW_SG3 DATA BEFORE AND AFTER REPAIRS	66
FIGURE 80. SH-3 NORTH BRIDGE OVER BNSF RAILROAD – PIER CAP TILTMETER TM1 AND TM2 DATA AFTER REPAIRS.....	67
FIGURE 81. SH-3 NORTH BRIDGE OVER BNSF RAILROAD – PIER CAP TILTMETER TM3 AND TM4 DATA AFTER REPAIRS.....	68
FIGURE 82. SH-3 NORTH BRIDGE OVER BNSF RAILROAD – PIER CAP TILTMETER TM5 DATA AFTER REPAIRS	68
FIGURE 83. SH-3 NORTH BRIDGE OVER BNSF RAILROAD – PIER CAP TILTMETER TM7 AND TM8 DATA AFTER REPAIRS.....	69
FIGURE 84. SH-3 NORTH BRIDGE OVER BNSF RAILROAD – COMPARISONS OF CRACKMETER CMP1 AND CMP2 DATA BEFORE AND AFTER REPAIRS.....	70
FIGURE 85. SH-3 NORTH BRIDGE OVER BNSF RAILROAD – COMPARISONS OF CRACKMETER CMP7 AND CMP8 DATA BEFORE AND AFTER REPAIRS.....	71
FIGURE 86. 19 TH STREET/I-35 BRIDGE	73
FIGURE 87. 19 TH STREET/I-35 BRIDGE PHOTOS SHOWING DISTRESS IN 2005.....	75
FIGURE 88. CENTER EXPANSION JOINT ON NORTH AND SOUTH BRIDGE AT 19 TH STREET/I-35 IN 2005	76
FIGURE 89. 19 TH STREET/I-35 BRIDGE SHEARED ANCHOR BOLTS IN 2009	77
FIGURE 90. CRACKING OF THE SOUTH EASTERN APPROACH SLAB ADJACENT TO SOUTH BRIDGE DECK IN 2009	77
FIGURE 91. U-SHAPED CRACKING AT 19 TH STREET/I-35 BRIDGE EASTERN ABUTMENT BACK WALL IN 2011	78
FIGURE 92. INSTRUMENTATION LAYOUT FOR THE EASTERN SIDE OF THE 19 TH STREET/I-35 BRIDGE.....	79
FIGURE 93. INSTRUMENTATION LAYOUT FOR THE WESTERN SIDE OF THE 19 TH STREET/I-35 BRIDGE	79
FIGURE 94. INSTRUMENTS ATTACHED TO SOUTH SIDE OF EASTERN APPROACH PAVEMENT NEAR APPROACH SLAB (BRIGHT, 2012).....	80
FIGURE 95. INSTRUMENTS ATTACHED TO SOUTH SIDE OF EASTERN APPROACH PAVEMENT (BRIGHT, 2012).....	81
FIGURE 96. ILLUSTRATION OF THE TILT TRENDS FOR 19 TH STREET/I-35 BRIDGE ABUTMENTS (FROM EST INC., 2008).....	82
FIGURE 97. EASTSIDE OF THE 19 TH STREET/I-35 BRIDGE – NORTHEAST TILTMETER (NE_TM) DATA BEFORE REPAIRS	83
FIGURE 98. EASTSIDE OF THE 19 TH STREET/I-35 BRIDGE – SOUTHEAST TILTMETER (SE_TM) DATA BEFORE REPAIRS	83
FIGURE 99. WESTSIDE OF THE 19 TH STREET/I-35 BRIDGE – NORTHWEST TILTMETER (NW_TM) DATA.....	84
FIGURE 100. WESTSIDE OF THE 19 TH STREET/I-35 BRIDGE – SOUTHWEST TILTMETER (SW_TM) DATA.....	84
FIGURE 101. CROSS-SECTION THROUGH THE BRIDGE DECK, ABUTMENT BACK WALL, AND APPROACH SLAB (EST 2008).....	85

FIGURE 102. INSTALLED CRACKMETER ATTACHED TO APPROACH PAVEMENT AND PARAPET ABOVE ABUTMENT WING WALL (BRIGHT, 2012)	87
FIGURE 103. EASTERN SIDE OF THE 19TH STREET/I-35 BRIDGE – NORTHEAST CRACKMETER NE_CM DATA BEFORE REPAIRS	88
FIGURE 104. EASTERN SIDE OF THE 19TH STREET/I-35 BRIDGE – SOUTHEAST CRACKMETER SE_CM DATA BEFORE REPAIRS	88
FIGURE 105. WESTERN SIDE OF THE 19TH STREET/I-35 BRIDGE – NORTHWEST CRACKMETER NW_CM DATA BEFORE AND AFTER REPAIRS	89
FIGURE 106. WESTERN SIDE OF THE 19TH STREET/I-35 BRIDGE – SOUTHWEST CRACKMETER SW_CM DATA BEFORE AND AFTER REPAIRS	89
FIGURE 107. ILLUSTRATION OF CRACKMETER DISPLACEMENT TRENDS (BRIGHT, 2012)	90
FIGURE 108. EASTERN SIDE OF THE 19TH STREET/I-35 BRIDGE – SOUTHEAST STRAIN GAGE SE_SG1 BEFORE REPAIRS	91
FIGURE 109. EASTERN SIDE OF THE 19TH STREET/I-35 BRIDGE – NORTHEAST STRAIN GAGE NE_SG1 BEFORE REPAIRS	92
FIGURE 110. EASTERN SIDE OF THE 19TH STREET/I-35 BRIDGE – SOUTHEAST STRAIN GAGE SE_SG3 BEFORE REPAIRS	92
FIGURE 111. WESTERN SIDE OF THE 19TH STREET/I-35 BRIDGE – NORTHWEST STRAIN GAGE NW_SG4 BEFORE AND AFTER REPAIRS	93
FIGURE 112. SOUTHEAST STRAIN GAGE SE_SG1 TREND ILLUSTRATION (BRIGHT, 2012)	94
FIGURE 113. NORTHEAST STRAIN GAGE NE_SG1 TREND ILLUSTRATION (BRIGHT, 2012)	95
FIGURE 114. LOCATIONS OF THE PROPOSED PRESSURE RELIEF JOINTS (#2 AND #3)	96
FIGURE 115. PROPOSED PRESSURE RELIEF JOINT WITH LOAD TRANSFER	98
FIGURE 116. PROPOSED PRESSURE RELIEF JOINT WITHOUT LOAD TRANSFER	99
FIGURE 117. BEJS JOINT IN TYPICAL INSTALLATION — NEW OR RETROFIT (EMSEAL, 2016)	100
FIGURE 118. NEW APPROACH PAVEMENT NEAR THE APPROACH SLAB AND COMPLETED BEJS PRESSURE RELIEF JOINT ON THE EAST SIDE OF THE 19TH STREET BRIDGE	101
FIGURE 119. INSTRUMENTATION LAYOUT FOR THE EASTERN SIDE OF THE 19TH STREET/I-35 BRIDGE AFTER REPAIRS	101
FIGURE 120. EASTERN SIDE OF THE 19TH STREET/I-35 BRIDGE – NORTHEAST CRACKMETER NE_CM3 DATA AFTER REPAIRS	102
FIGURE 121. EASTERN SIDE OF THE 19TH STREET/I-35 BRIDGE – SOUTHEAST CRACKMETER SE_CM4 DATA AFTER REPAIRS	103
FIGURE 122. EASTERN SIDE OF THE 19TH STREET/I-35 BRIDGE – COMPARISON OF SOUTHEAST TILTMETER SE_TM DATA BEFORE AND AFTER REPAIRS	104
FIGURE 123. EASTERN SIDE OF THE 19TH STREET/I-35 BRIDGE – COMPARISON OF NORTHEAST TILTMETER NE_TM DATA BEFORE AND AFTER REPAIRS	105
FIGURE 124. EASTERN SIDE OF THE 19TH STREET/I-35 BRIDGE – COMPARISON OF NORTHEAST CRACKMETER DATA BEFORE AND AFTER REPAIRS	106
FIGURE 125. EASTERN SIDE OF THE 19TH STREET/I-35 BRIDGE – SOUTHEAST CRACKMETER DATA BEFORE AND AFTER REPAIRS	107
FIGURE 126. EASTERN SIDE OF THE 19TH STREET/I-35 BRIDGE – SOUTHEAST STRAIN GAGE 1 (SE_SG1) BEFORE AND AFTER REPAIRS	108
FIGURE 127. EASTERN SIDE OF THE 19TH STREET/I-35 BRIDGE – SOUTHEAST STRAIN GAGE 2 (SE_SG2) BEFORE AND AFTER REPAIRS	109
FIGURE 128. EASTERN SIDE OF THE 19TH STREET/I-35 BRIDGE – NORTHEAST STRAIN GAGE 1 (NE_SG1) BEFORE AND AFTER REPAIRS	110

FIGURE 129. EASTERN SIDE OF THE 19TH STREET/I-35 BRIDGE – NORTHEAST STRAIN GAGE 2 (NE_SG2) BEFORE AND AFTER REPAIRS111

FIGURE 130. FINITE ELEMENT MESH WITH BOUNDARY CONDITIONS.....113

FIGURE 131. UNSATURATED FINITE ELEMENT ANALYSIS DEFORMED MESH114

FIGURE 132. SATURATED FINITE ELEMENT ANALYSIS DEFORMED MESH.....115

1.0 General

ODOT is experiencing a number of problems related to the interactions between bridge abutments and adjacent roadways. These problems include expansion joints closing, roller support bearings tilting, and beams pushing against abutment backwalls. Design, construction, repair, and maintenance guidelines to alleviate adverse effects of interactions between ODOT bridge abutments (non-integral), bridge decks, and adjacent roadways are developed in this project based on field observations, instrumentation of selected bridges, and computer simulations.

For several bridge sites where ODOT has noticed distress due to possible interactions with adjacent roadways, background information was first collected. Site reconnaissance visits and visual inspection of all the distressed bridge sites were conducted. Based on the background information collected and the field visits, three bridges were selected for detailed instrumentation and instrumentation plans were developed. The bridges selected included National Bridge Inventory (NBI) No. 25440 (19th Street Moore - I-35 under), NBI No. 18141 (US-64 Westbound over Shell Creek near Sands Springs), and NBI No. 19824 and NBI No. 19825 (SH-3 North and South over BNSF Railroad in Ada). The selected instrumentation included sensors to measure strains at various locations of approach slabs, approach pavements, and bridge decks; relative displacements between approach slabs and approach pavements; relative tilt of the abutment backwalls and pier caps; and temperatures at various locations. In addition to these three bridges, strains adjacent to expansion joints near I-244 bridges over N. Detroit Avenue and Martin Luther King Jr. Boulevard (formerly N. Cincinnati Avenue) in Tulsa and NBI No. 12643 (SH-76 over Rush Creek – Garvin County) were periodically monitored using demountable mechanical strain gage (DEMEC) targets.

2.0 Overview of Work Done

The following tasks were performed in this project.

- (i) instrumentation of all selected bridges
- (ii) data collection and analyses
- (iii) Removal and reinstallation of instrumentation, respectively, prior to and after the repairs to the SH-3 North Bridge
- (iv) Removal and reinstallation of instrumentation, respectively, prior to and after the installation of a pressure relief joint on the west side of the 19th Street Bridge
- (v) Computer simulations of the lateral deformations of the approach embankments at SH-3 Bridges.

2.1 Instrumentation Used

This section describes the particular model and type of sensors used to instrument the bridges as well as the information on the logging system used to collect data from the sensors. The sensors consisted of strain gages, crackmeters, tiltmeters, thermistors, and inclinometers. All the instruments were equipped with vibrating wire transducers (except the thermistors) and connected to data loggers located near the abutments underneath the bridge decks and powered by batteries.

2.1.1 Strain Gage

The Geokon Model 4000 vibrating wire strain gage (Geokon Inc., 2013a) was used in this project (Figure 1). This particular model of strain gage is designed to measure small incremental strains over time. It is not suitable for rapidly changing or dynamic strains. It has a range of 3000 microstrain and a resolution of 1 microstrain.

Essentially, there are 3 pieces to the strain gage, the protective tube which houses the plucking wire, the coil/thermistor housing, and the mounting blocks (Figure 2). The strain gage can be modified for use on pavement surfaces with the addition of groutable anchors that are grouted or epoxied into drilled holes.



Figure 1. Geokon model 4000 vibrating wire strain gage (Geokon Inc., 2013a)

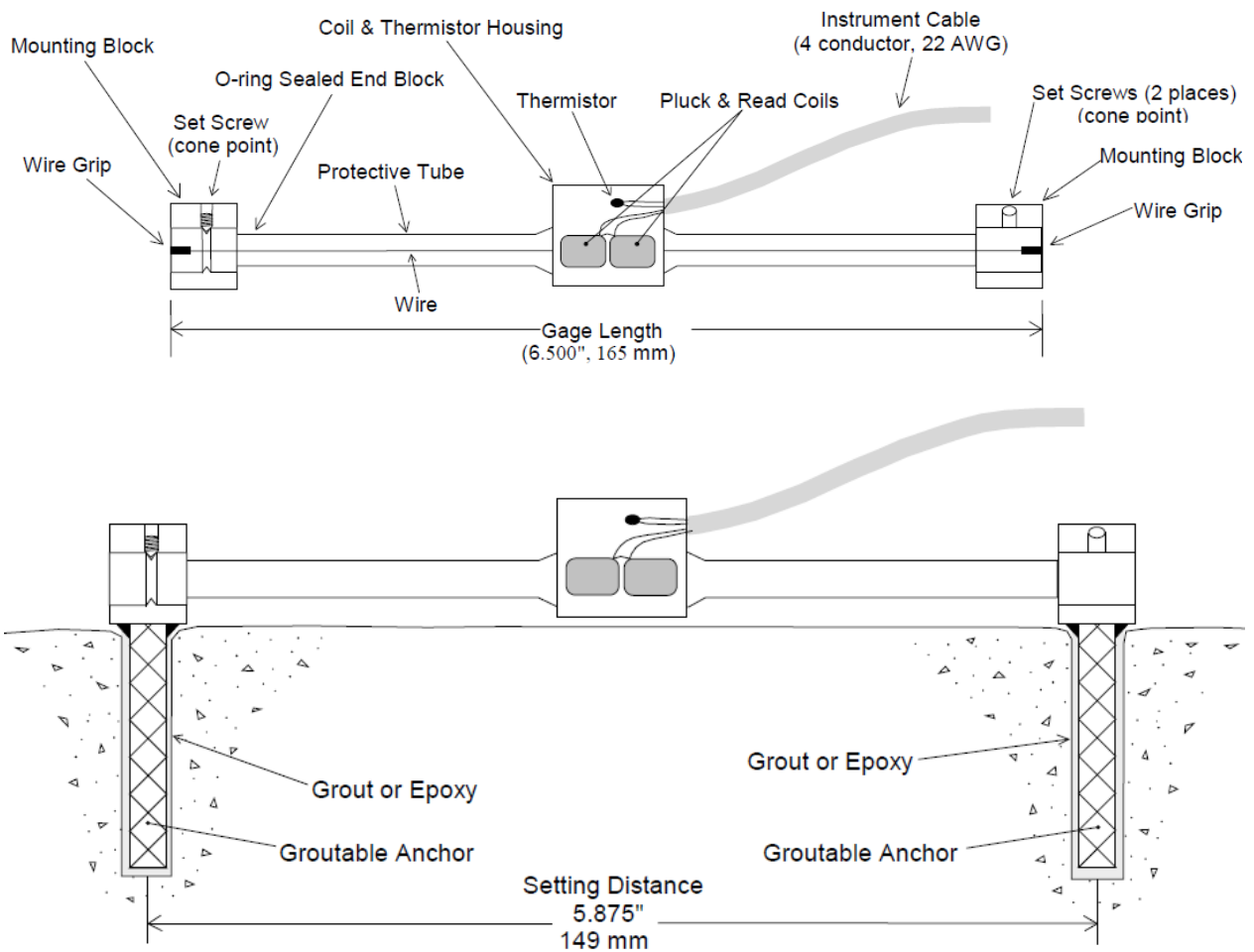


Figure 2. Strain gage schematic (Geokon Inc., 2013a)

Strain is measured by the relative movement between the anchors which causes the wire within the protective tube to reach a particular tension. A measurement is taken when the wire in the protective tube is plucked so that a vibration at a particular frequency is transferred from the vibrating wire to the electromagnetic coil, which then measures the resonant frequency of the vibration and sends this information via the cable to the data logging system. By applying the gage and batch factors, this frequency in hertz is transformed to microstrain.

An increase in microstrain from the initial set point indicates that the strain gage is being pulled with a tensile force and a decrease in strain indicates that the strain gage is being compressed. So for example, when expansion of the approach pavement occurs the strain gage will register an increase in microstrain and vice versa for pavement contractions.

2.1.2 Thermistors

The Geokon Model 3800 thermistor (Geokon Inc., 2013b) probe was used to measure the temperature of the bridge and the approach pavements at various locations (Figure 3). The thermistors were installed next to the strain gages, crackmeters, and tiltmeters.



Figure 3. Geokon model 3800 thermistor (Geokon Inc., 2013b)

These thermistors are enclosed in PVC housing as shown in Figure 3; each has a length of 50 mm and a diameter of 12 mm. The thermistors have a temperature range of -30 to 120 degrees Celsius, an accuracy of ± 0.5 degrees Celsius, and a resolution of 0.1 degrees Celsius. To measure temperature, the thermistor utilizes semiconductors that work similar to thermal resistors. The thermistor beads that are inside the PVC encasing consist of metal oxides that are resistant to temperature change, the bead's resistance to electrical current, in ohms, corresponds to a particular temperature. This information along with thermal coefficients can be used to calculate the temperature at the location of the thermistor.

The thermistors were installed into ½ inch diameter drilled holes with a 2 inch depth. Once the hole was drilled out, the thermistor probe was simply inserted into the drilled hole. Afterward the thermistor was covered with expandable foam to insulate it and help prevent pullout. Thermistors were placed approximately 6” away from the tiltmeters and strain gages so that the temperature of the structure could be obtained.

2.1.3 Tiltmeters

The Geokon Model 6350 vibrating wire tiltmeter (Geokon Inc., 2013c) was used to measure the relative tilt of the abutments and pier caps (Figure 4). Each abutment had 2 tiltmeters placed on both ends of the abutment. Monitoring the relative tilt of each abutment provides valuable supporting data on the interactions between the bridge deck and the approach slab. In addition tiltmeters were also installed on pier caps of the SH-3 North Bridge over BNSF railroad. This particular model of tiltmeter is for long-term, small changes in inclination of large structures. The tiltmeter has a range of ± 10 degrees and an accuracy/resolution of ± 8 arc seconds, or 0.0022 degrees.



Figure 4. Geokon model 6350 vibrating wire tiltmeter (Geokon Inc., 2013c)

The tiltmeter is able to measure rotation using a calibrated weight within the device that is supported by an elastic hinge and a vibrating wire attached to an electromagnetic coil (Figures 5 and 6). Depending on the direction in which the tiltmeter rotates, the weight either pulls or pushes on wire causing a certain amount of tensile strain within the wire and bends the elastic hinge accordingly. This weight rotation can be dampened with high viscosity silicone oil to keep sudden, vibratory rotations from over stressing the wire; however, it is optional and usually not

required for most structures. This entire apparatus is housed in a stainless steel, water tight casing. To prevent damage to the device while being shipped the weight is locked into place with a clamp screw. When the tiltmeter is ready to be used, this locking screw is replaced by a shorter Phillips head screw that does not lock the weight into place. Attaching this screw is necessary in order to keep the device water tight. Taking a measurement is similar to the strain gage in that the vibrating wire is plucked and the resulting natural frequency represents a particular strain and thus a particular inclination which is measured by the electromagnetic coil.

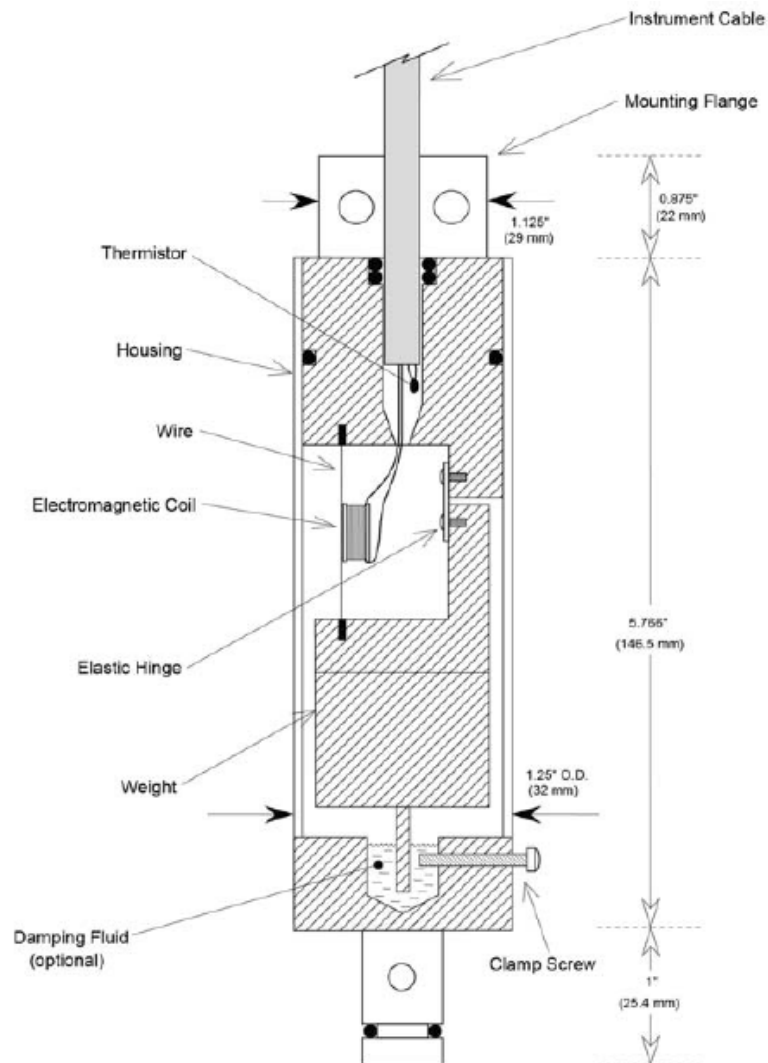


Figure 5. Different sections of Geokon model 6350 tiltmeter (Geokon Inc., 2013c)

An increase in the digit value from the device indicates that the tiltmeter is experiencing a positive angle increase and is rotating in a clockwise direction as shown in Figure 6. The

opposite is true for negative angle increase; the device will rotate counter clockwise. Each tiltmeter is delivered with a calibration sheet. This calibration sheet is specific to each tiltmeter and provides the digits and gage factors that correspond to an angular tilt for that particular tiltmeter. Calibration of the tiltmeter is not required; however, the inclination of the tiltmeter upon installation needs to correspond to the amount of digits that equate to zero angular tilt.

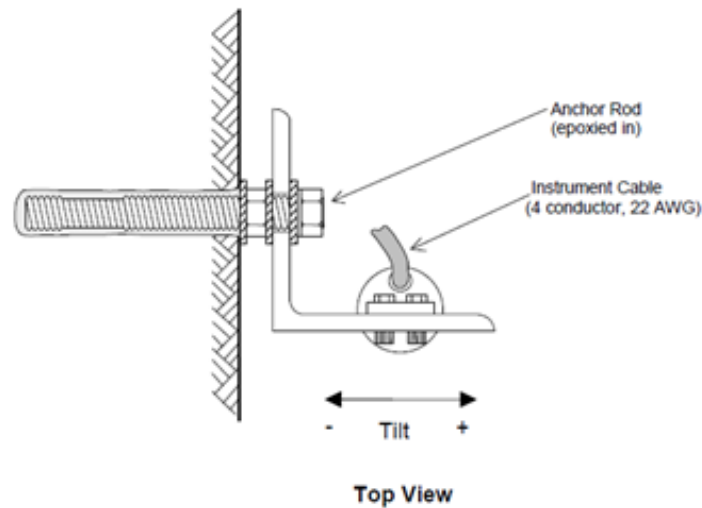


Figure 6. Top view of an installed tiltmeter (Geokon Inc., 2013c)

2.1.4 Crackmeters

The Model 4420 vibrating wire crackmeter (Geokon Inc., 2013d) is designed to measure displacement across concrete joints in bridges and buildings (Figure 7). This makes the instrument ideally suited to measure the displacement between different sections of bridges. This particular model of crackmeter has a 50 mm stroke.



Figure 7. Geokon model 4420 vibrating wire crackmeter (Geokon Inc., 2013d)

As seen in Figure 8, the crackmeter measures displacement with a wire that runs through the transducer housing and connects the coupling at the right end of the instrument with a heat treated, stress relieved, spring on the left (located in the transducer housing). This spring is connected to a vibrating wire sensing element, similar to the ones previously discussed. When the right end of the instrument is pulled the transducer shaft is pulled out of the housing and the spring elongates. When the vibrating wire element plucks the wire it senses this increase in tension and sends the corresponding natural frequency to the data logger where it is converted to digits. These digits directly correspond to a particular displacement length when additional factors are applied.

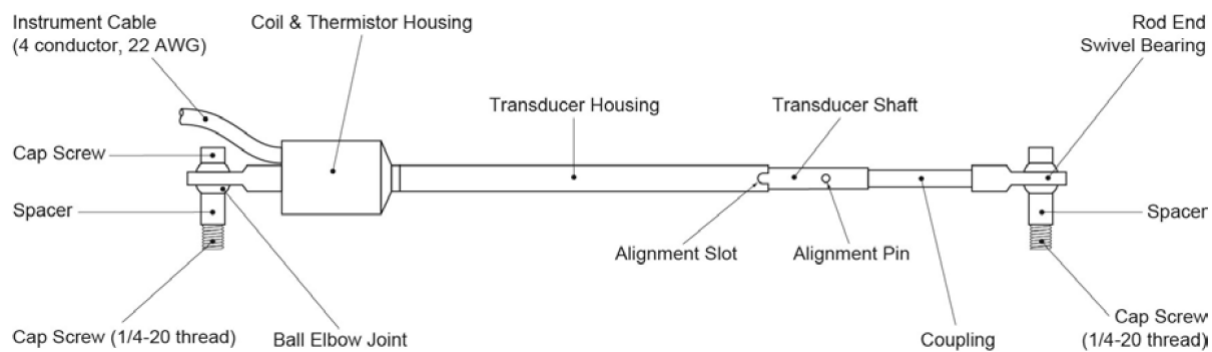


Figure 8. Different sections of Geokon model 4420 vibrating wire crackmeter (Geokon Inc., 2013d)

An increase in the digit value indicates that positive displacement is taking place and tensile forces are acting on the device. For example, it means that the distance between an approach slab and a wing wall is increasing and the approach slab is contracting (assuming that the wing wall is stationary). The opposite is true for a decrease in digits. That is, the distance between an approach slab and wing wall is decreasing and the approach slab is expanding.

2.1.5 Data Logging System

The Geokon Model 8021 Micro-1000 data logger (Geokon Inc., 2013e) shown in Figures 9 and 10 was used to record, process, and store the data from the vibrating wire instruments by utilizing the Geokon Model 8032 multiplexer and the Geokon Multilogger software. Each data logger can support up to 6 multiplexers and depending on the multiplexer's configuration the data logger can read up to a maximum of 192 instruments sequentially. The system is contained

in a weather proof enclosure to withstand hostile environmental conditions (Figure 9). The portion of the Mirco-1000 data logger that controls the system with program instructions is the Campbell Scientific CR measurement and control system; it receives programming instructions such as the instrument model attached, time interval instructions and the number of multiplexers attached.

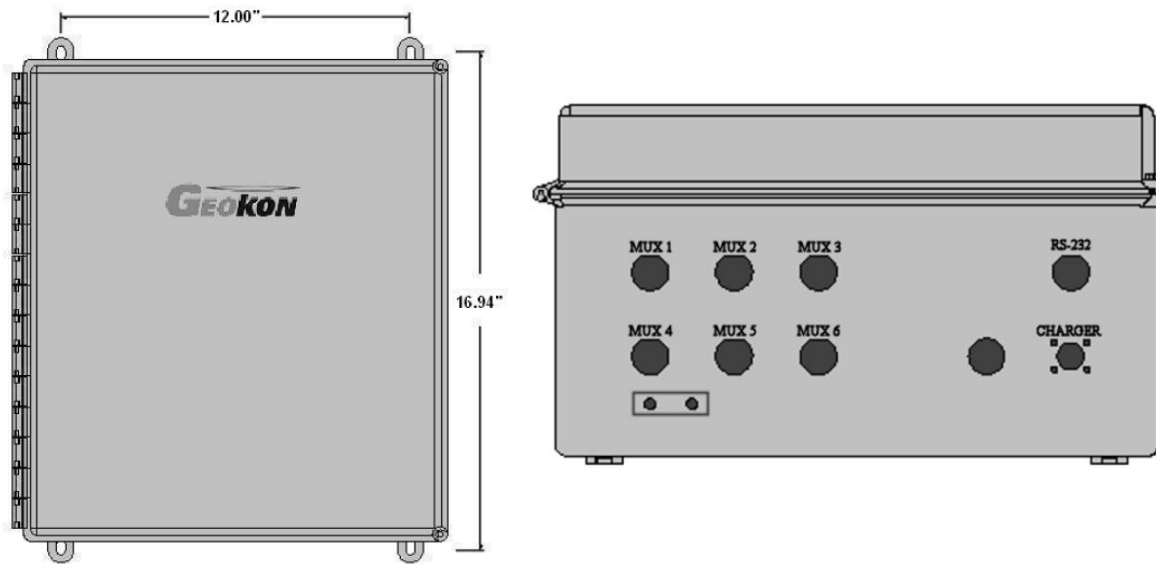


Figure 9. Geokon model 8021 Micro-1000 data logger; left picture is front view and the right picture is bottom view (Geokon Inc., 2013e)

The Campbell scientific AVW200 is the portion of the data logging system that provides an excitation by plucking the vibrating wires embedded in each instrument. Each instrument in turn plucks the internal vibrating wire within the instrument to take a reading. The AVW200 is also responsible for processing and recording the returned frequency signal from each instrument. The data logger is powered by an internal 12 Volt DC lead acid battery; however, in field conditions this battery should only be used as a backup for when power interruptions occur. The main power supply can come from different sources, in the case of this project each Mirco-1000 data logger was attached to a large deep cycle marine battery. The logger can continually take readings until the battery voltage drops below 9.6 volts at which point the readings become unreliable. The time it takes to reach 9.6 volts depends on a variety of factors such as the number of instruments attached to the logger, the interval between readings, and the battery temperature. For purposes of this project the battery will reach 9.6 volts in about 3 months of continuous use. Approximately every 2 months the deep cycle battery was swapped with a fully

charged battery. The Micro-1000 data logger has a variety of ports on the bottom portion of the device (Figure 9). The 6 serial ports on the left of the device are for the attachment of up to 6 Model 8032 multiplexers. The RS-232 port in Figure 9 is used to communicate, download data, and program the Micro-1000 data logger via a serial cable to a computer using the Multilogger software. The port below the RS-232 port is used to supply power to the logger from the external battery. The two leads seen under multiplexer ports are used to ground the data logger in the event of a power surge. The last port to the left of the charger port is for other extraneous wires that may need to be fed into the data logger.



Figure 10. Inside of the Geokon model 8021 Micro-1000 data logger box

The model 8032 multiplexer (Geokon Inc., 2013f) expands the amount of channels that can be read and thus increases the amount of instrumentation that can be attached to the data logger (Figure 11). The multiplexer can be set up in two ways, with a 32 channel or a 16 channel configuration. The 32 channel configuration is for instruments that only have 2 wires with which to send information; an example would be a thermistor. In this configuration, two separate 2 vibrating wire instruments can be attached to a single multiplexer channel. The 16 channel configuration is for instruments that have 4 wires to send information with; an example would be a Model 4000 strain gage. Figure 12 shows the channels inside the multiplexer. The white and green wires send information on the internal temperature of the gage while the red and black wires send information for the instrument's primary measurements; for a strain gage,

the primary measurement would be strain. For purposes of this project the multiplexers were set in the 16 channel configuration mode, so only 16 instruments could be attached to a single multiplexer. This means that a single instrument was read by a single multiplexer channel. Prior to field installation, the Micro-1000 data logger had to have each multiplexer port configured specifically for the Model 8032; then each individual multiplexer channel had to be configured to the type of instrument that would be attached to that channel.



Figure 11. Geokon model 8032 multiplexer (left) and its data logger (right) (Geokon Inc., 2013f)

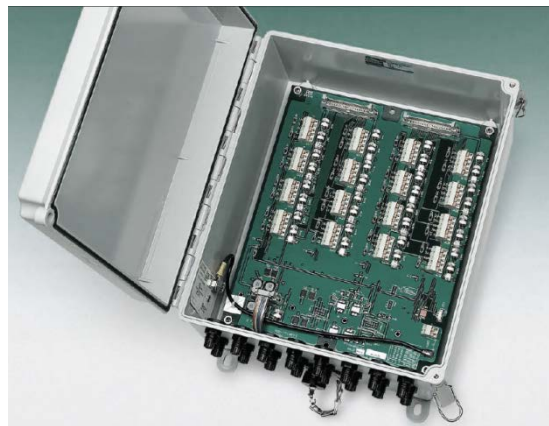


Figure 12. Channels inside the multiplexer (Geokon Inc., 2013f)

2.2 Data Collection and Analysis

The instrumentation layouts for the bridges are presented and the data collected from the bridges are analyzed and discussed in this section. For each bridge, the data collected before the repairs are discussed first and then the data collected after the repairs are discussed.

2.2.1. The US 64 Westbound over Shell Creek

The US 64 Westbound over Shell Creek (NBI No. 18141) is located in Tulsa County, Oklahoma. This bridge is experiencing number of problems related to the interactions between bridge abutments and adjacent roadways. These problems include, expansion joints closing (Figure 13), roller support bearings tilting (Figure 14), and beams pushing against abutment backwalls (Figures 14 and 15).

For the US 64 Westbound Bridge over Shell Creek, only the west abutment (where the distress was more severe) was instrumented. The locations of the instruments are shown in Figure 16. After about 4 months of data collection, on November 25, 2012, most of the sensor cables were stolen and the data collection was interrupted. All the data collected on this bridge is presented and discussed in this section. The following abbreviations are used for instruments, strain gage = SG, thermistor = TH, tiltmeter = TM, and crackmeter = CM.



Figure 13. A closed expansion joint on the Shell Creek Bridge



(a) On May 6, 2011



(b) On May 26, 2011

Figure 14. Northern most rocker bearing (before and after straightening) and girder on the west abutment of the Shell Creek Bridge



Figure 15. A beam pushing against an abutment backwall on the Shell Creek Bridge

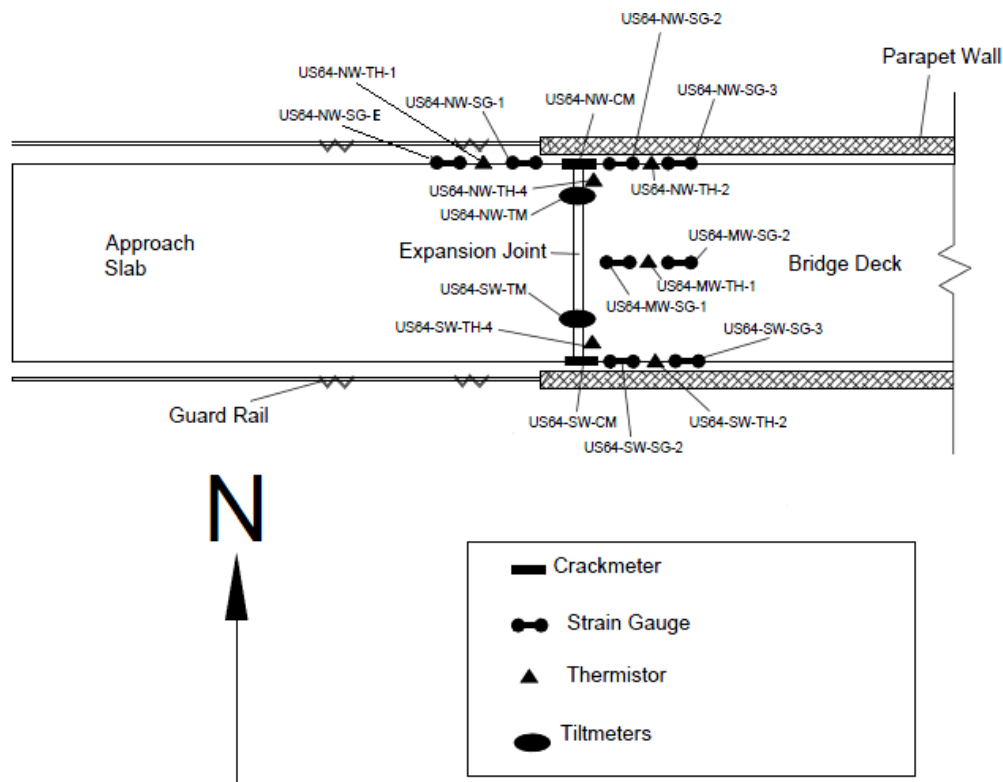


Figure 16. Instrument locations for the Shell Creek Bridge

2.2.1.1 Abutment Rotation

Tiltmeters are located on both ends of westbound abutment back walls as shown in Figure 16. The figures in this section show the data trends for both tiltmeters. A negative trend in the tiltmeter data indicates the abutment is tilting toward the approach slab and a positive trend indicates that the abutment is tilting toward the bridge deck. This applies to all of the tiltmeter data presented.

Figure 17 depicts SW-TM tiltmeter data on the south side of the abutment backwall. The spikes seen in the tiltmeter data are caused by vehicle vibrations. It can be seen that the trend in the tiltmeter data corresponds inversely with temperature trends. As the average temperature decreases from July through October, the tilt increases. Similar trend can also be seen in for the tiltmeter on the north side (Figure 18). These data indicates that as the deck cools the abutment backwall is rotating towards deck.

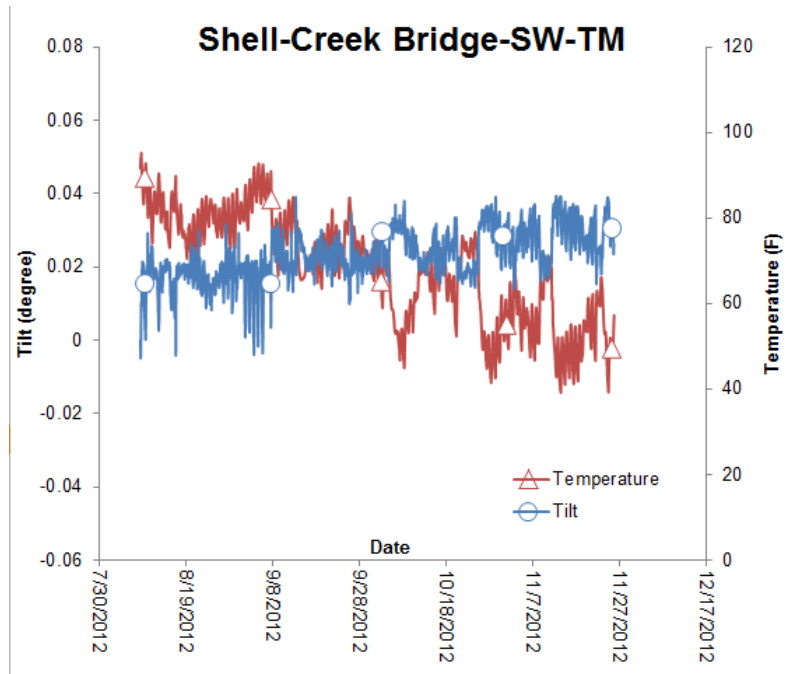


Figure 17. US 64 over Shell Creek Bridge – Southwest Tiltmeter data (SW_TM)

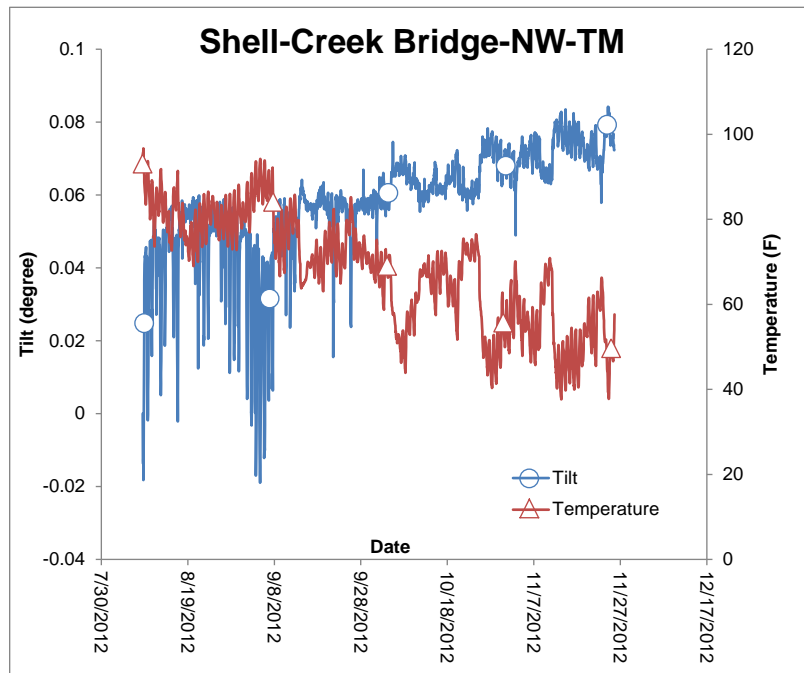


Figure 18. US 64 over Shell Creek Bridge – Northwest Tiltmeter data (NW_TM)

2.2.1.2 Relative Displacement between the Bridge Deck and the Approach Slab

Crackmeters are attached between the bridge deck and the approach slab, near the expansion joint, as shown in Figure 16. Figure 19 and Figure 20 show measured displacements and temperatures for crackmeters SW-CM and NW-CM, respectively. As the temperature decreases, deck and the approach slab move away from each other and the relative displacement between them increases as shown in Figure 19 and Figure 20.

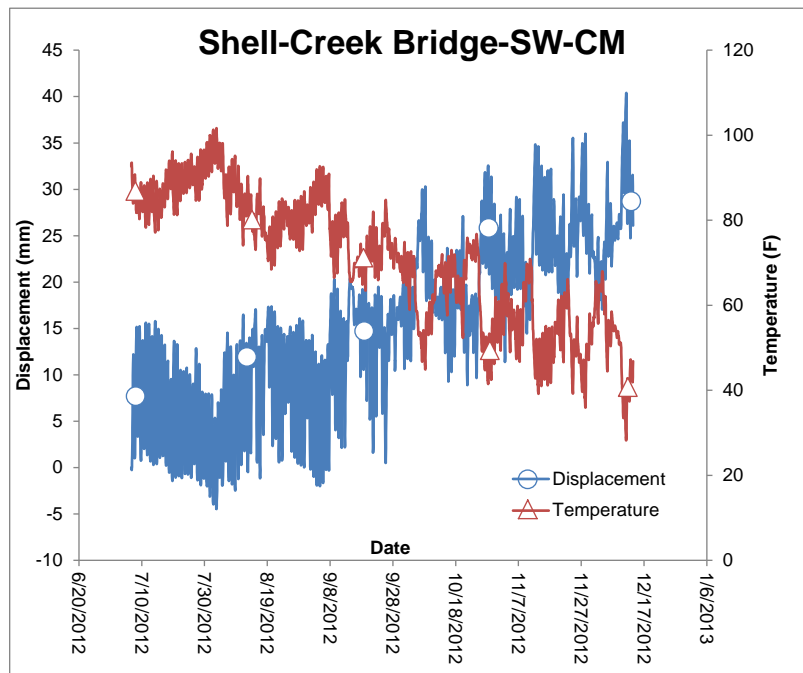


Figure 19. US 64 over Shell Creek Bridge – Southwest Crackmeter data (SW_CM)

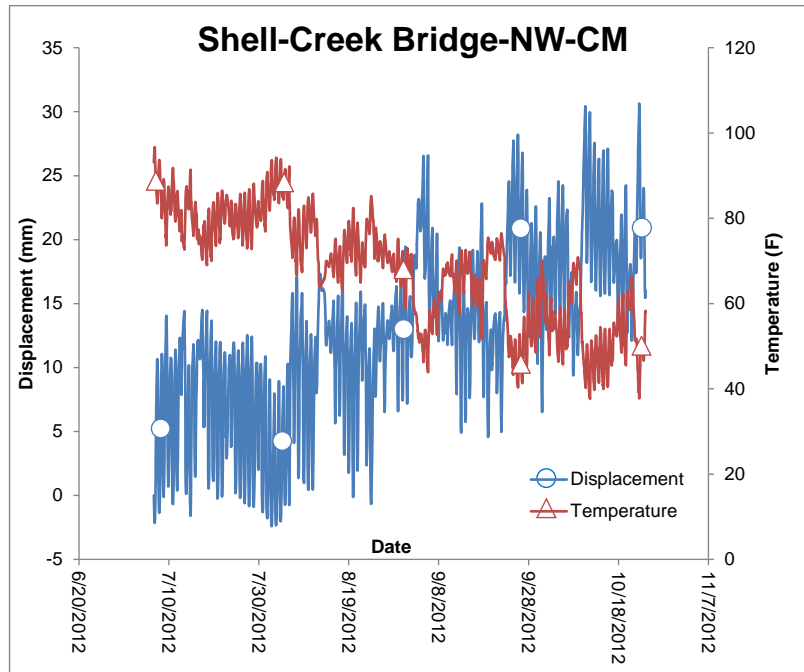


Figure 20. US 64 over Shell Creek Bridge – Northwest Crackmeter data (NW_CM)

2.2.1.3 Axial Strains

Strain gages were installed with a thermistor at different locations as shown in Figure 16. Figure 21 and Figure 22 show strain trends for strain gage NW-SG1 (located on the approach slab) and NW-SG3 (located under the bridge deck), respectively. It can be seen from these figures that as the temperature decreases the strains in the approach slab increases and the strain in the deck decreases and vice versa. These trends indicate that the deck and the approach slab are locked into each other near the expansion joint and as the deck shrinks during cooling, the approach slab is expanding into the gap created by the shrinking deck. This also indicates that there will be compressive stresses transmitted between the deck and the approach slab during heating.

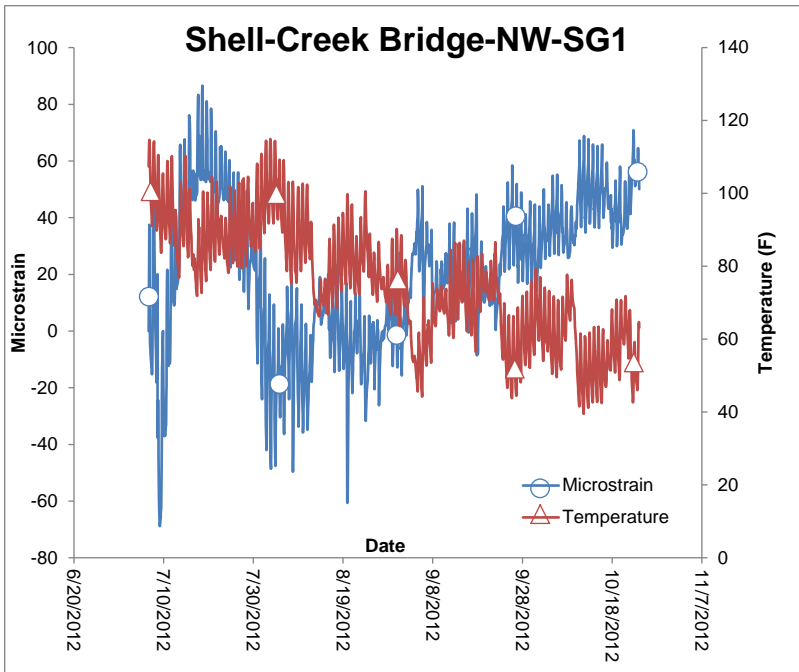


Figure 21. US 64 over Shell Creek Bridge – Northwest Strain Gage 1 (NW_SG1)

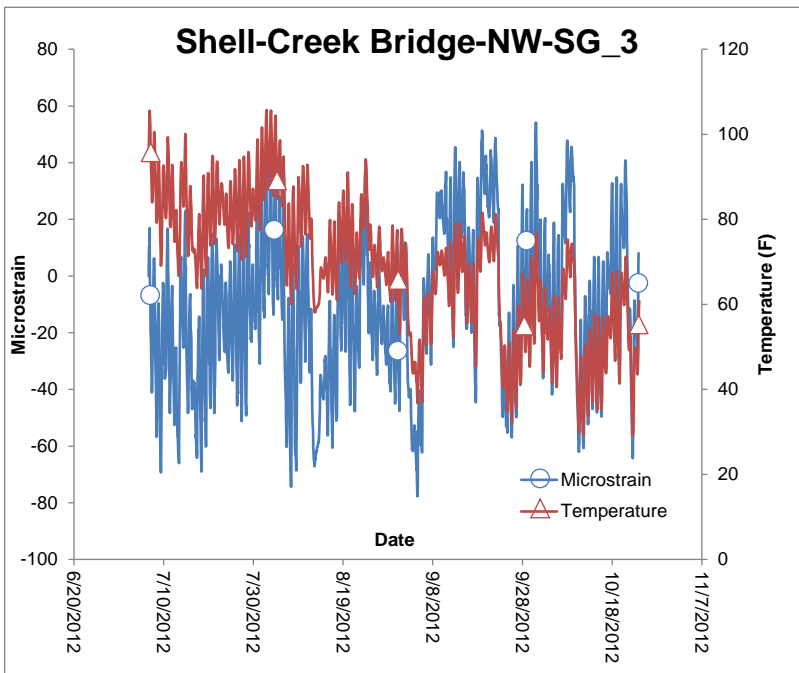


Figure 22. US 64 over Shell Creek Bridge -Northwest Strain Gage 3 (NW_SG3)

2.2.2. Monitoring of Expansion Joint Widths

This section presents data obtained using demountable mechanical strain gage (DEMEC) measurements across expansion joints at several bridges in Tulsa and a bridge on SH 76 near Purdy, Oklahoma. These measurements were taken at 1-2-month intervals over wide range of temperatures to verify whether the new expansion joints constructed on these bridges during repairs are functioning as expected. The bridges in Tulsa (Figure 23) are on I-244 east and westbound over North Detroit Ave. and Martin Luther King Jr. Blvd. (formerly North Cincinnati Ave.). The NBI numbers for these bridges are 18027, 18029, 18024 and 18028. The SH 76 Bridge (NBI No. 12643) is over Rush Creek. For all the expansion joints, measured widths are compared with the calculated joint widths obtained by starting from a width of 2 in. at 60° F and adjusting for temperature changes by Equation (1) given below.

$$\Delta = \alpha L \Delta T \quad (1)$$

Where: Δ = change in length, in.

α = coefficient of thermal expansion, 6.5×10^{-6} in./in. $^{\circ}$ F

L = initial length, in.

ΔT = change in temperature, $^{\circ}$ F



Figure 23. I-244 Bridges

2.2.2.1 I-244 Bridges

The expansion joints on I-244 bridges for which results are presented are shown in Figures 24-27.

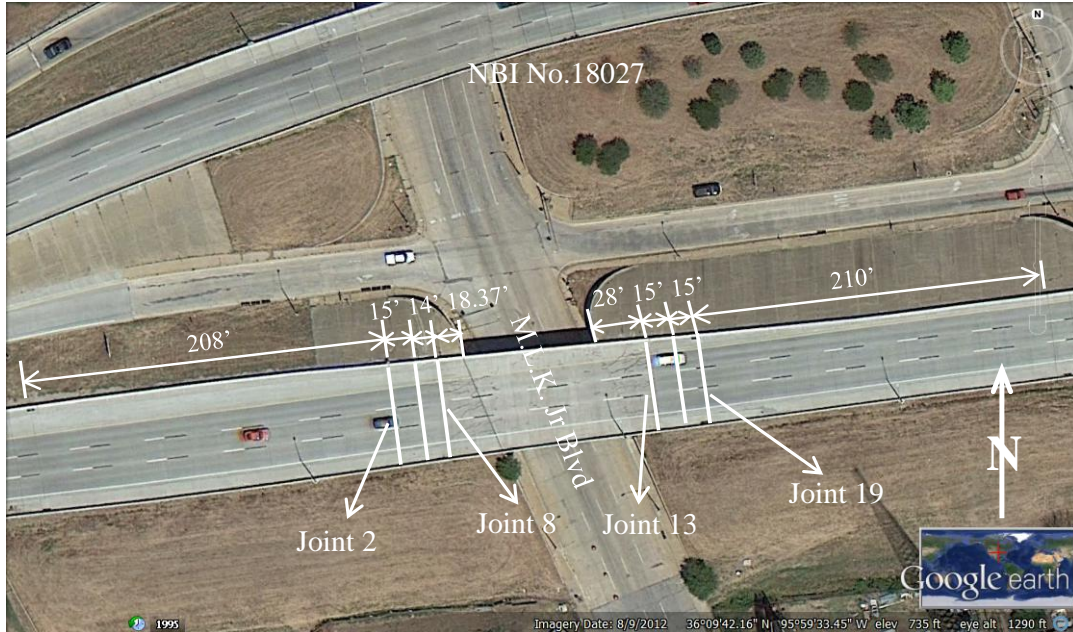


Figure 24. Joints on I-244 East over Martin Luther King Jr. Blvd. (NBI No. 18027)

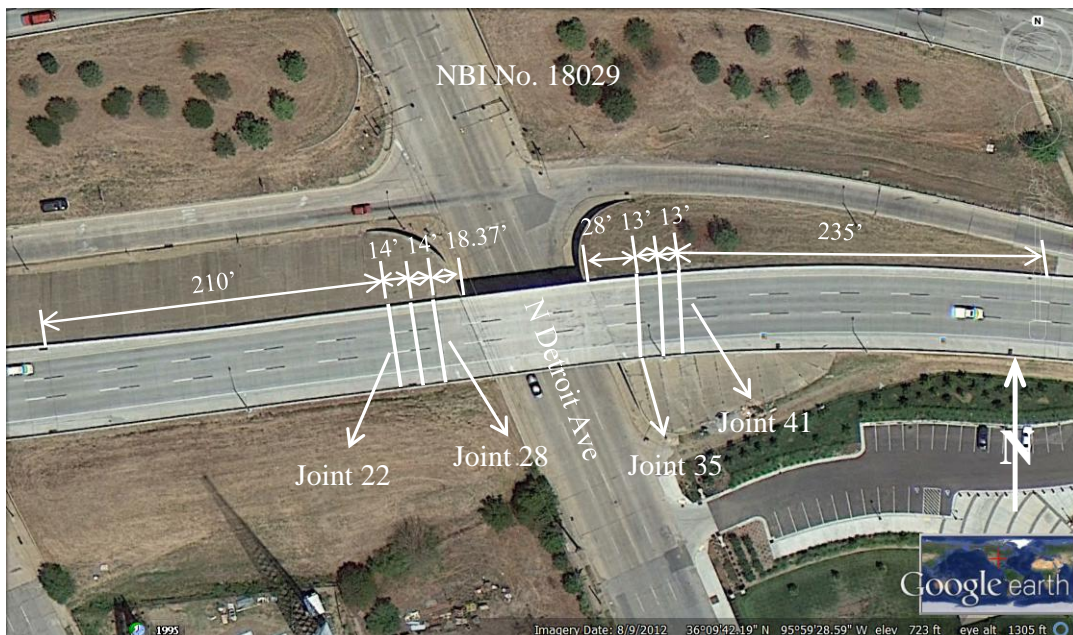


Figure 25. Joints on I-244 East over N. Detroit Ave. (NBI No. 18029)

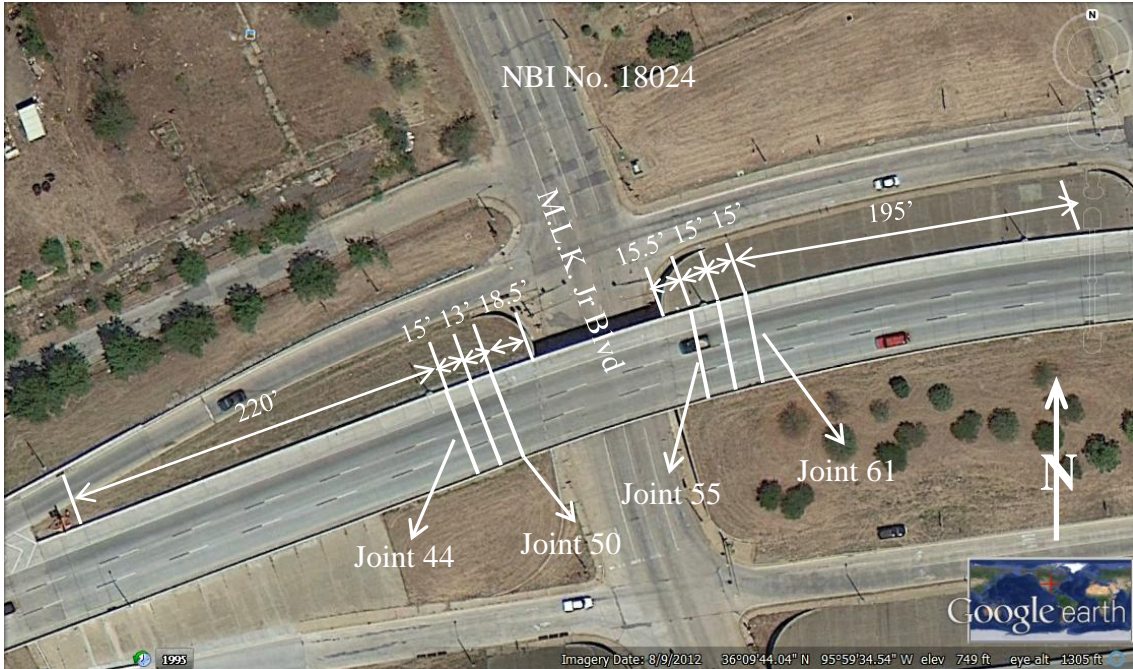


Figure 26. Joints on I-244 West over Martin Luther King Jr. Blvd. (NBI No. 18024)

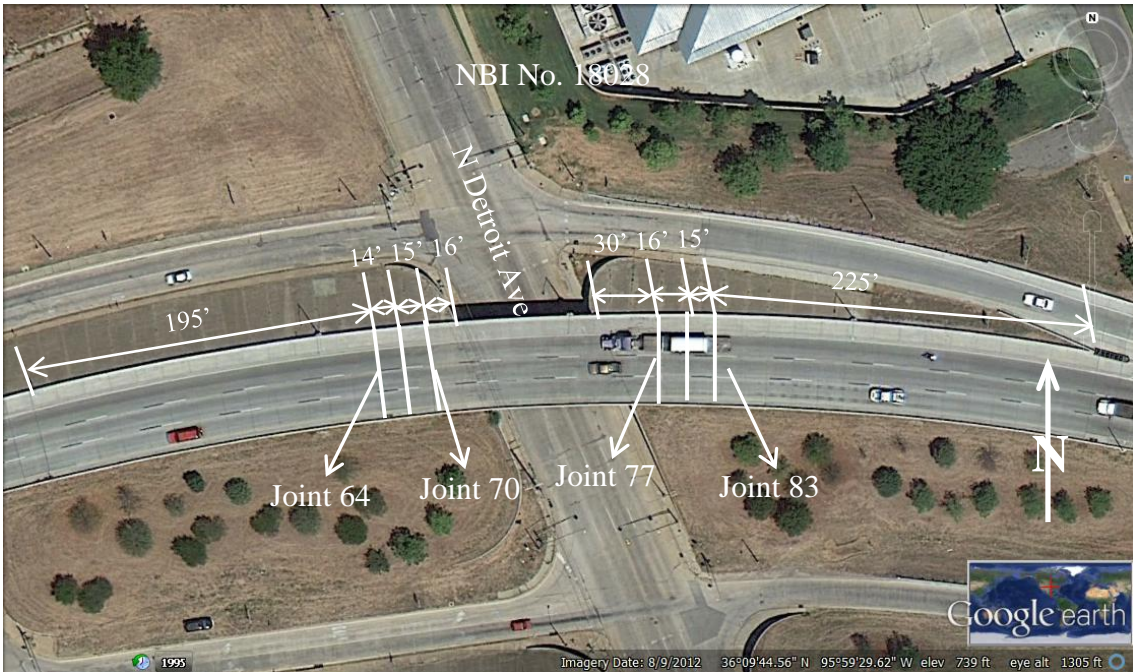


Figure 27. Joints on I-244 West over N. Detroit Ave. NBI No. 18028

The variations of joint widths with temperature for I-244 bridges are shown in Figures 28-31. Except for Joint 70 (Figure 31), for all other interior joints, the measured variations

reasonably matched the calculated variations. The reason that the calculated variations and the measured variations deviate for exterior joints is likely due to the fact that the slab lengths (shown in Figures 24-27) used in calculating the joint widths may not be the actual lengths contributing to the expansion and contraction of the exterior joints. The measured variations for the exterior joints are, however, similar to those for the interior joints. Based on these observations, it appears that these expansion joints on the I-244 Bridges are performing as expected at this time.

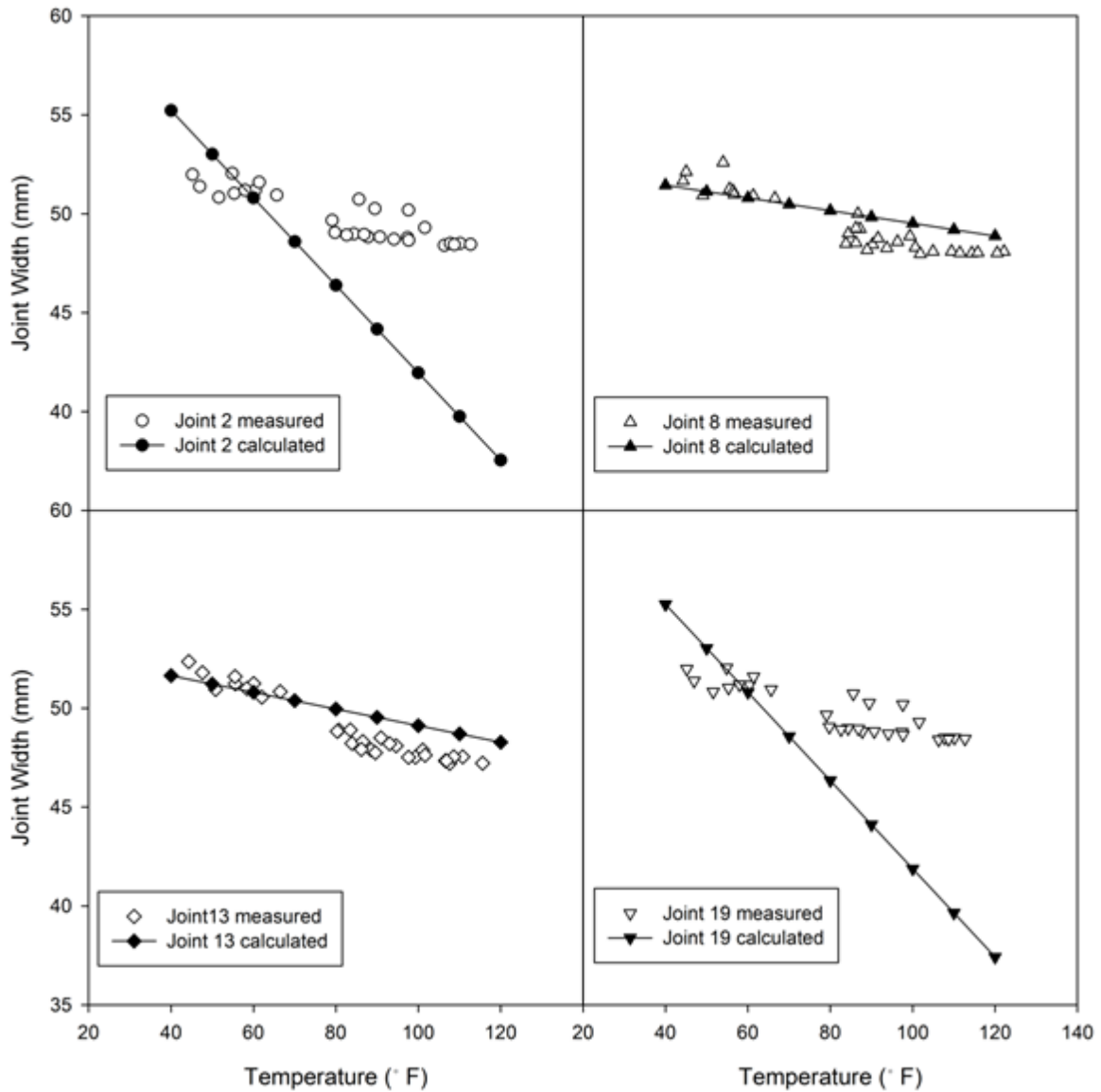
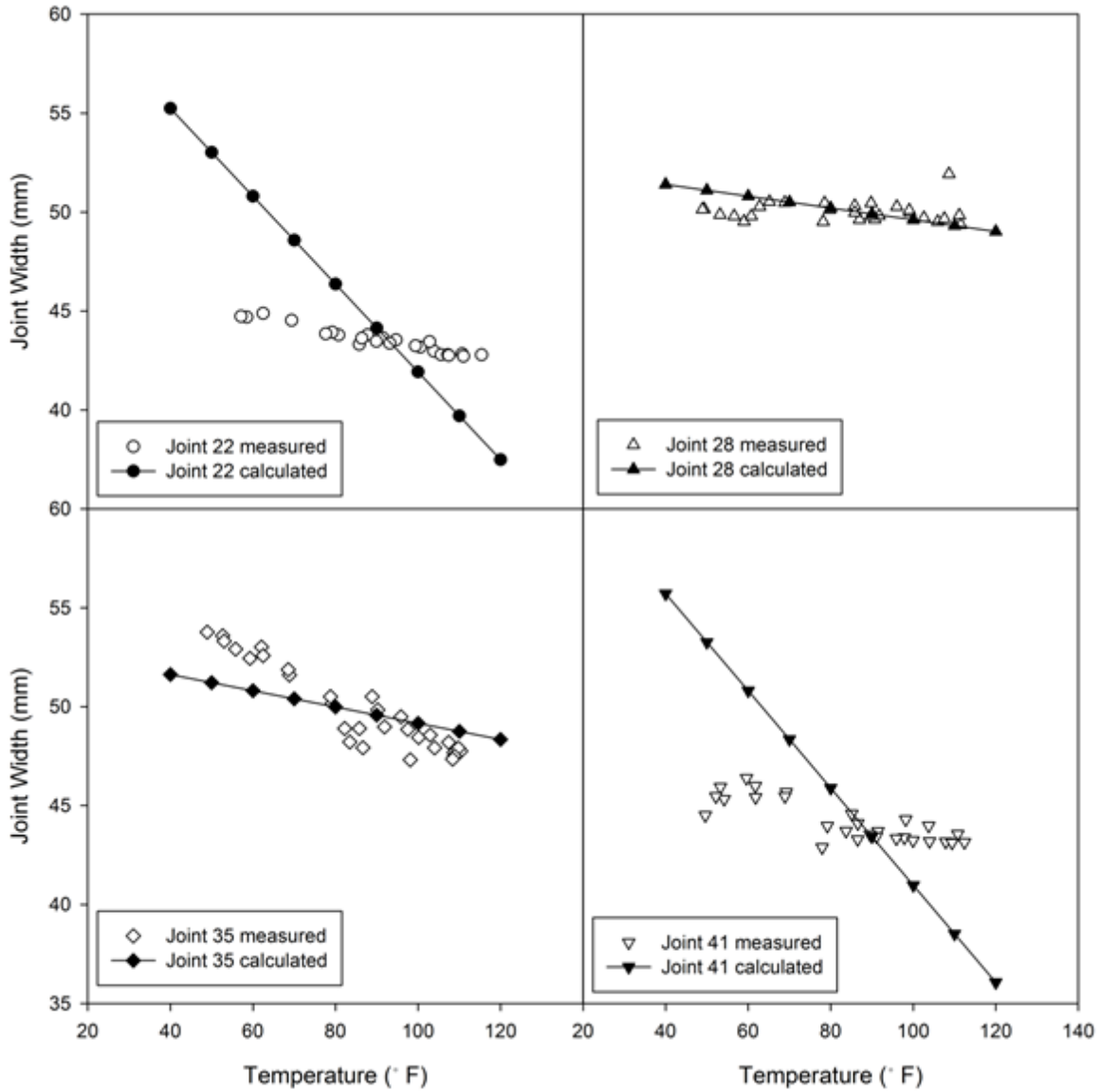


Figure 28. Variation of joint widths with temperature for I-244 East over Martin Luther King Jr. Blvd. (NBI No. 18027)



**Figure 29. Variation of joint widths with temperature for I-244 East over N. Detroit Ave.
(NBI No. 18029)**

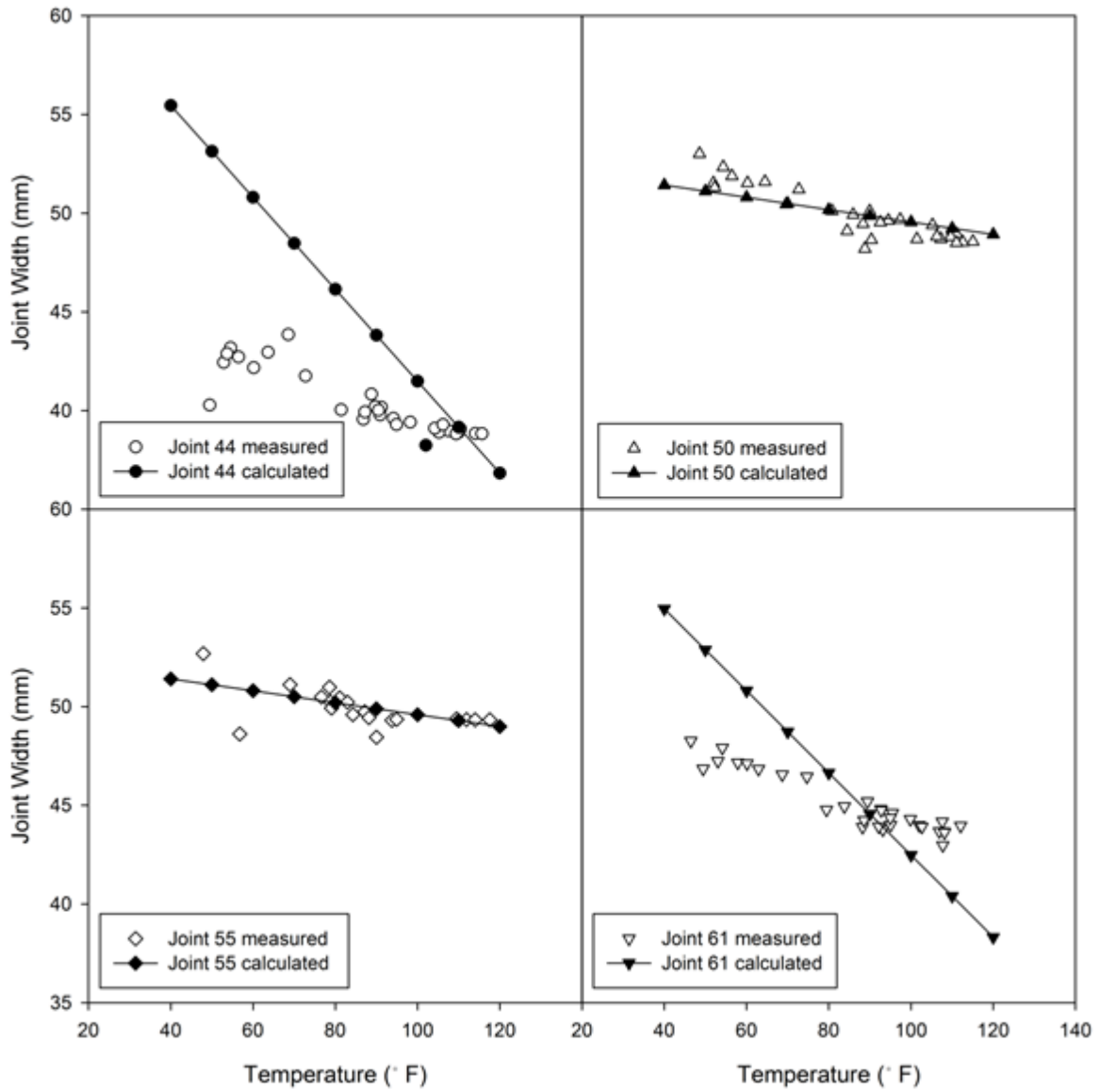


Figure 30. Joint Widths of Expansion Joints for I-244 West over Martin Luther King Jr. Blvd. (NBI No. 18024)

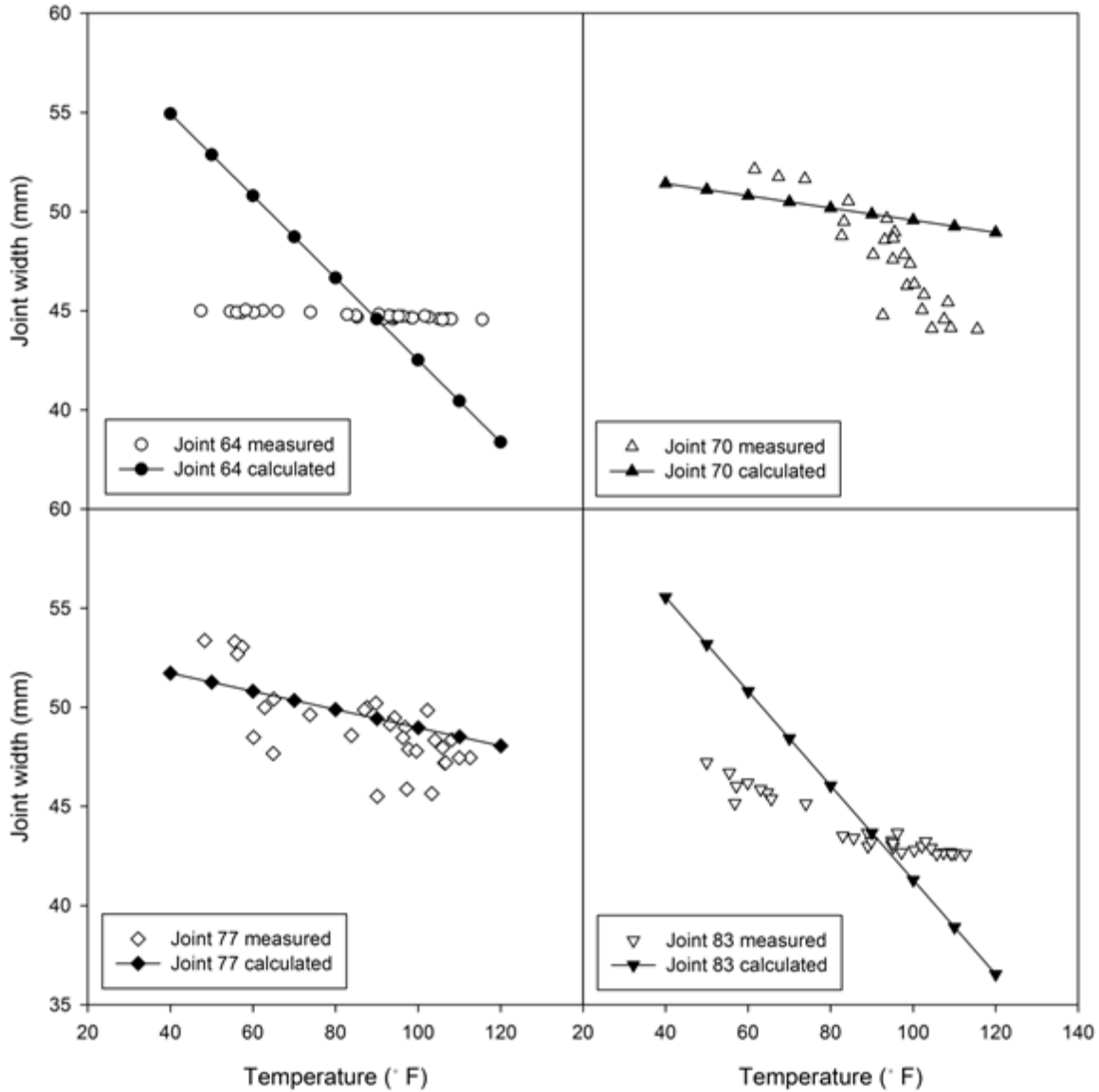


Figure 31. Joint Widths of Expansion Joints for I-244 West over N. Detroit Ave. (NBI No. 18028)

2.2.2.2 SH 76 Bridge over Rush Creek

The expansion joints where measurements were taken for this bridge are shown in Figure 32. Measurements were taken on both east and west sides of the joints. The joint widths were measured and calculated in the same manner as for the I-244 Bridges. The measured joint widths are compared to the calculated widths in Figure 33. Based on this comparison, these joints also appeared to be functioning properly at this time.



Figure 32. SH 76 over Rush Creek

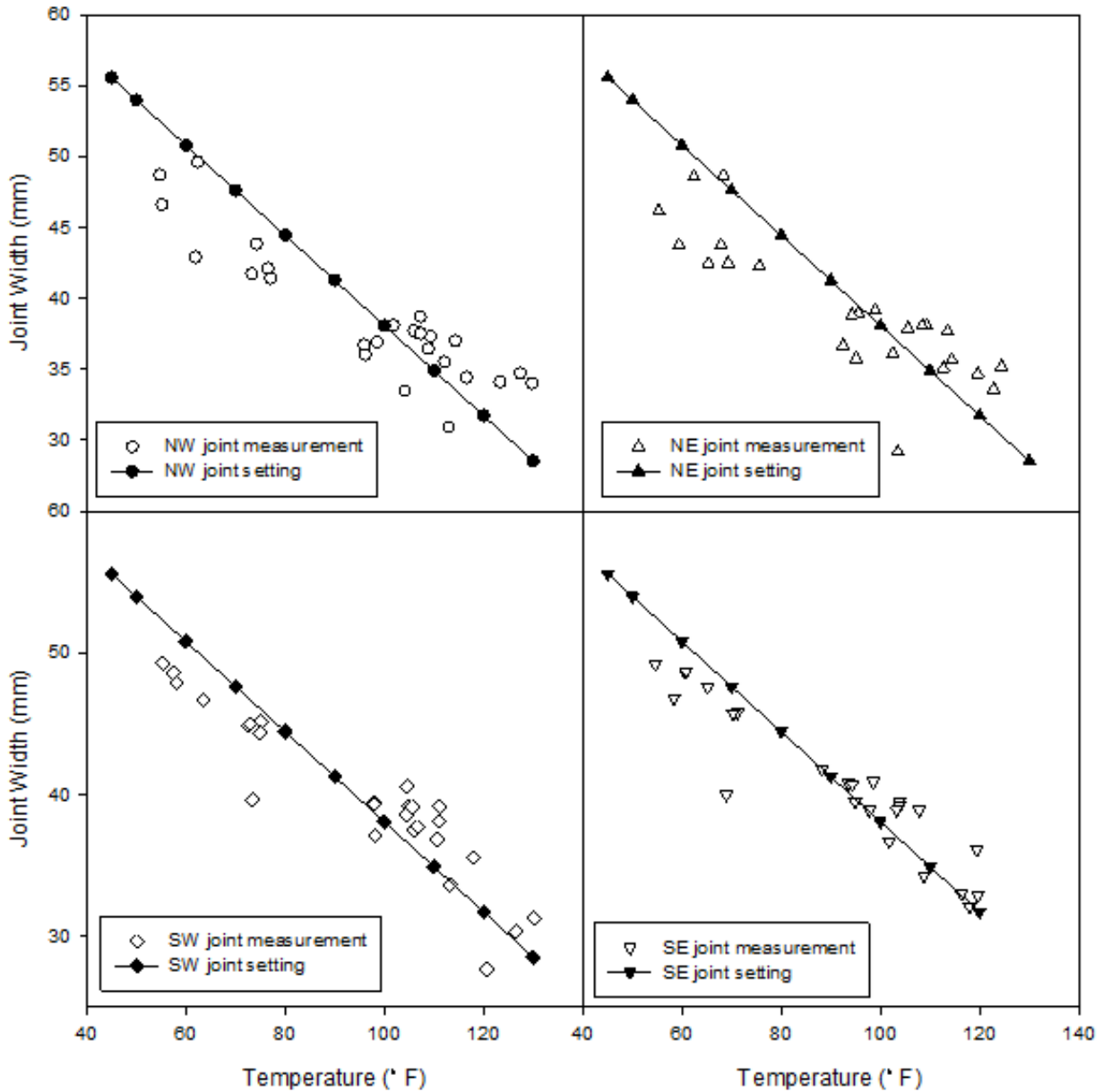


Figure 33. Joint widths of expansion joints on SH 76 over Rush Creek

2.2.3. The SH-3 Bridges over BNSF Railroad

The SH-3 bridges over BNSF railroad are located near Ada, Oklahoma. These five span bridges are 344 ft long and were built in 1980 (Figure 34). The elevation of the SH-3 North Bridge is shown in Figure 35. These bridges have experienced a number of problems related to the interactions between bridge abutments and adjacent roadways. These problems included expansion joints closing, roller support bearings tilting, and beams pushing against abutment

backwalls (Figures 36 and 37). These problems were noticed as early as in 1983. It is believed these problems were related to the lateral deformation of the embankments on top of the soft clay layer (see Figure 35) early in the life of the bridges. Rotation of the top of the anchor bolts towards the abutment backwall (Figure 36) and buckling/cracking of the slope wall (Figure 37) are strong evidence for lateral deformations of the approach embankments.

The eastern side (Figure 38) was first selected for instrumentation due to the taller approach embankment (45 ft) on this side and later additional instruments were added to the western side, the pier caps, and expansion joints of the North Bridge.

Instrumentation consisted of installing various sensors at key locations in order to collect useful data regarding strain, temperature, displacement, and rotation. The installed instruments collected data at this site until the repairs to the North Bridge started in August 2015. The instruments were moved out of the way of the construction activities starting on August 6, 2015 and the data collection stopped at this site on August 26, 2015 and resumed after repairs in February 2016.

Two Geokon Model 6300 Vibrating Wire In-Place Inclinator systems were also installed on the east and west approach embankments between the North and the South Bridge. The locations of the east and west inclinometers are shown in Figure 39. The inclinometer is appropriate for long-term monitoring of deformations in embankments. The basic principle is the utilization of tiltmeters to make accurate measurement of inclination, over segments, in a borehole drilled into the embankment being studied. The continuous nature of the instrument allows for very precise measurement of changes in the borehole profile to be measured. The instruments were installed in standard grooved inclinometer casing. The data are presented as deflections at the pivot points of the inclinometer (Figure 40).



Figure 34. SH-3 bridges over BNSF railroad

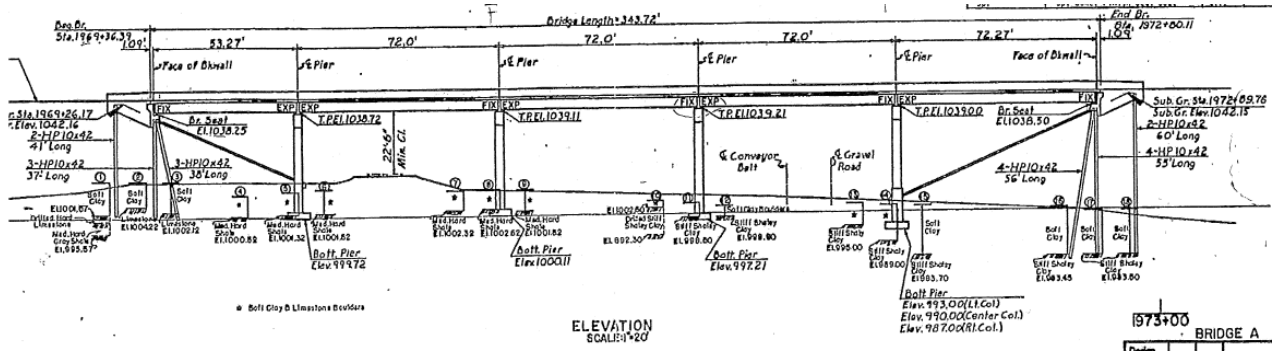


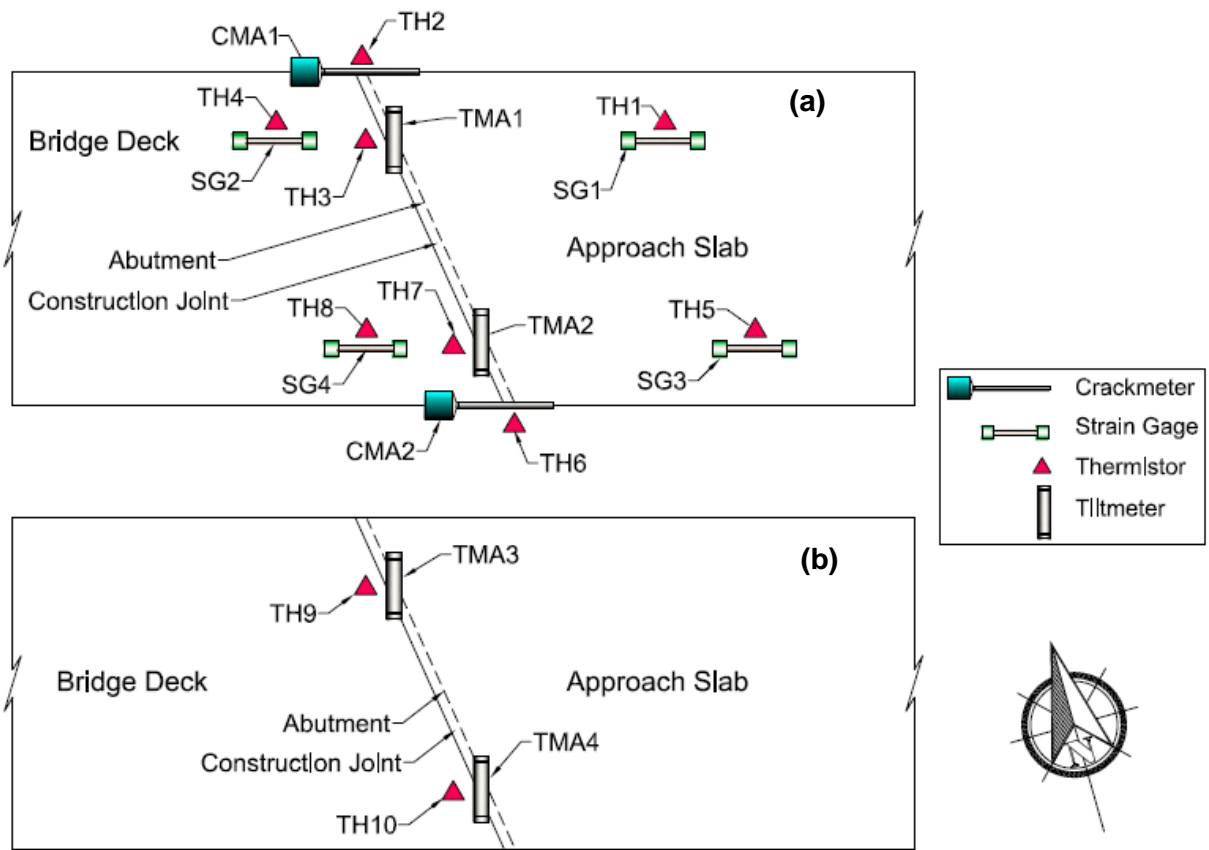
Figure 35. Elevation of the SH-3 north bridge over BNSF railroad



Figure 36. Beams pushing against abutment backwalls and a bent anchor bolt



Figure 37. Cracks in the slope-wall



**Figure 38. Eastern side of SH-3 bridges over BNSF railroad – instrumentation locations:
 (a) north bridge (b) south bridge**

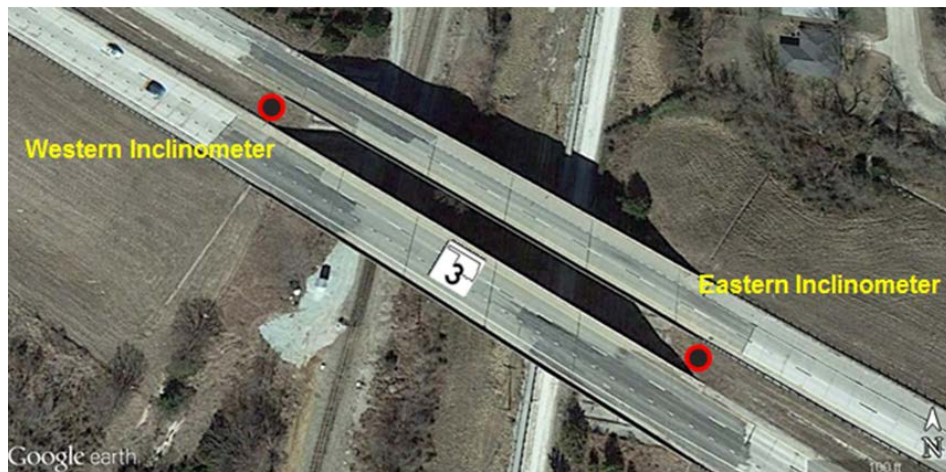


Figure 39. SH-3 bridges over BNSF railroad – locations of the inclinometers (Google Inc., 2013a)

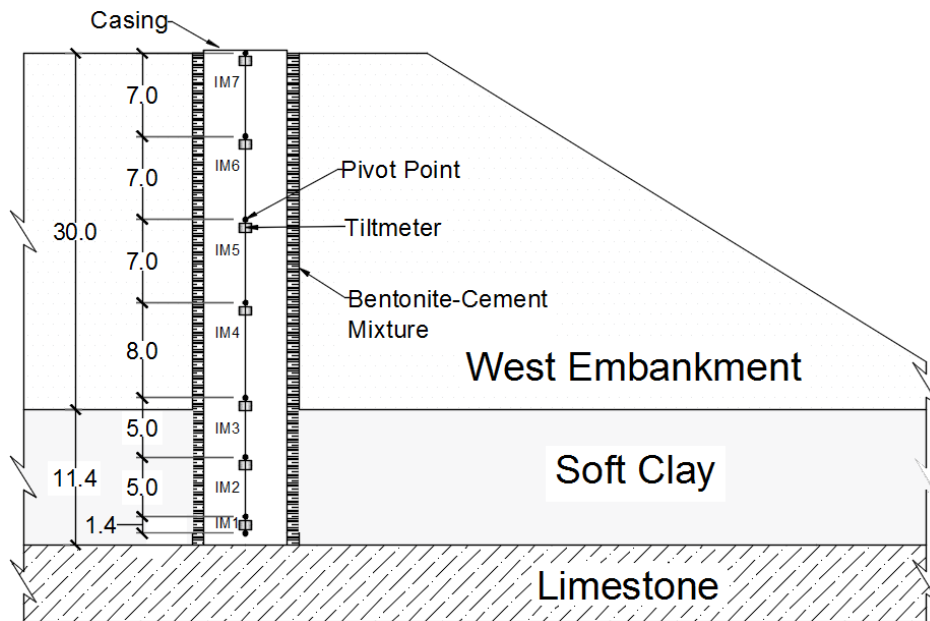
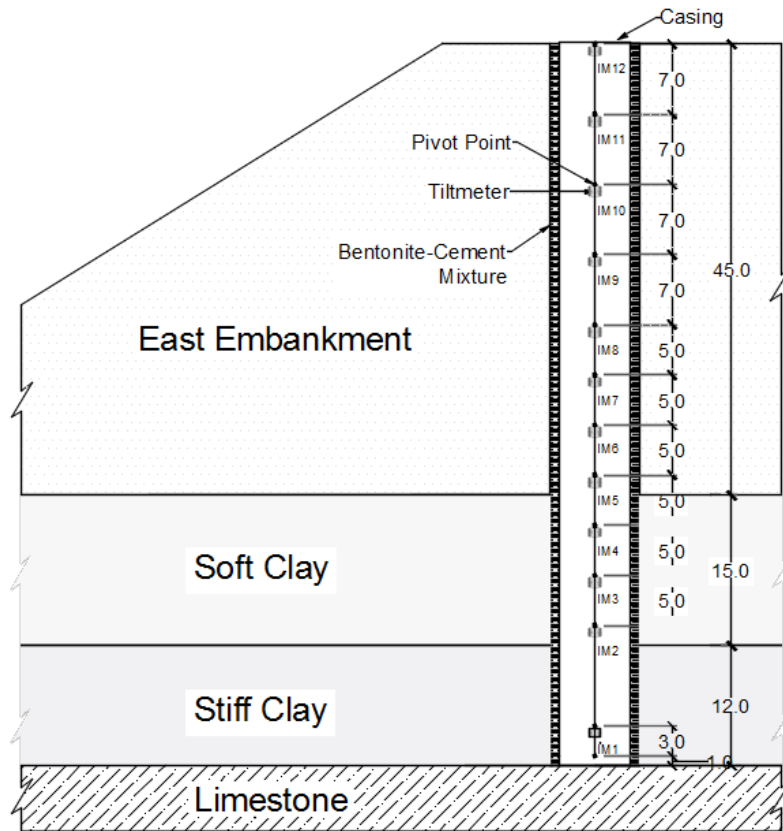


Figure 40. SH-3 bridges over BNSF railroad – tiltmeter locations within the eastern and western inclinometers (all dimensions are in feet)

2.2.3.1 Rotations of East Abutments before Repairs

The figures in this section show data trends for selected tiltmeters. A negative trend in the tiltmeter data indicates the abutment is tilting toward the approach slab and a positive trend indicates that the abutment is tilting toward the bridge deck. This applies to all of the tiltmeter data presented.

Figure 41 depicts TMA3 and TMA4 tiltmeter data installed on the east abutment backwall of the South Bridge. It can be seen that the trends in the tiltmeter data corresponds inversely with temperature trends. Similar trends can also be seen for the tiltmeter TMA1 and TMA2 on the east abutment backwall of the North Bridge (Figure 42). These tiltmeters indicate that the abutment back walls rotate toward the approach slab as the temperature increases and then rotate back toward the bridge deck as the temperature decreases. In both abutment backwalls, more tilt can be seen in the insides of the abutments (TMA2 and TMA3) than outsides (TMA1 and TMA4). This indicates that more forces are being transmitted through the insides of the abutments due to the interactions between the North and the South Bridge.

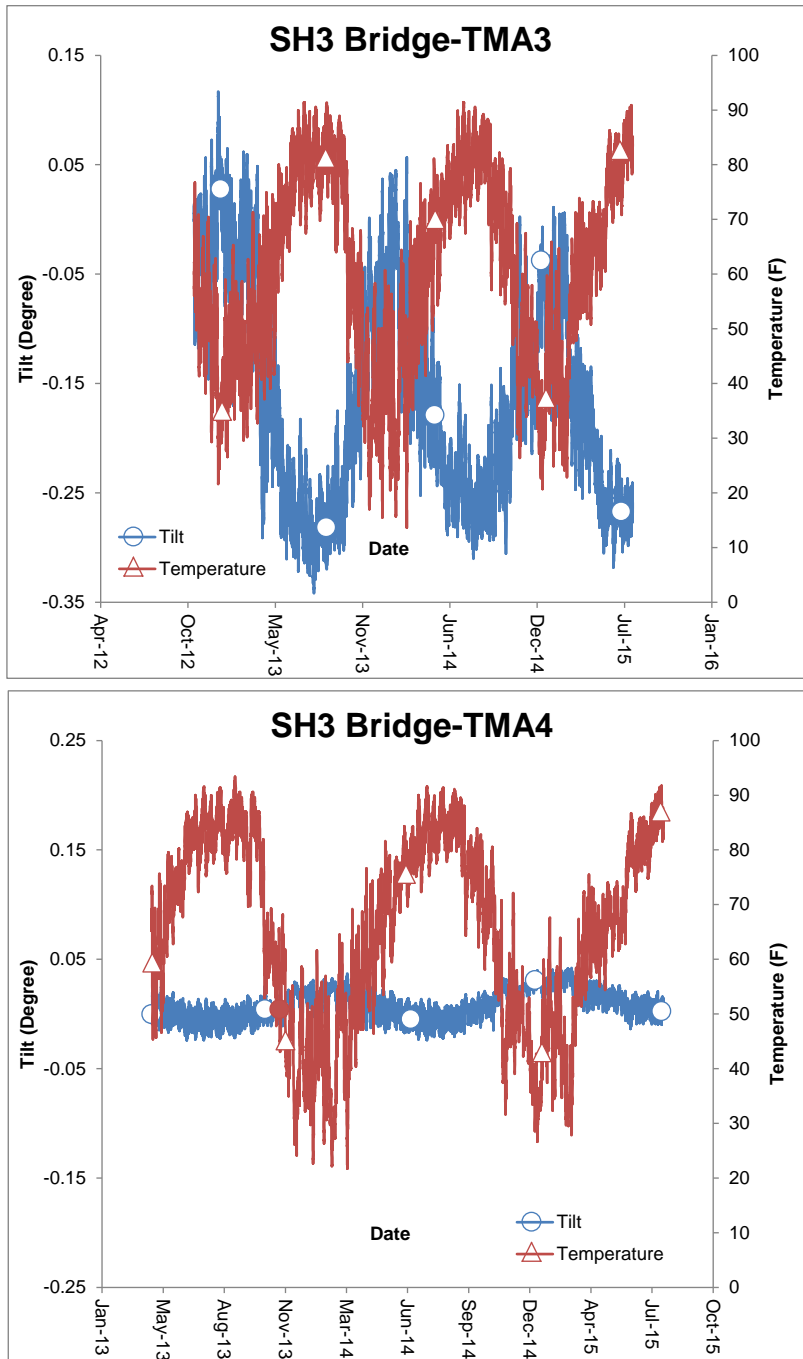
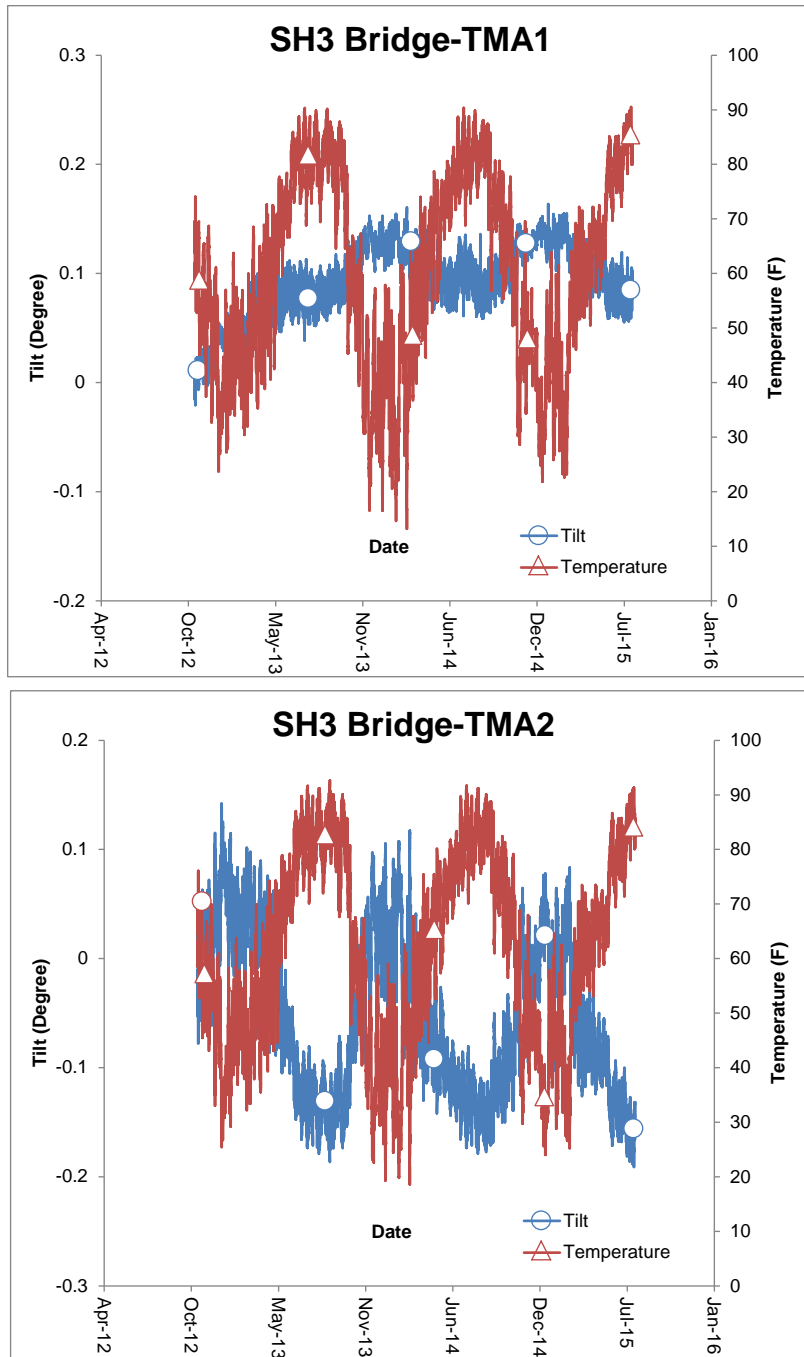


Figure 41. East abutment of SH-3 south bridge over BNSF railroad – TMA3 and TMA4 tiltmeter data before repairs



**Figure 42. East abutment of SH-3 north bridge over BNSF railroad – TMA1 and TMA2
tiltmeter data before repairs**

2.2.3.2 Displacement of the Bridge Deck Relative to the Abutment Wing Wall before Repairs

Crackmeters were attached to the bridge deck and the abutment wing wall of the North Bridge, across the construction joint, as shown in Figure 43. Figures 44 and 45, respectively, show the trends in displacements and temperatures for the crackmeters CMA1 and CMA2. As the temperature increases, the relative displacement between the bridge deck and the abutment wing wall increases and when the temperature decreases this displacement decreases.



Figure 43. East abutment of SH-3 north bridge over BNSF railroad – CMA2 crackmeter

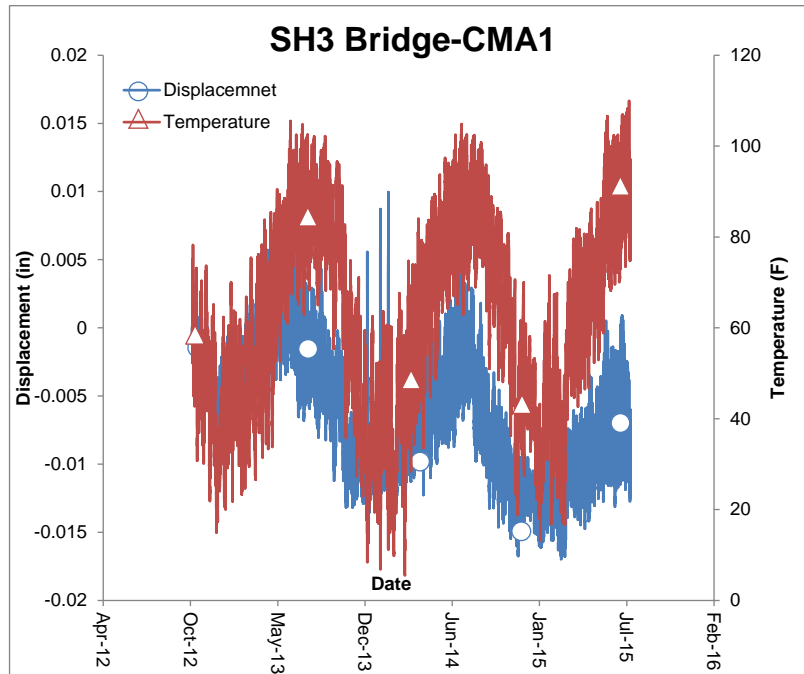


Figure 44. East abutment of SH-3 north bridge over BNSF railroad – CMA1 crackmeter data before repairs

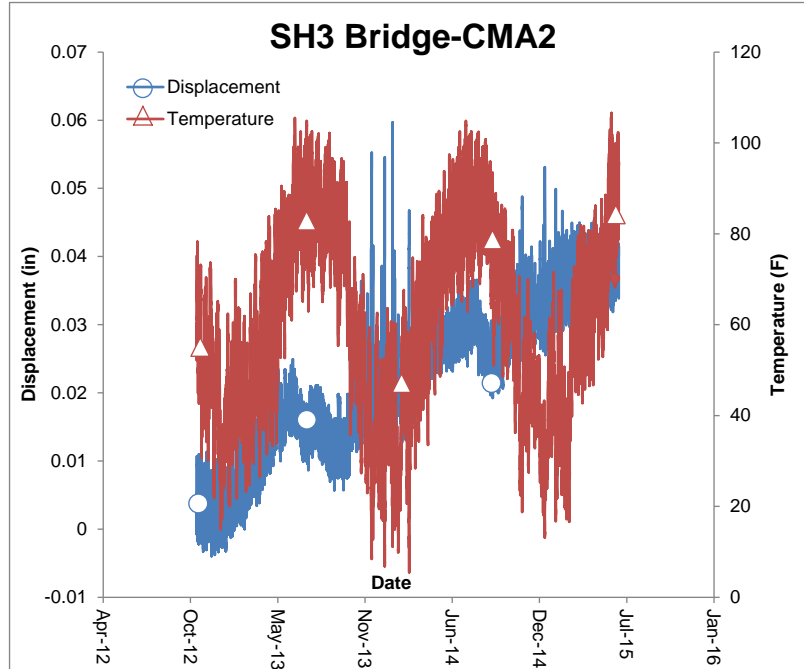


Figure 45. East abutment of SH-3 north bridge over BNSF railroad – CMA2 crackmeter data before repairs

2.2.3.3 Axial Strains – East Side before Repairs

Strain gages were installed with thermistors at eight different locations on the east and west sides of the North Bridge (see Figure 46). Figures 47 and 48, respectively, show strain and temperature trends for the strain gages NE_SG1 and NE_SG3 (located on the approach slab) and NE_SG2 and NE_SG4 (located under the bridge deck close to the abutment).

By looking at the seasonal trend for NE_SG1 and NE_SG3, it can be seen that, in general, when the temperature increases there is also an increase in axial strain and when the temperature decreases, the strain decreases. The opposite is true for NE_SG2 and NE_SG4; increasing temperatures cause a decrease in axial strains and vice versa.

These observed trends seem to indicate that while the approach slab is behaving as expected, that is, expanding as the temperature increases (likely away from the bridge) and contracting as the temperature decreases, the deck near the abutment is behaving in the opposite manner. As the temperature increases, the deck is compressing near the abutment due to the closed expansion joints and vice versa as shown in Figure 49.

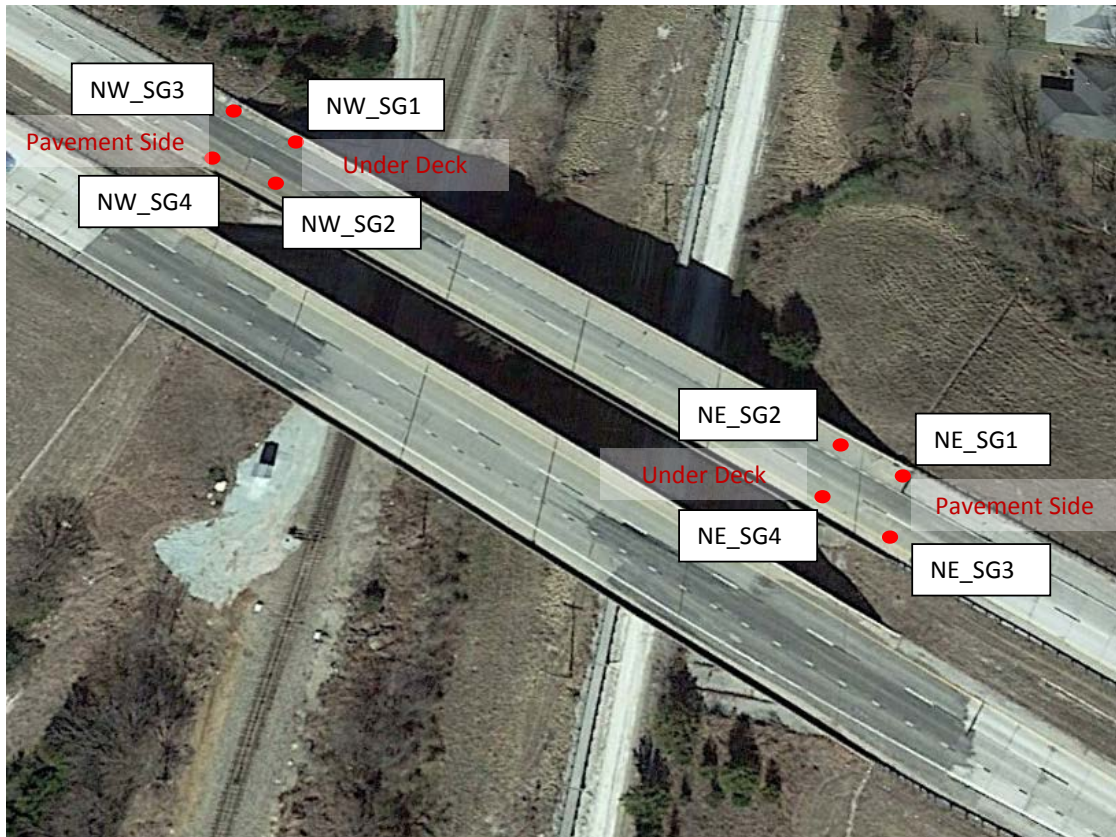


Figure 46. SH-3 bridges over BNSF railroad – strain gage locations

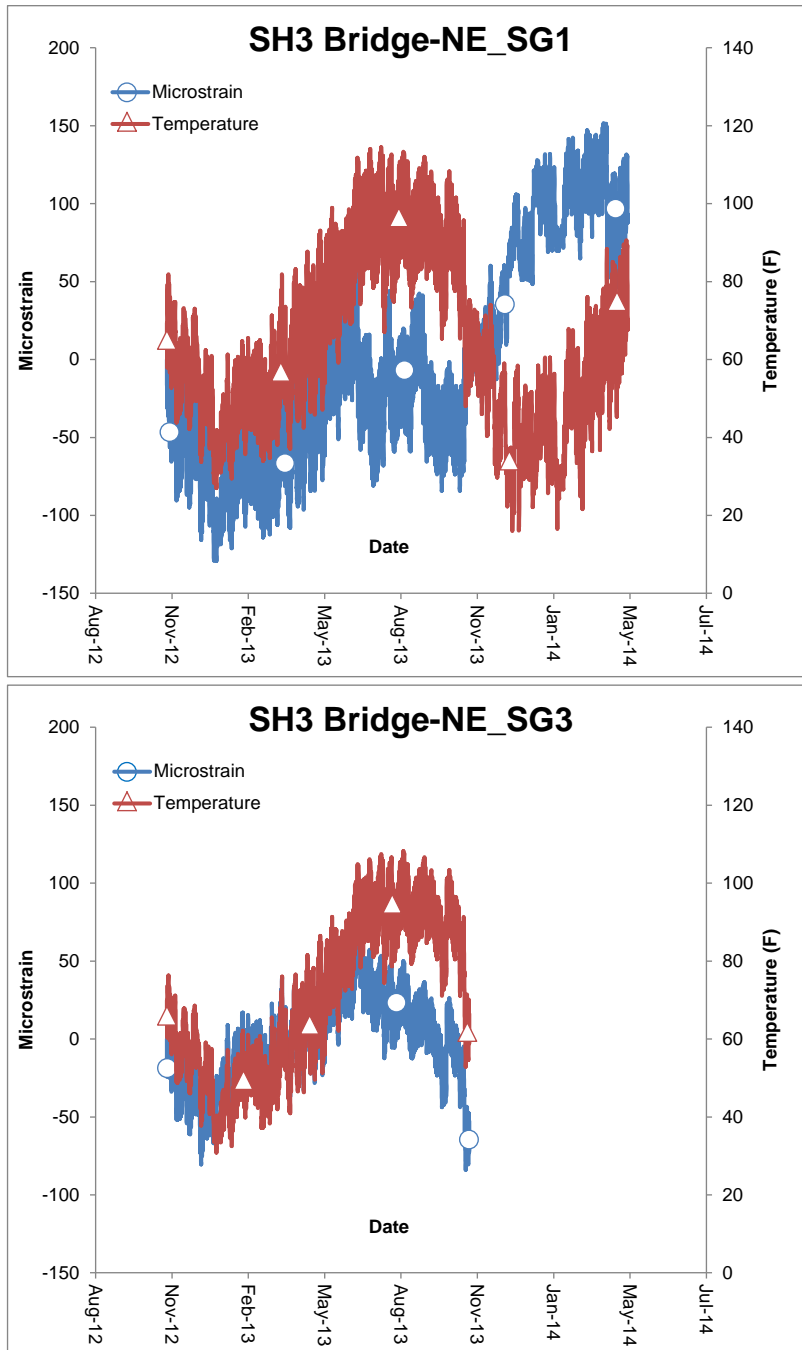


Figure 47. Eastern side of SH-3 north bridge over BNSF railroad – NE_SG1 and NE_SG3 strain gage data before repairs

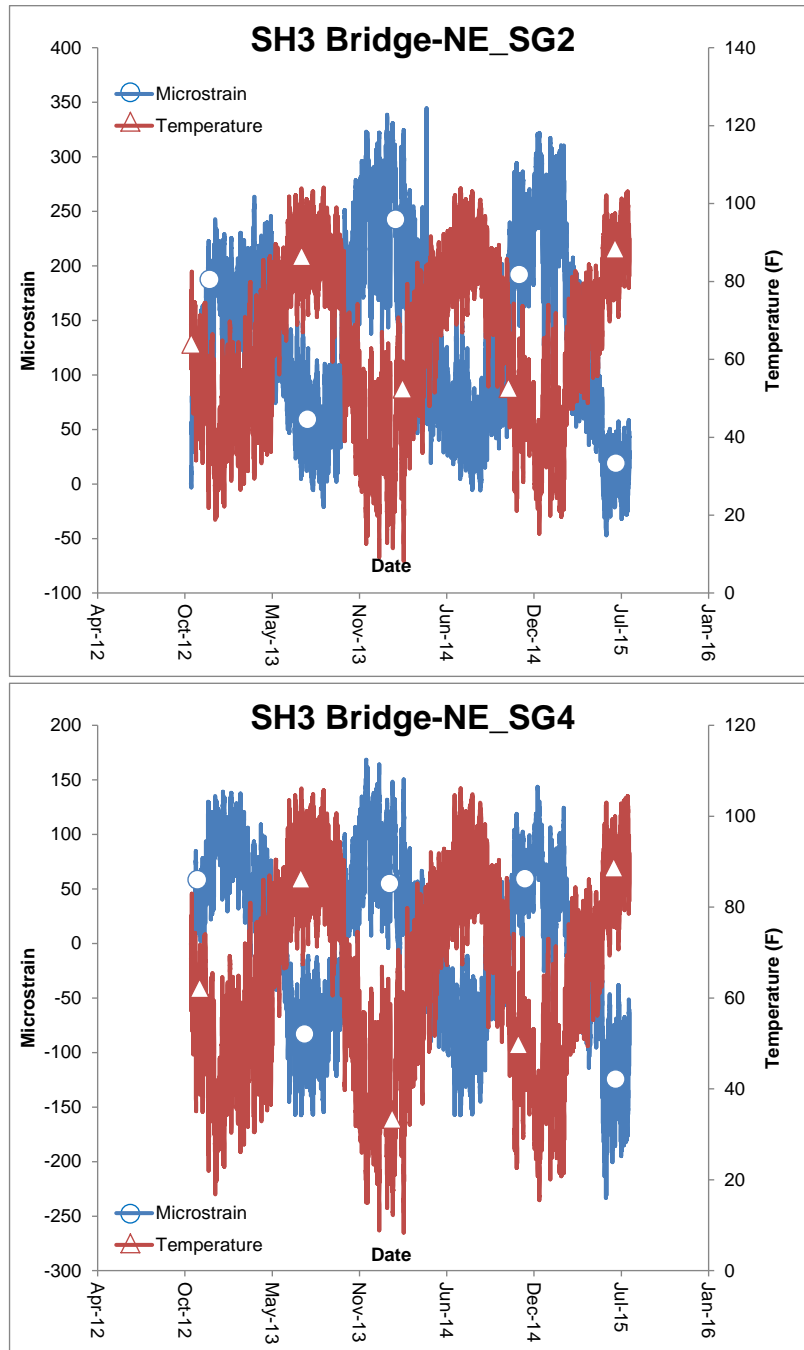


Figure 48. Eastern side of SH-3 north bridge over BNSF railroad – NE_SG2 and NE_SG4 strain gage data before repairs

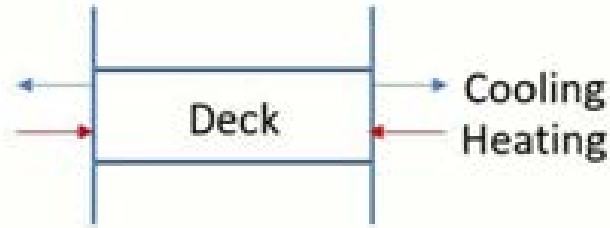


Figure 49. Stresses in the bridge deck near the abutments during heating and cooling due to closed expansion joints

2.2.3.4 Axial Strains – West Side before Repairs

Two strain gages and two thermistors were installed on the underside of the western deck of the North Bridge near the abutment. Two additional strain gages and two thermistors were also installed on north and south sides of the western approach pavement near the approach slab (see Figure 46). Data from NW_SG1 and NW_SG2 and corresponding thermistors, installed on the underside of the deck, are shown in Figure 50 and 51, respectively. Data from NW_SG3 and the corresponding thermistor, installed on the approach pavement, are shown in Figure 52. By looking at the trends in NW_SG3, it can be seen that when the temperature increases there is also an increase in axial strain and when the temperature decreases, the strain decreases. This means that the approach slab is expanding (likely away from the bridge) as the temperature increases and contracting as the temperature decreases. The opposite is true for NW_SG1 and NW_SG2 (more for NW_SG2 than NW_SG1). As the temperature increases, the deck is compressing near the abutments and expanding as the temperature decreases. This behavior is consistent with what was observed on the eastern side.

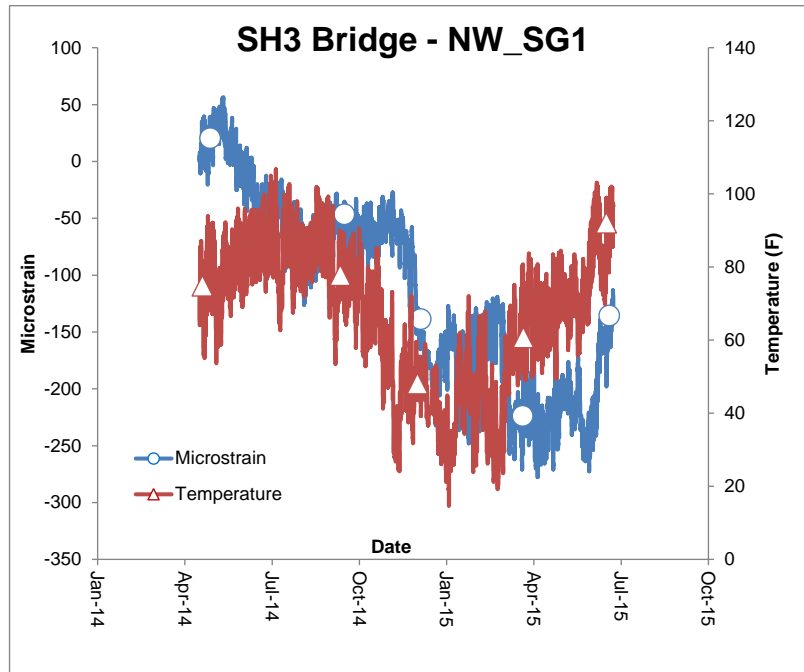


Figure 50. Western side of SH-3 north bridge over BNSF railroad – NW_SG1 data before repairs

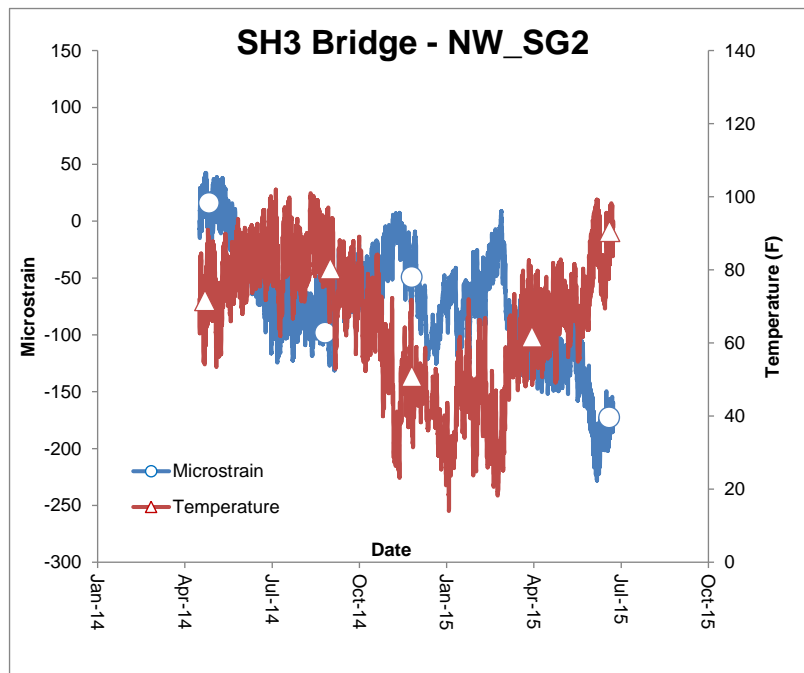


Figure 51. Western side of SH-3 north bridge over BNSF Railroad – NW_SG2 data before repairs

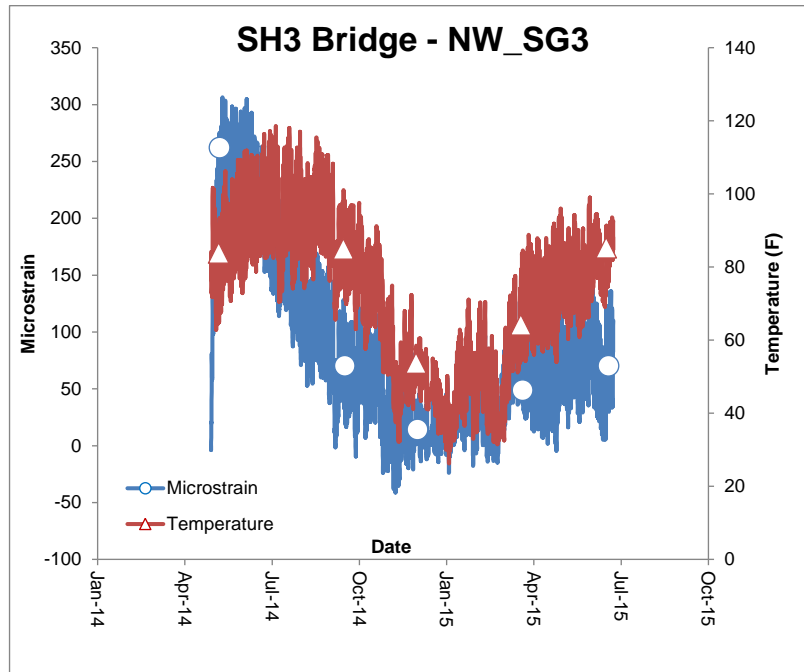


Figure 52. Western side of SH-3 north bridge over BNSF railroad – NW_SG3 data before repairs

2.2.3.5 Eastern Approach Embankment Displacements before Repairs

Selected inclinometer data are presented in Figures 53 and 54 (see Figure 39 for the locations). The deflection profile of the embankment on August 24, 2013 is shown in Figure 55. The data from the instruments indicate that the expansion joints are essentially closed and as the bridge heats the deck is pushing against the approach slab which in turn is transmitting these forces into the abutment and the approach embankment. As the bridge cools, the deck, abutment, and the embankment are all relaxing. While the trend in the measured inclinometer data is consistent with the above described behavior, the deflection magnitudes need further analyses and verification.

It is also believed that the lateral movements of the approach embankments on top of the underlying soft clay layer soon after the construction of the bridge caused the expansion joints to close. Very small east to west movement in the soft clay layer can still be seen in Figure 54 (note that positive deflection values imply movement from the approach pavement towards the middle of the bridge or east to west movement).

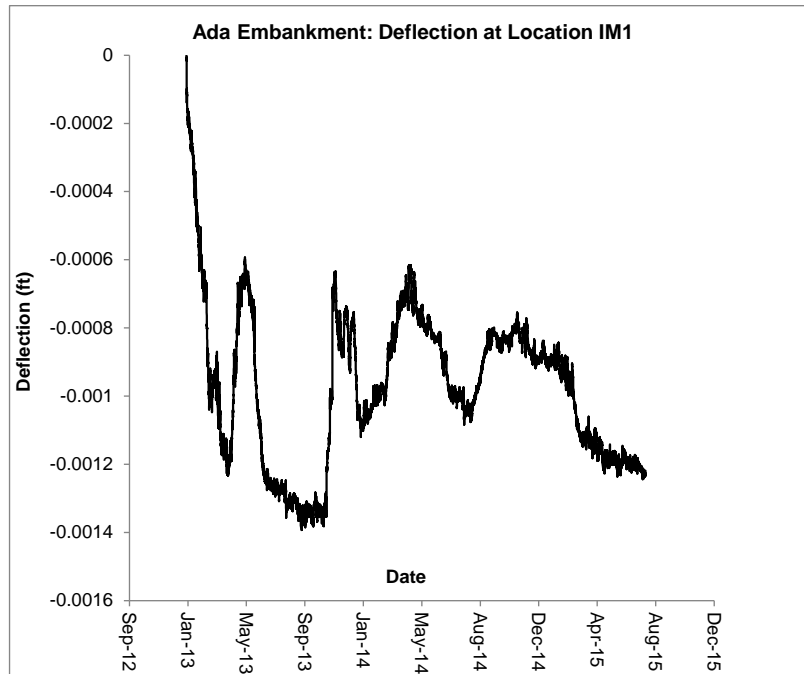


Figure 53. SH-3 bridges over BNSF railroad – eastern embankment deflection at location IM1

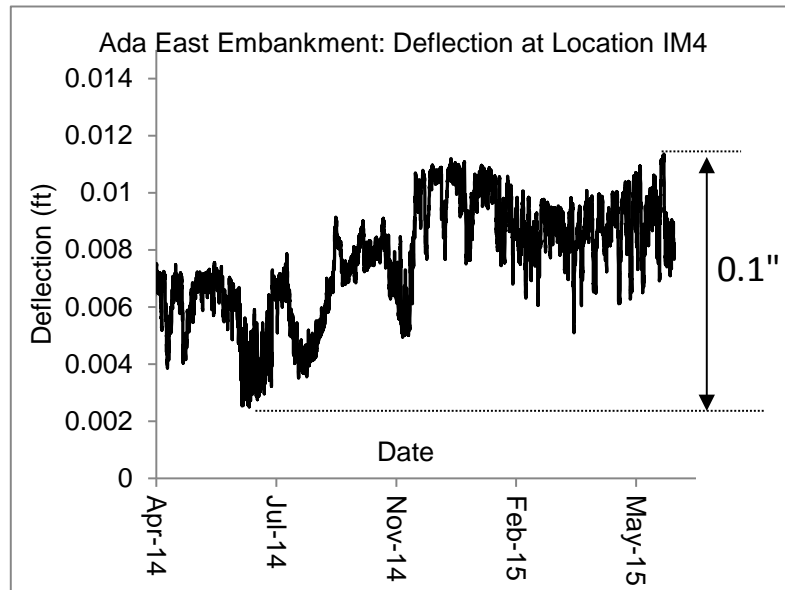


Figure 54. SH-3 bridges over BNSF railroad – eastern embankment deflection at location IM4

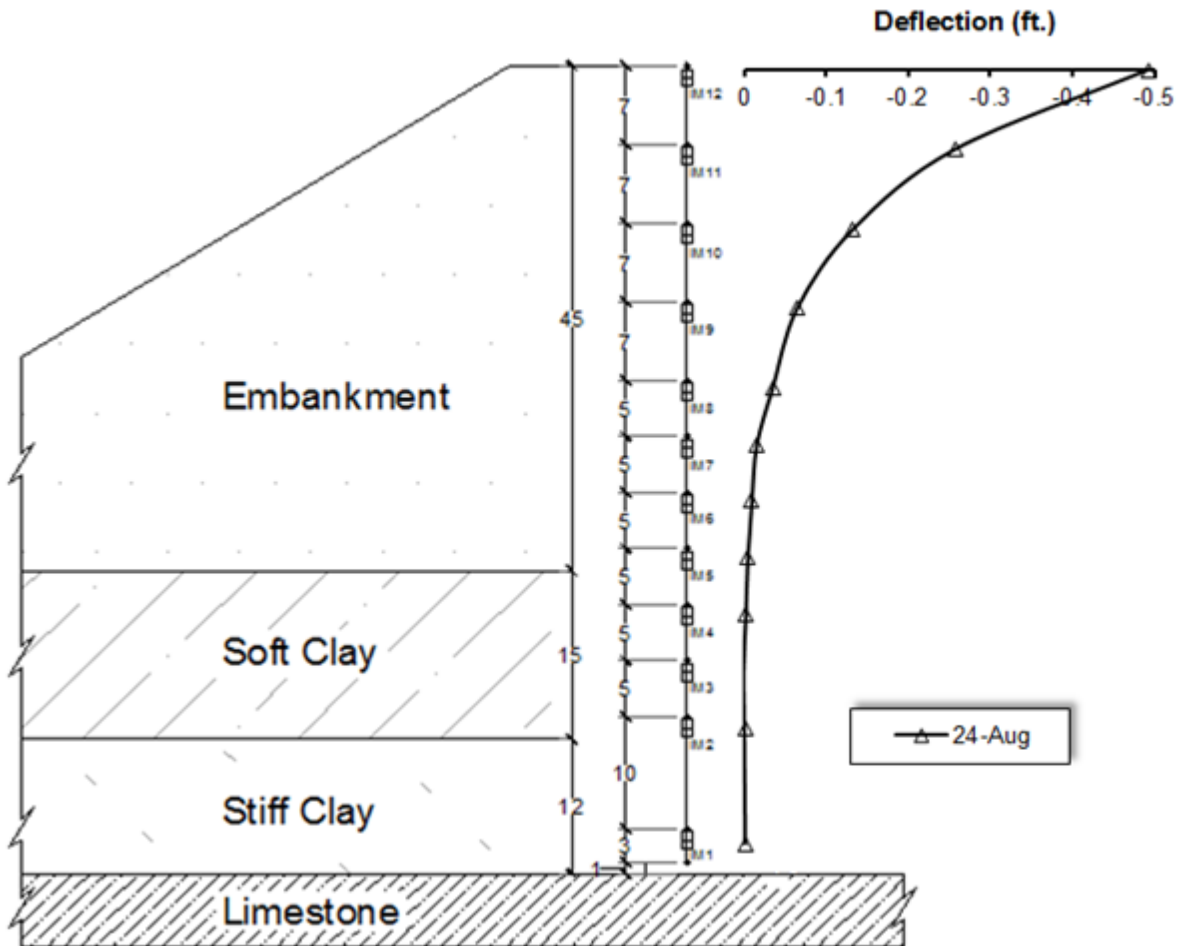


Figure 55. SH-3 bridges over BNSF railroad – eastern embankment deflection profile on August 24, 2013

2.2.3.6 Western Approach Embankment Displacements before Repairs

An inclinometer was installed within the western approach embankment on May 20, 2014 to investigate the similarities and differences in behavior between the eastern and western approach embankments (see Figure 39). The height of this inclinometer is about 40'. This inclinometer consisted of 7 tiltmeters joined by connecting steel tubes and connected to a different data acquisition system on the western abutment of the north bridge. Selected data are presented in Figures 56 - 61. Note that positive deflection values imply movement from the approach pavement towards the middle of the bridge or west to east movement. Both the eastern and western inclinometers had approximately same top elevations. In general, east to west movements on top of the both embankments were observed. During the monitoring period,

the maximum east to west movement of top of the western embankment was about 0.036 ft (0.4 in.). The daily variations of movements are on the order of 0.015 ft (0.18 in.). These movements are much more reasonable than what was observed on the eastside. Unfortunately, this inclinometer was damaged beyond repair, likely by a mower, on June 9, 2015.

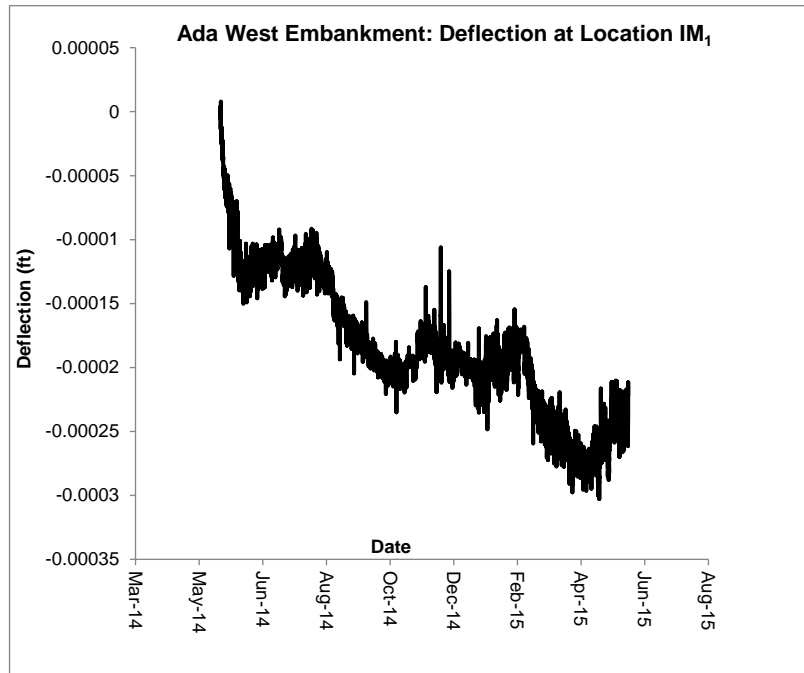


Figure 56. SH-3 bridges over BNSF railroad – western embankment deflection at location IM1

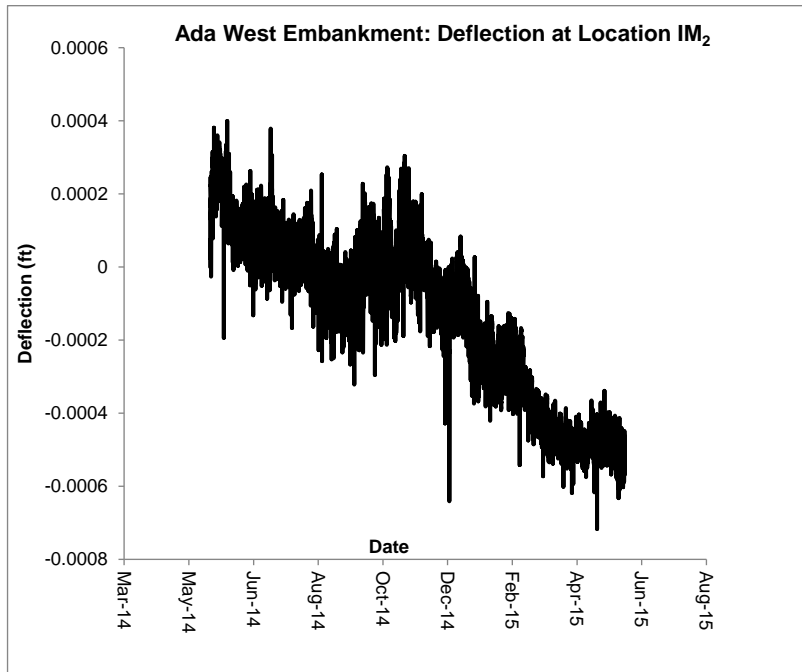


Figure 57. SH-3 bridges over BNSF railroad – western embankment deflection at location IM₂

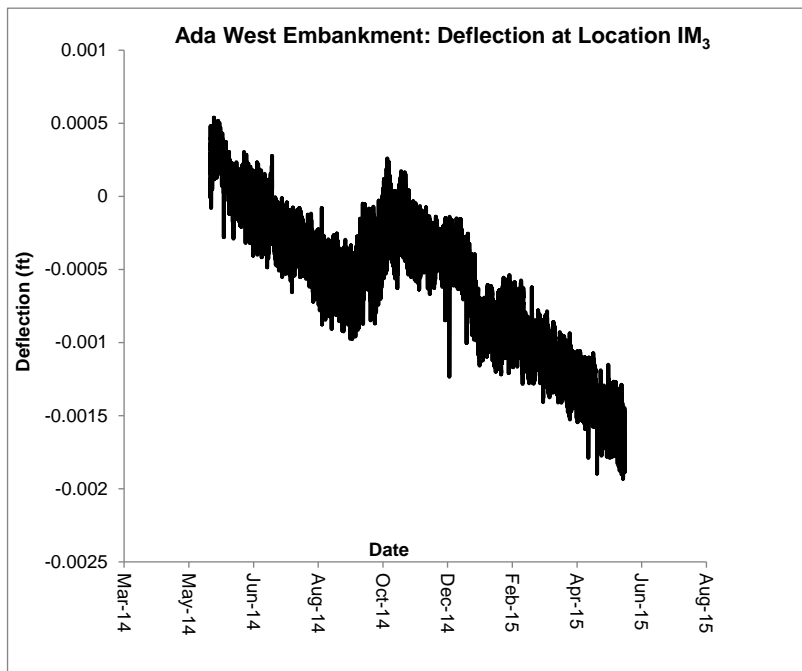


Figure 58. SH-3 bridges over BNSF railroad – western embankment deflection at location IM₃

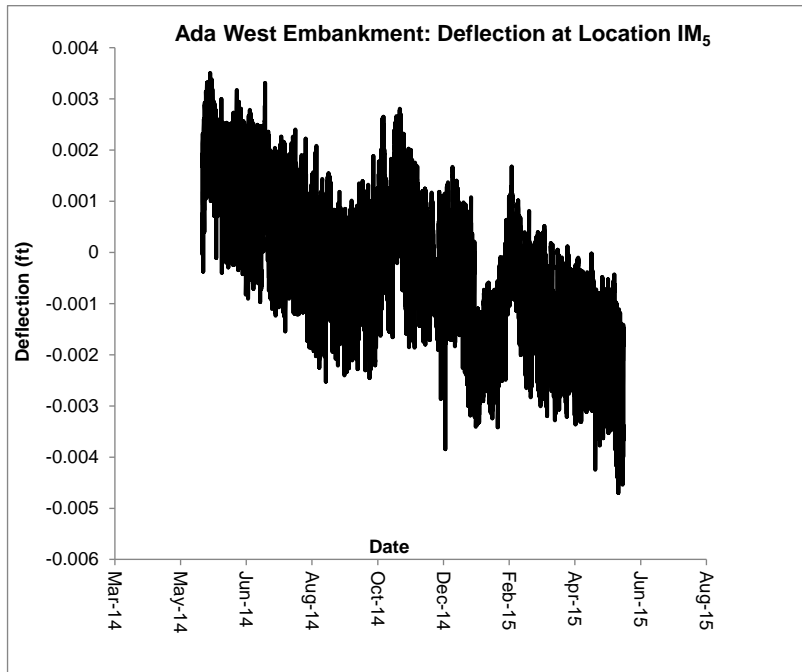


Figure 59. SH-3 bridges over BNSF railroad – western embankment deflection at location IM5

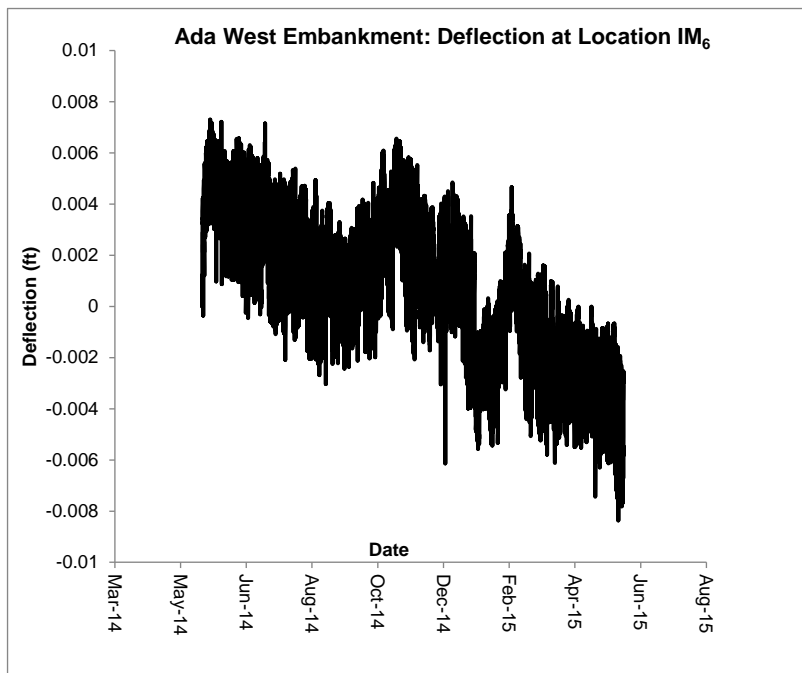


Figure 60. SH-3 bridges over BNSF railroad – western embankment deflection at location IM6

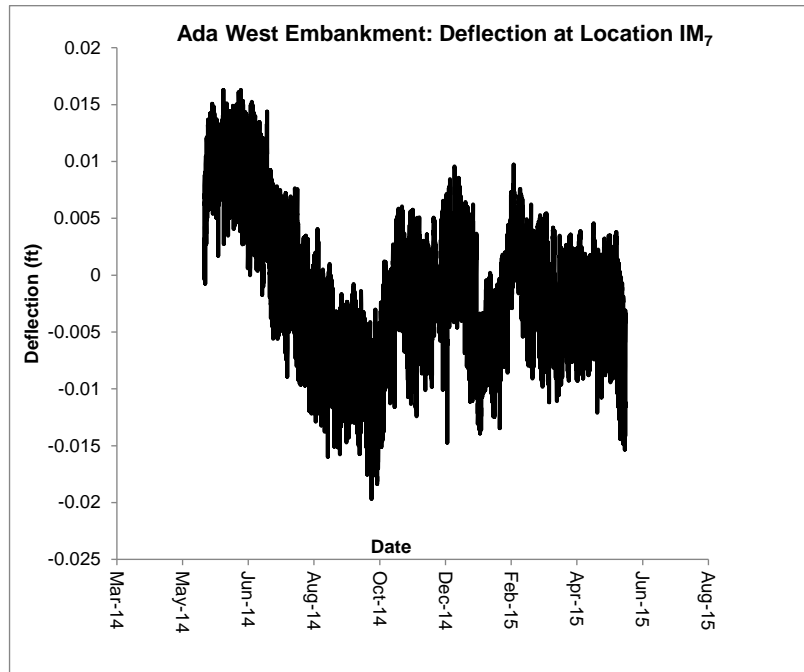


Figure 61. SH-3 bridges over BNSF railroad – western embankment deflection at location IM7

2.2.3.7 Tilting of Pier Caps before Repairs

In order to monitor the tilting of the piers before and after repairs a total of eight tiltmeters were installed on pier caps of the north bridge. Two tiltmeters were installed on each pier cap, one on the north side and the other on the south side. These tiltmeters were connected to the closest data acquisition system on the east or the west abutment. Instrumentation on Pier No. 4 is shown in Figure 62. Locations of pier cap instrumentation are given in Figure 63. All tiltmeter data and corresponding temperature data are presented in Figures 64 and 65. There was generally an opposite trend between tilt and temperature variations. When the temperature increased, expanding girders pushed on the fixed ends (see Figure 63). These forces caused the tilting of the piers. This is why the daily variations of tilt were lot smaller at Pier No. 1 on top of which the girders were allowed to expand on both sides. When the temperature increased, all the piers were tilting toward Abutment No. 2 (eastern abutment), except Pier No. 1. A decrease in temperature caused a tilt away from Abutment No. 2.



Figure 62 Pier cap instrumentation on Pier No. 4 of the SH-3 north bridge

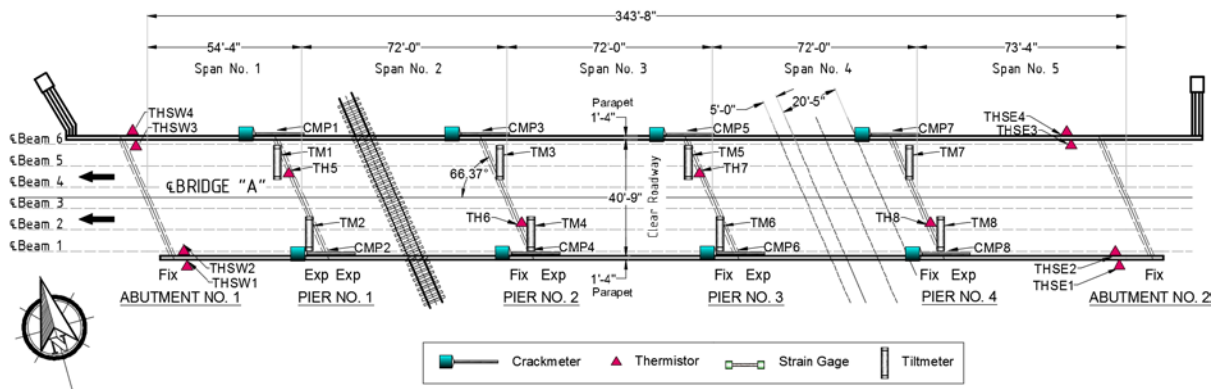


Figure 63. Locations of pier cap and road surface instrumentation on SH-3 north bridge

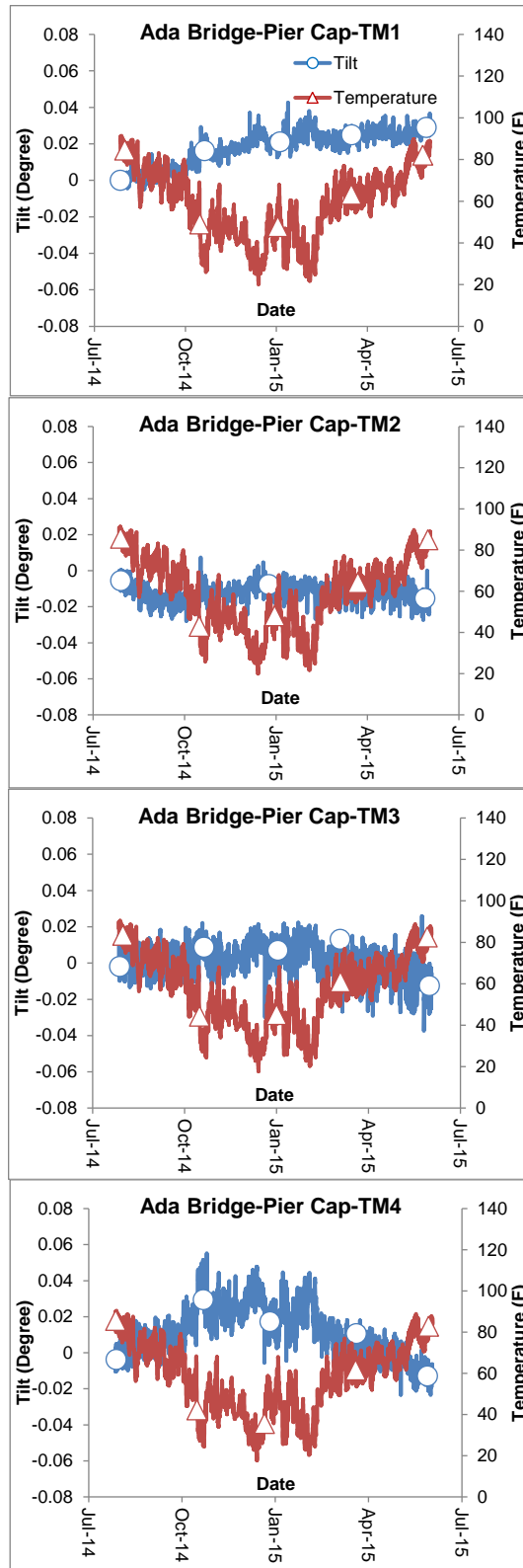


Figure 64. SH-3 north bridge over BNSF railroad – pier cap tiltmeter TM1-4 data before repairs

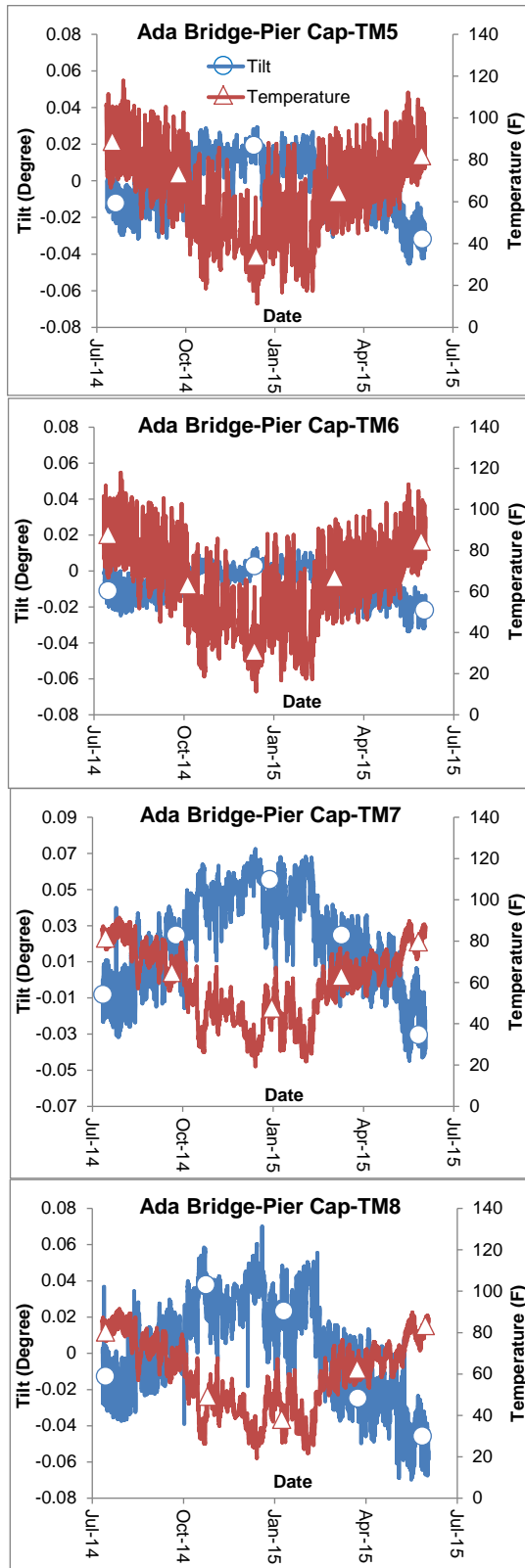


Figure 65. SH-3 north bridge over BNSF railroad – pier cap tiltmeter TM5-8 data before repairs

2.2.3.8 Movements around Expansion Joints before Repairs

A total of eight crackmeters (2 per expansion joint) were installed on the parapet walls across the expansion joints of the north bridge on February 19, 2015 to directly measure the movements of the expansion joints before and after the repairs. The locations of these crackmeters (CMP1-8) are shown in Figure 63.

Expansion joint movements along with temperature variations for the western and eastern sections of the north bridge are shown in Figures 66 and 67, respectively. Based on the recorded data during the monitoring period, temperature varied between 15° F and 105° F. Measured displacements during this period were between 0.06"-0.23". However, the estimated displacement was 0.51" indicating that most of the expansion joints were practically locked before the repairs.

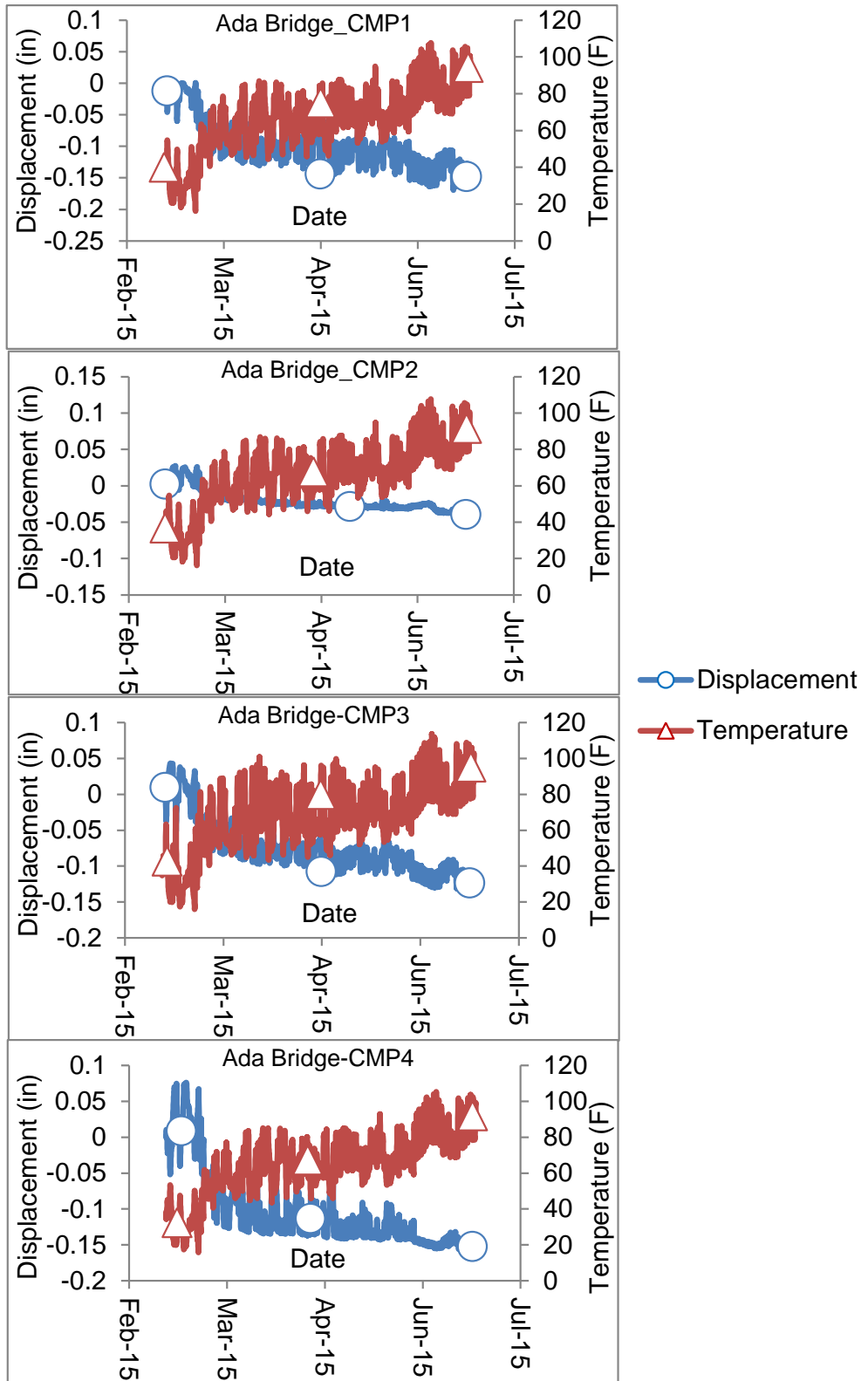


Figure 66. Expansion joints of SH-3 north bridge over BNSF Railroad - CMP1-4 crackmeter data before repairs

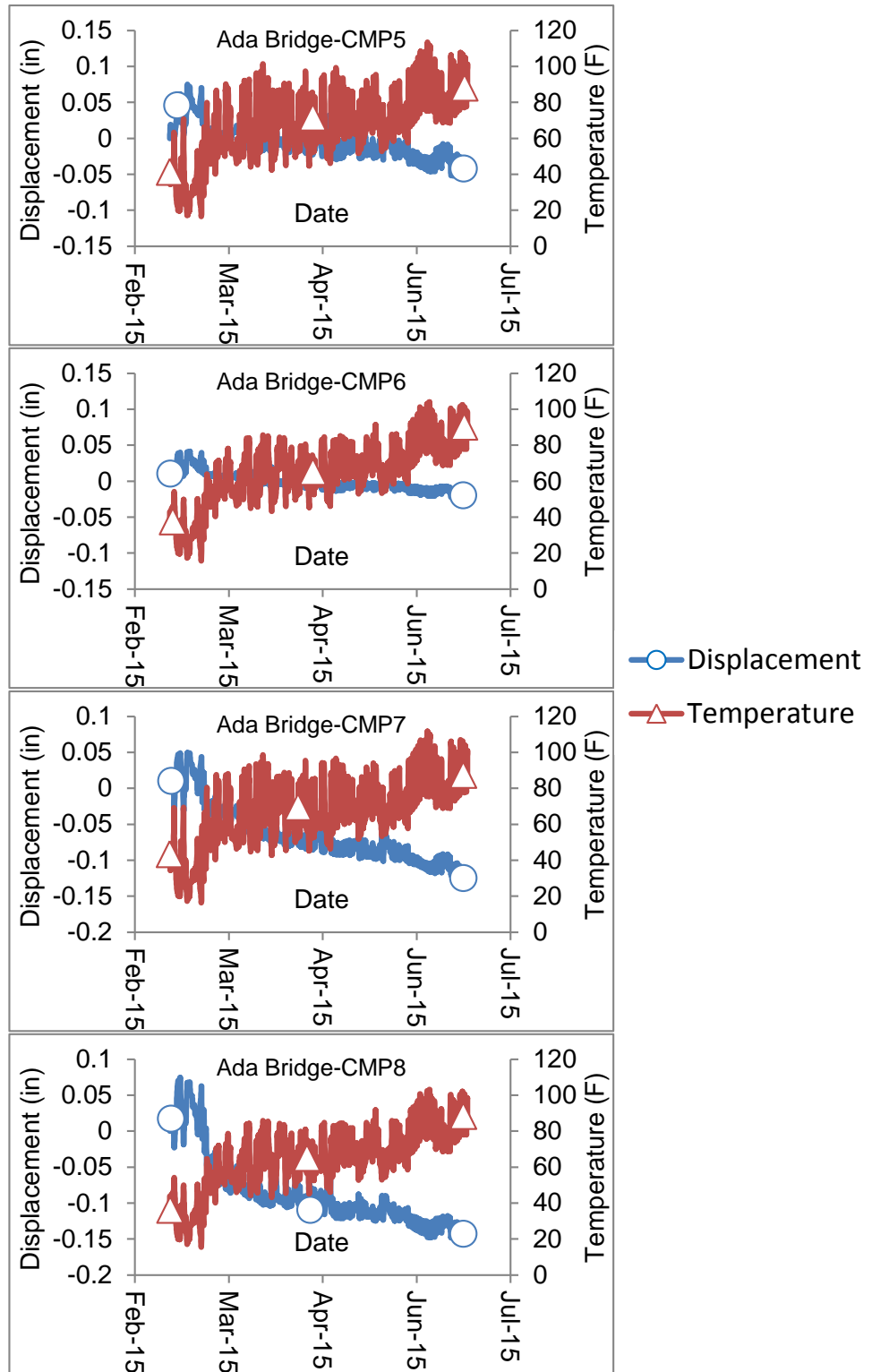


Figure 67. Expansion joints of SH-3 north bridge over BNSF railroad - CMP5-8 crackmeter data before repairs

2.2.4. The SH-3 North Bridge over BNSF Railroad after Repairs

The repairs to SH-3 north bridge, as shown in Figure 68, were done from August 2015 to January 2016. Two new sealed expansion joints were constructed at Piers No.1 and No.4. The design details of these expansion joints are given in Figure 69. The existing expansion joints at Piers No. 2 and No. 3 were eliminated and construction joints were created at these locations. The design details of these construction joints are given in Figure 70. The construction joints at the abutments were also rehabilitated. The design details of the rehabilitated construction joints at the abutments are given in Figure 71. In addition, several bearing assemblies and beam pedestals were repaired.

All the instruments, except the tiltmeter TM6 on the Pier Cap 3, were reinstalled. Data collection on both east and west sides restarted in February 2016. Data collected after the repairs are presented here and compared to data collected before the repairs to evaluate the effectiveness of the repairs. Same time intervals from 2014 and 2016 are selected to compare the data before and after the repairs.

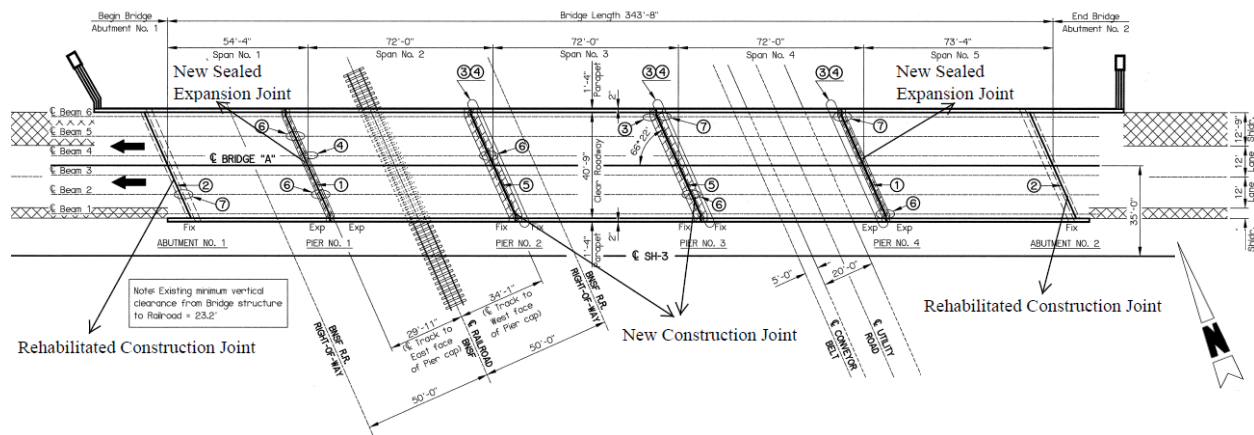


Figure 68. Repair details for SH-3 north bridge over BNSF railroad

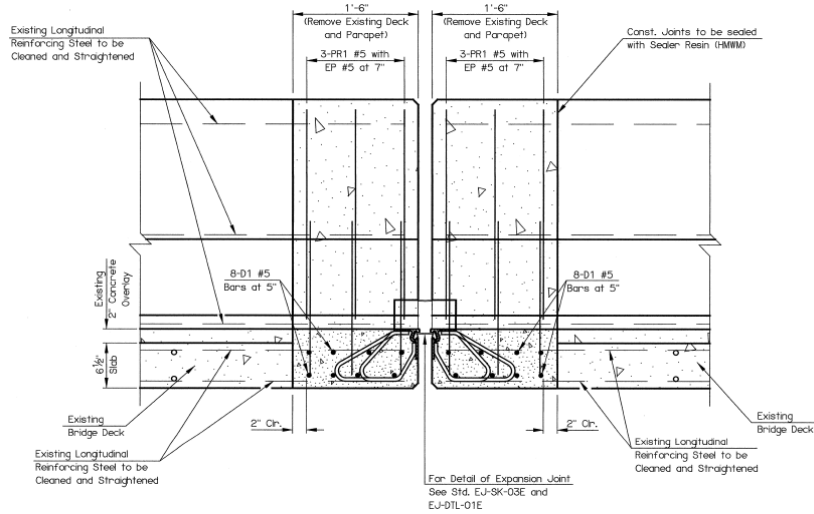


Figure 69. Details of the new sealed expansion joints at Pier No. 1 and Pier No. 4 for SH-3 north bridge over BNSF railroad

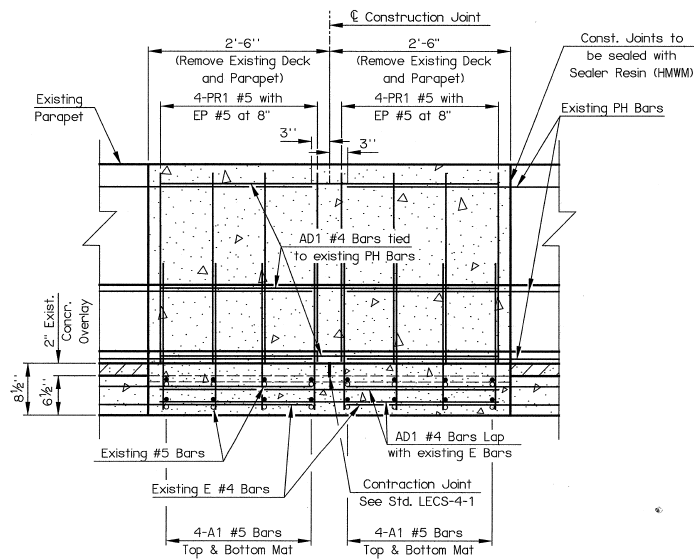


Figure 70. Details of new construction joints at Pier No. 2 and Pier No. 3 for SH-3 north bridge over BNSF railroad

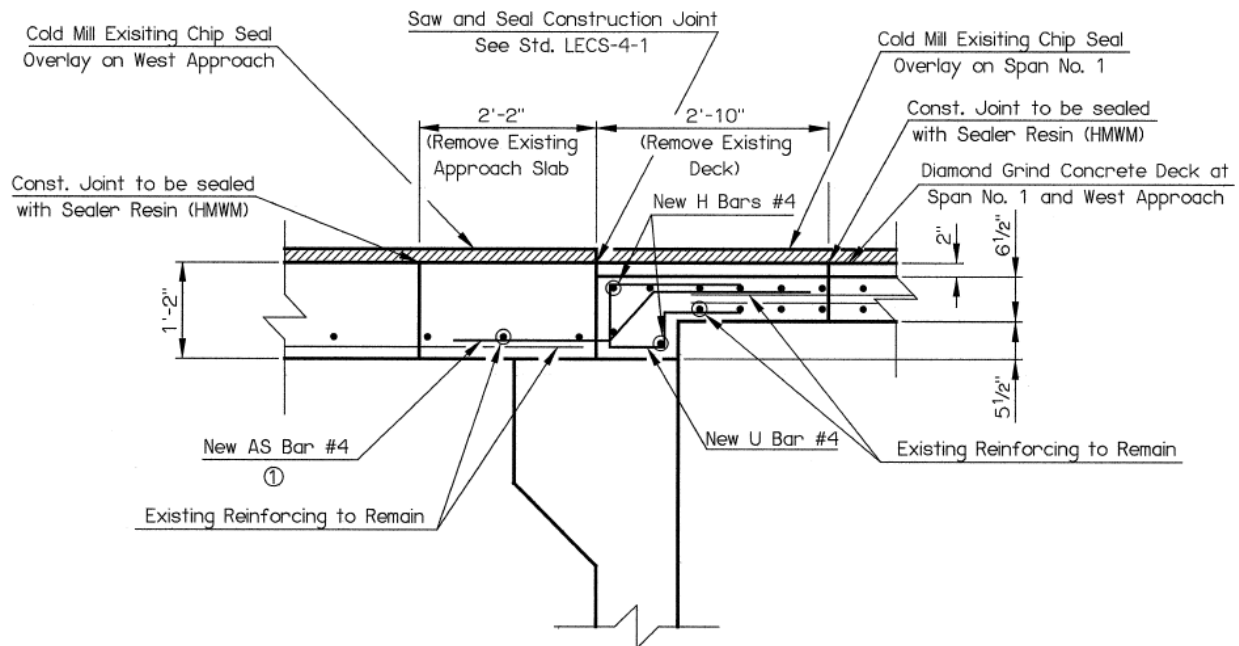


Figure 71. Details of rehabilitated construction joints at abutments for SH-3 north bridge over BNSF railroad

2.2.4.1 Rotations of the East Abutment after Repairs

Data from tiltmeters TMA1 and TMA2 installed on the east abutment backwall (see Figure 38) of the north bridge before and after repairs are compared in Figure 72. While the trends are similar before and after the repairs, significantly more tilt is being recorded on TMA2 than TMA1 after the repairs. It appears that the new expansion joint at Pier No. 4 has isolated the eastern most portion of the deck and now the skew of the bridge is causing more tilt of the abutment backwall on the south side.

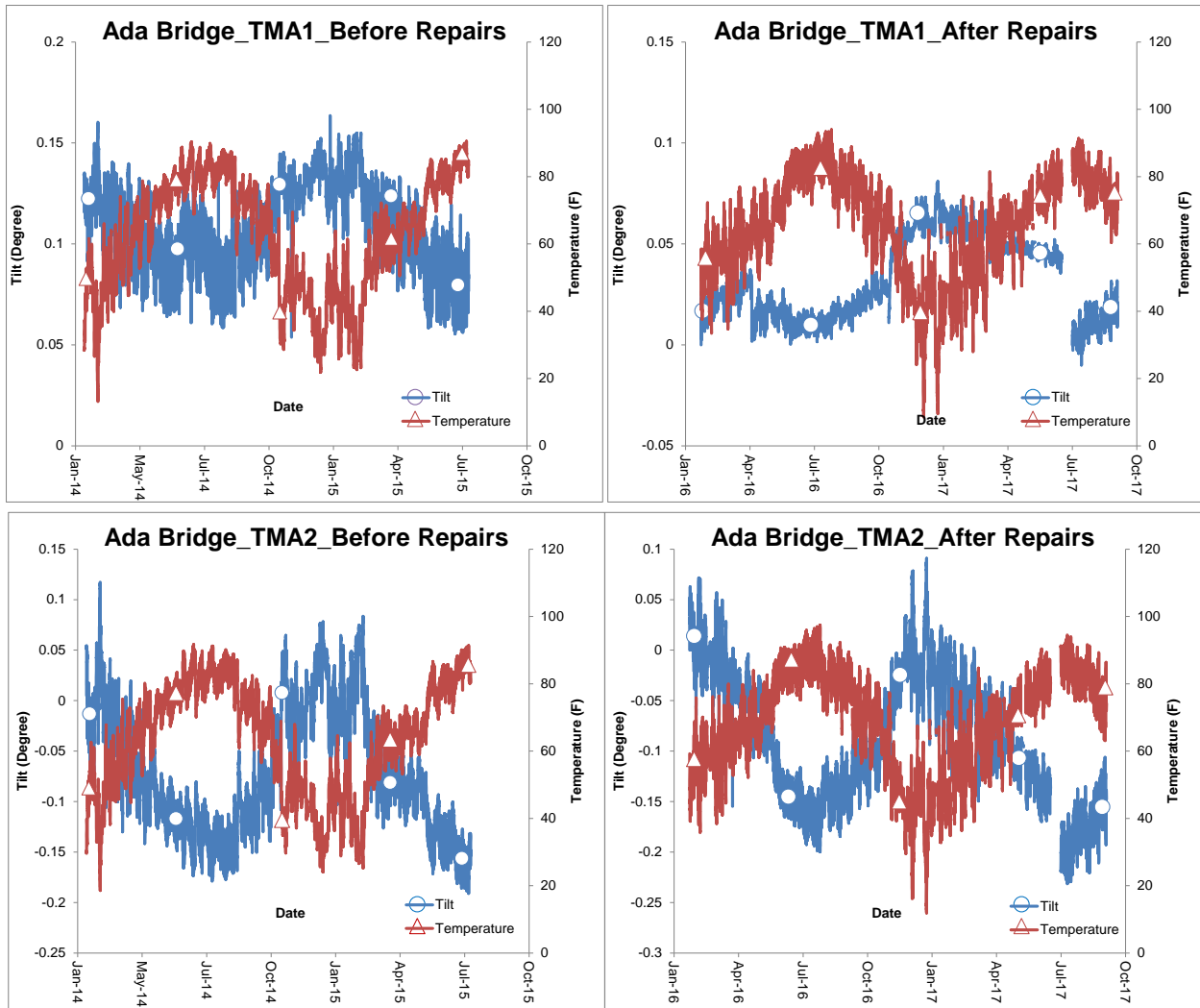


Figure 72. East abutment of SH-3 north bridge over BNSF Railroad – Comparisons of TMA1 and TMA2 tiltmeter data before and after repairs

2.2.4.2 Displacement of the Bridge Deck Relative to the Abutment Wing Wall after Repairs

Figures 73 and 74 show the trends in displacements and temperatures for the crackmeters CMA1 and CMA2 (Figure 38). In general, the opposite trends in displacements and temperatures can be observed before and after the repairs for CMA1. When the temperature increases there is a decrease in the relative displacement between the bridge deck and the abutment wing wall and when the temperature decreases, the displacements increase. For CMA2, similar trends in displacements and temperatures can be observed before and after the repairs. Substantially more daily variations in displacements can be seen

after the repairs for CMA1 and CMA2, especially when the cooling trend starts in July/August 2016. This likely means that there is additional room at Pier No. 4 for expansion and contraction of the bridge deck to occur. The results seem to indicate that the new expansion joint at Pier No. 4 is working as intended.

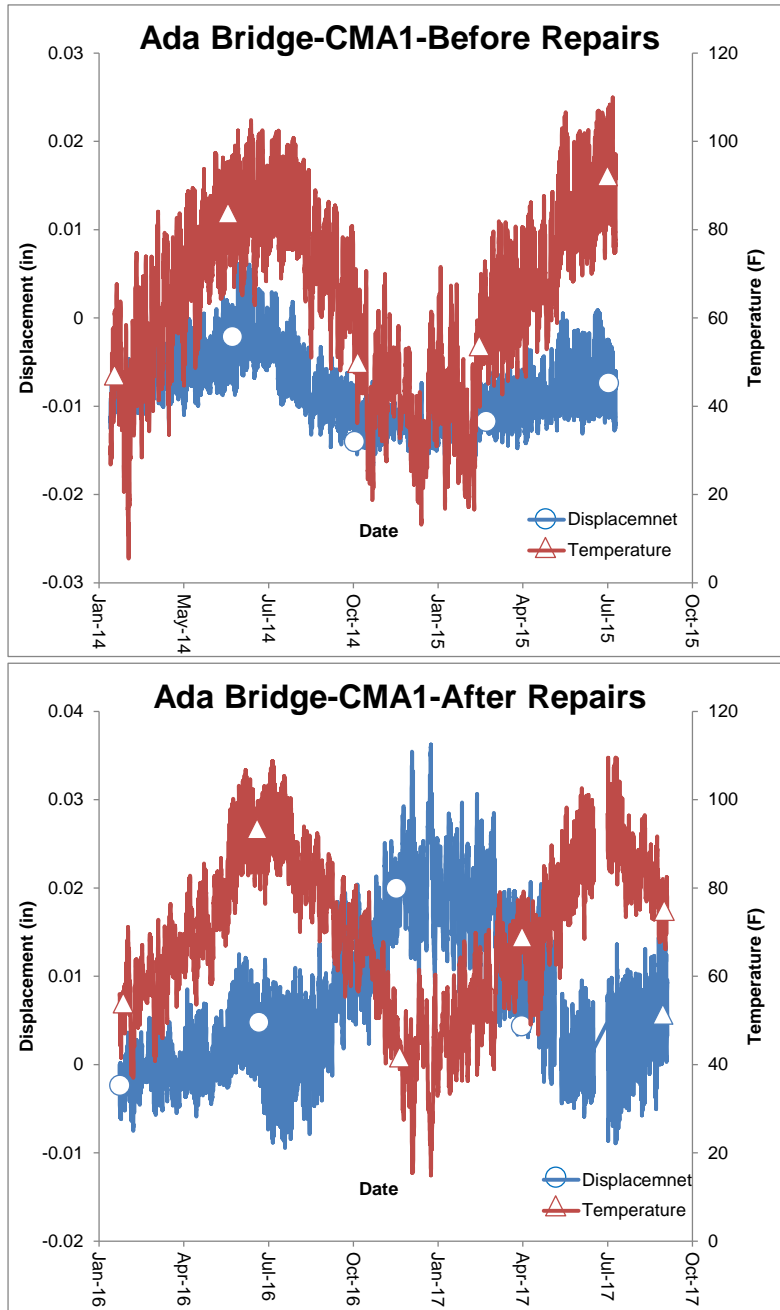


Figure 73. East abutment of SH-3 north bridge over BNSF railroad – comparison of CMA1 crackmeter data before and after repairs

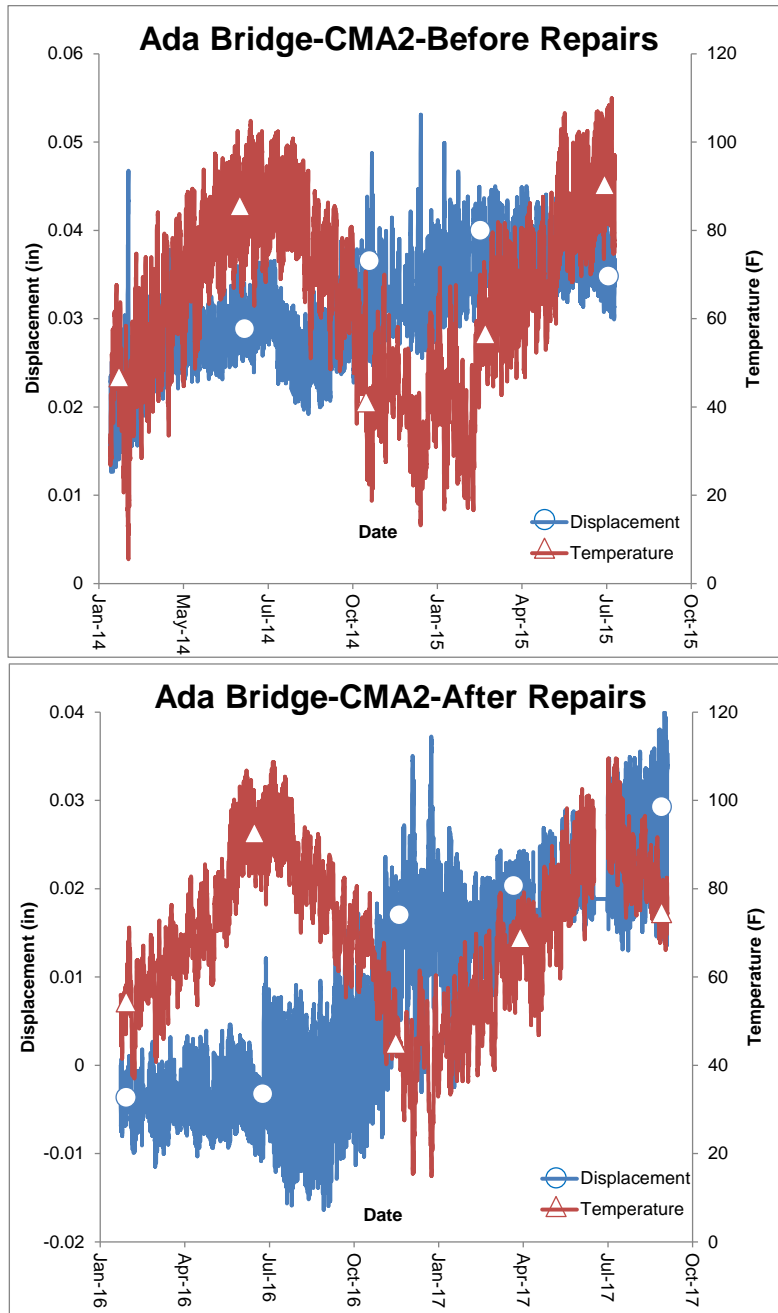


Figure 74. East abutment of SH-3 north bridge over BNSF railroad – Comparison of CMA2 crackmeter data before and after repairs

2.2.4.3 Axial Strains – Eastern Side after Repairs

Figures 75 and 76 show strain and temperature trends for the strain gages NE_SG1 and NE_SG2 (Figure 38) before and after repairs. The trends in axial strains at NE_SG1 (approach

pavement) and NE_SG2 (under the deck) are similar before and after repairs, i.e., increasing temperatures cause an increase in axial strains at NE_SG1 and a decrease in axial strains at NE_SG2. Smaller strains at NE_SG1 and at NE_SG2 are recorded after the repairs. These observations indicate that the eastern most portion of the deck is now freely expanding and contracting into the new expansion joint at Pier No. 4.

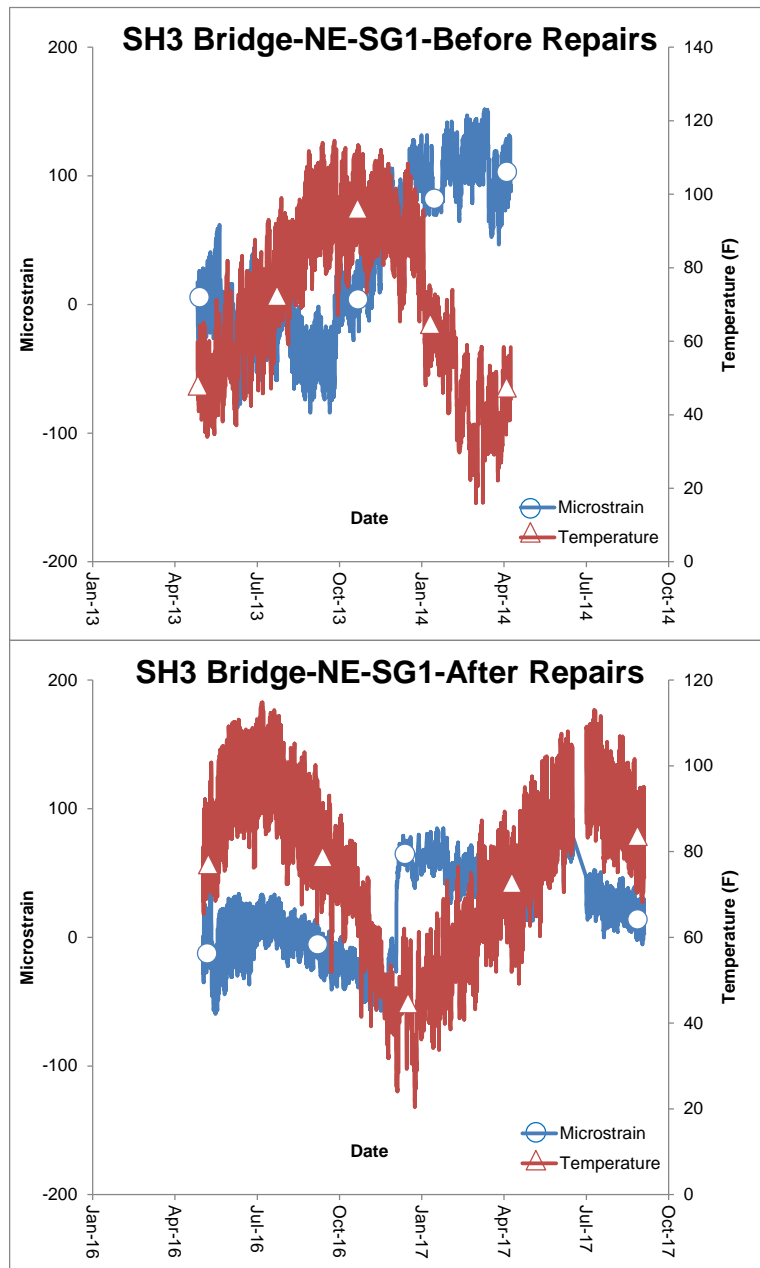


Figure 75. Eastern side of SH-3 north bridge over BNSF railroad – comparison of NE_SG1 strain gage data before and after repairs

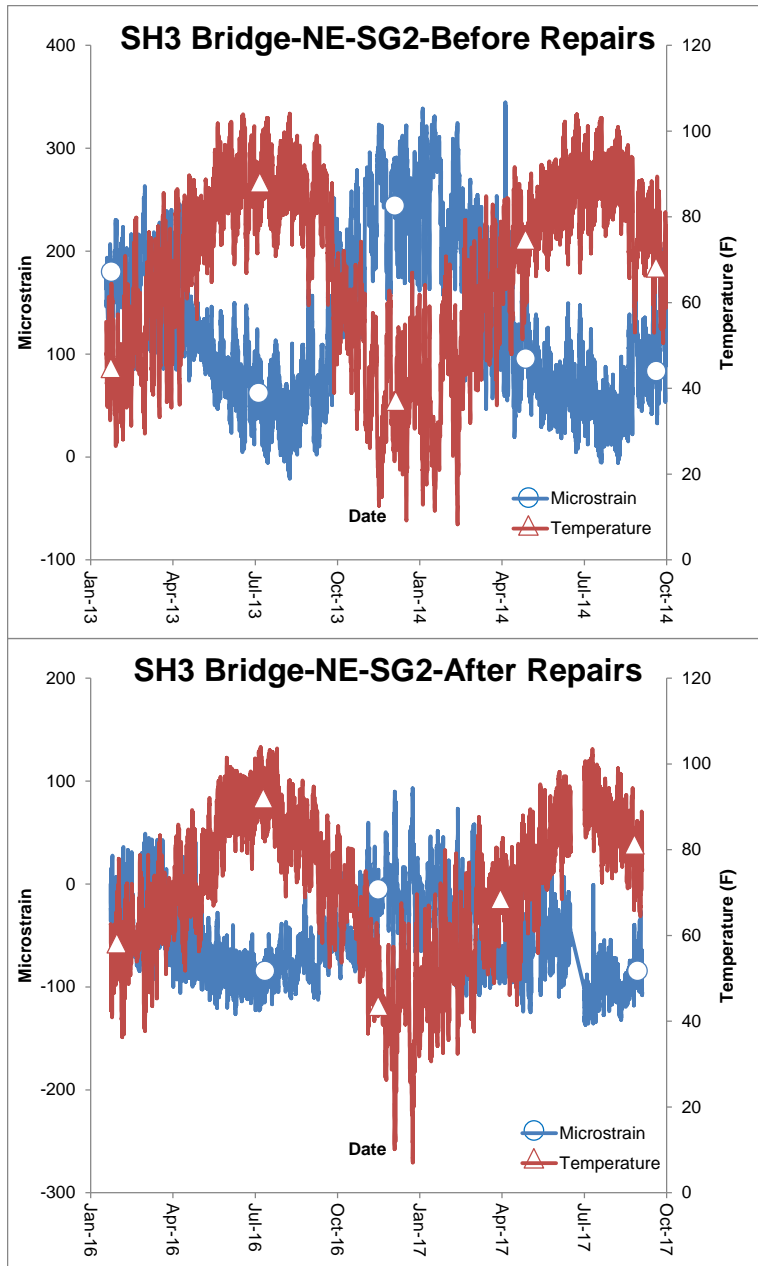


Figure 76. Eastern side of SH-3 north bridge over BNSF railroad – comparison of NE_SG2 strain gage data before and after repairs

2.2.4.4 Axial Strains – Western Side after Repairs

Data from NW_SG1, NW_SG2 and NW_SG3 and corresponding thermistors on the western side of the north bridge before and after repairs are shown in Figure 77, 78 and 79, respectively. NW_SG3, installed on the approach pavement, shows somewhat smaller

strains after the repairs. Smaller strains are also recorded in NW_SG1 and NW_SG2 installed underneath the deck after the repairs. These observations indicate that the western most portion of the deck is now freely expanding and contracting into the new expansion joint at Pier No. 1.

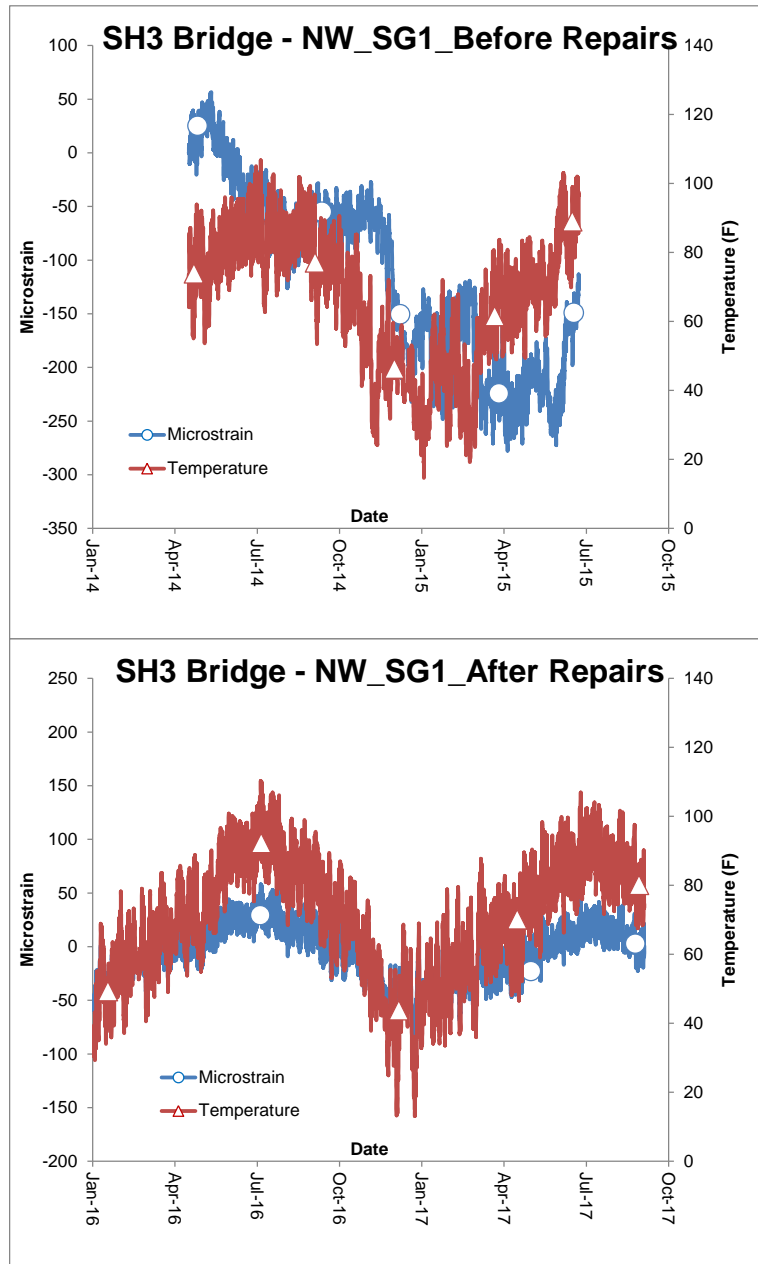


Figure 77. Western side of the SH-3 north bridge over BNSF railroad – Comparison of NW_SG1 data before and after repairs

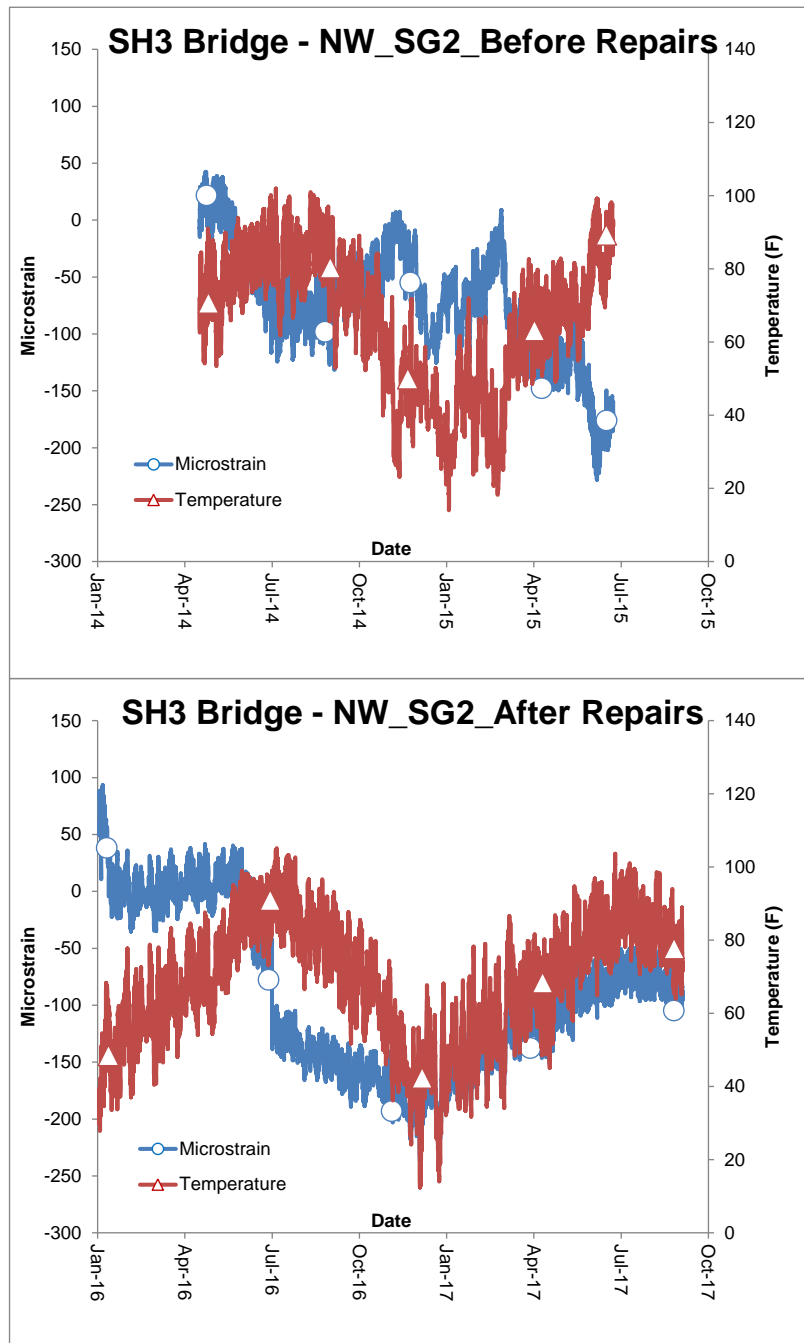


Figure 78. Western side of the SH-3 north bridge over BNSF railroad – comparison of NW_SG2 data before and after repairs

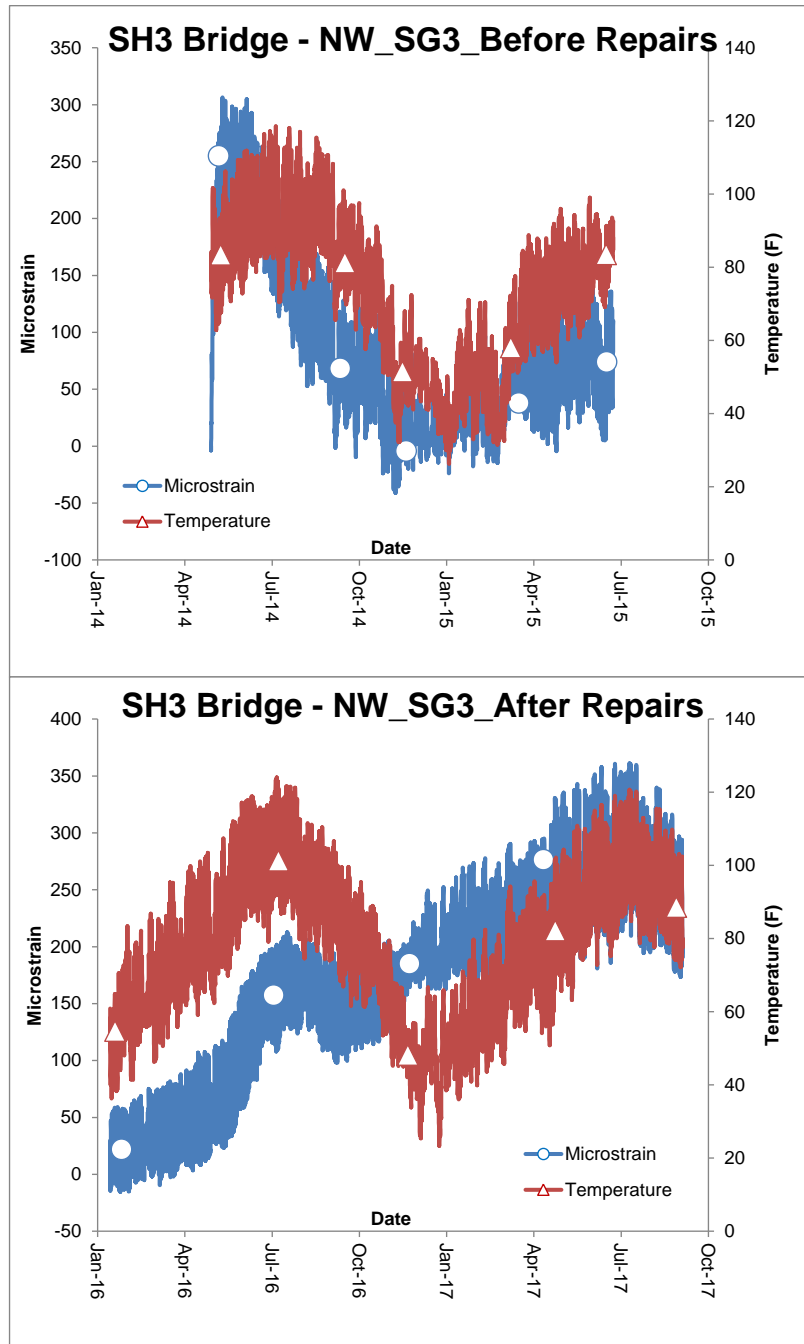


Figure 79. Western side of SH-3 north bridges over BNSF railroad – comparison of NW_SG3 data before and after Repairs

2.2.4.5 Tilting of Pier Caps after Repairs

All tiltmeter data and corresponding temperature data for tiltmeters installed on pier caps of the north bridge are presented in Figures 80 – 83. Some of the tiltmeter data is too noisy and may indicate malfunctioning tiltmeters. There is generally an opposite trend between tilt and temperature variations for TM1-4 and TM7-8. Substantially more daily variations in tilt can be seen after the repairs. Same trend between tilt and temperature variations is observed for TM5. When the temperature increases, the Pier No.3 is tilting away from Abutment No. 2 (eastern abutment). These observations seem to indicate that the repairs to SH-3 North Bridge are working as intended.

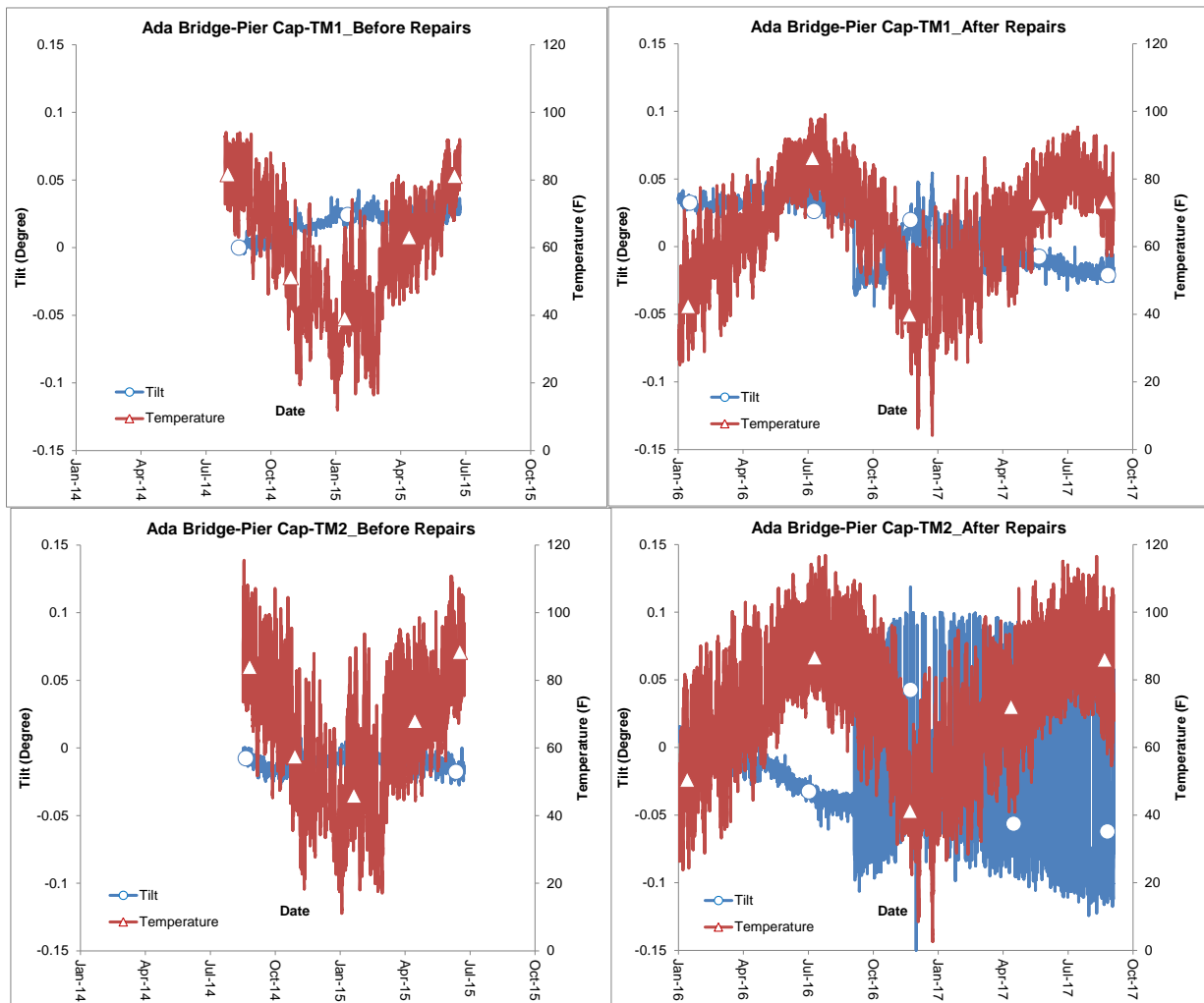


Figure 80. SH-3 north bridge over BNSF railroad – pier cap tiltmeter TM1 and TM2 data after repairs

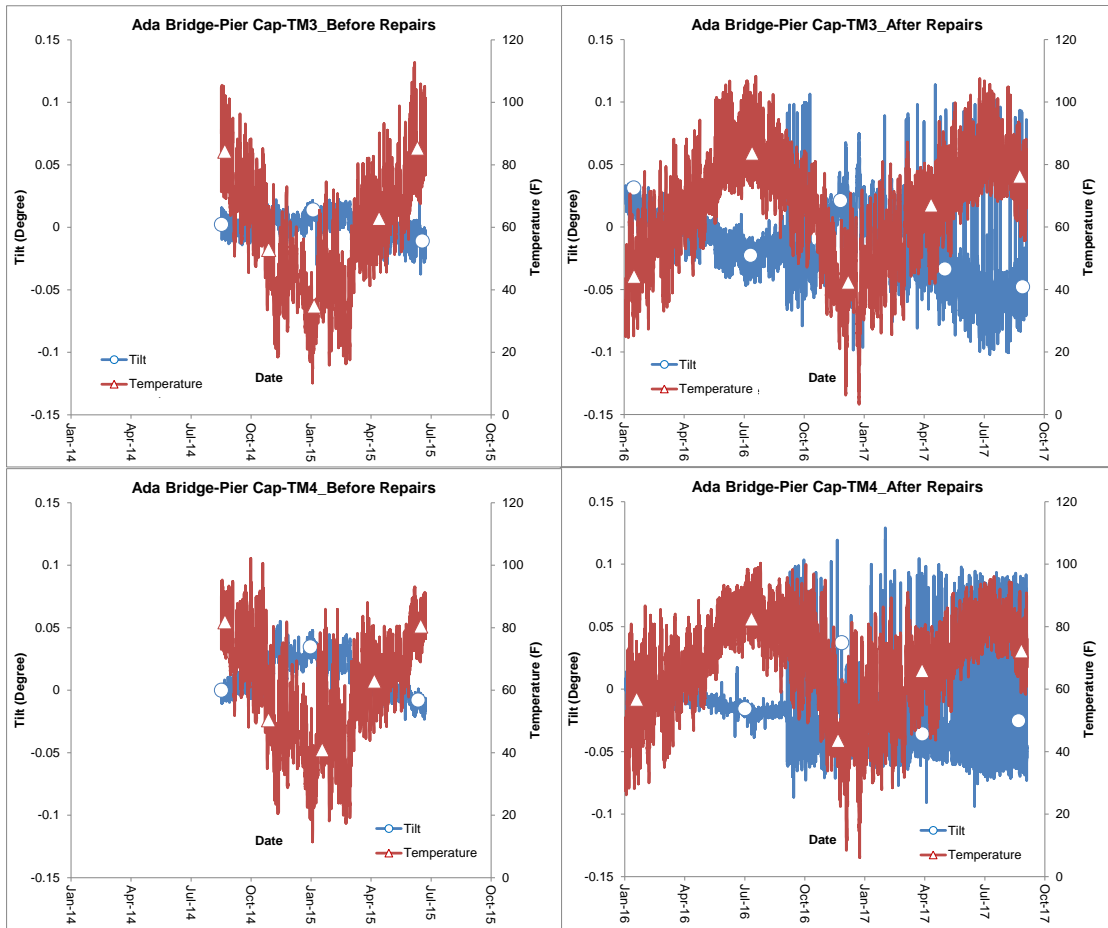


Figure 81. SH-3 north bridge over BNSF railroad – pier cap tiltmeter TM3 and TM4 data after repairs

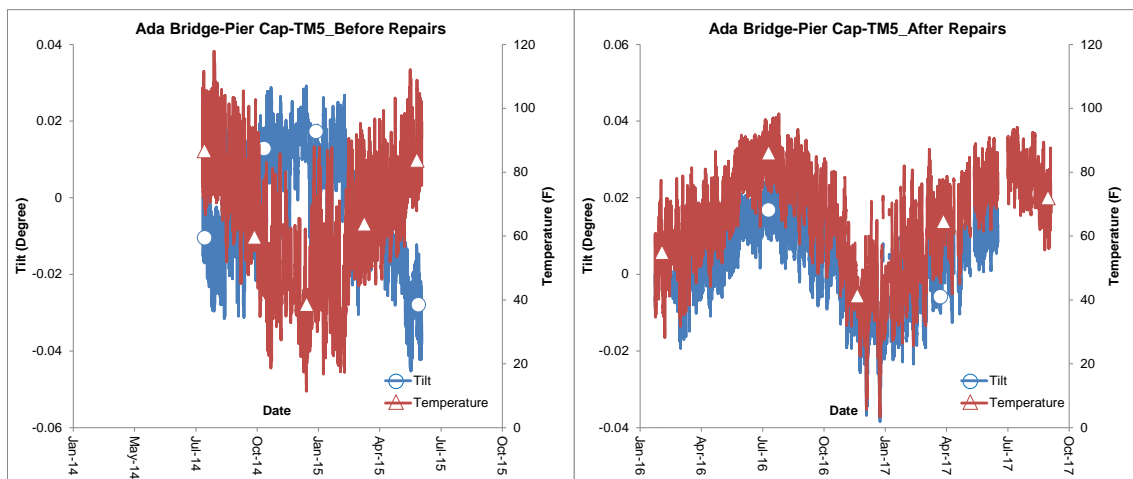


Figure 82. SH-3 north bridge over BNSF railroad – pier cap tiltmeter TM5 data after repairs

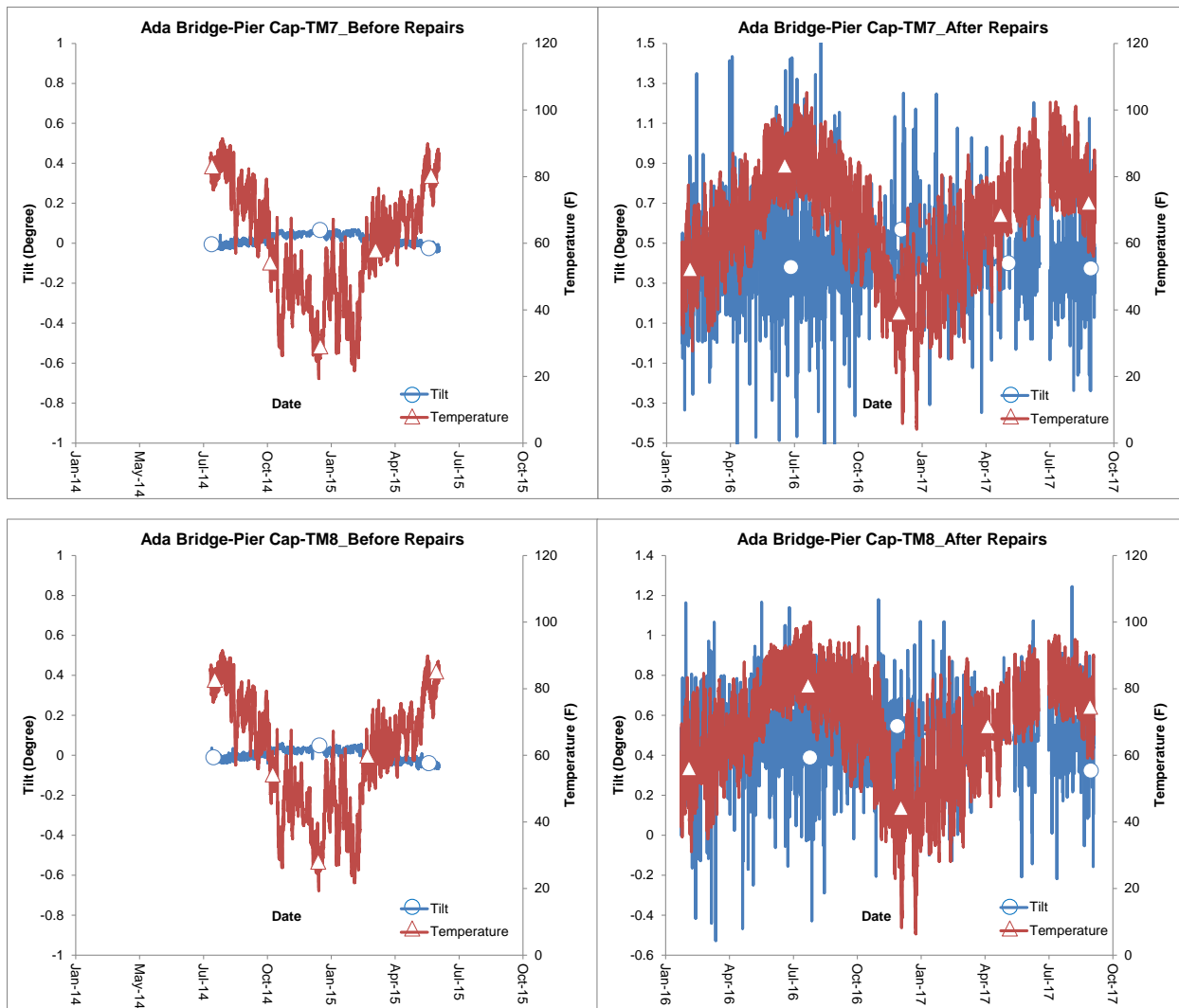


Figure 83. SH-3 north bridge over BNSF railroad – pier cap tiltmeter TM7 and TM8 data after repairs

2.2.4.6 Movements around Expansion Joints after Repairs

Expansion joint movements along with temperature variations before and after repairs at Pier Nos. 1 (CMP1 and CMP2) and 4 (CMP7 and CMP8) are compared in Figures 84 and 85, respectively. Substantially more daily variations in expansion joint movements can be seen after the repairs. Based on the recorded data during the monitoring period in 2016 and 2017, temperature varied between 2° F and 104° F at Pier No. 1 and between 28° F and 120° F at Pier No. 4. The measured displacements at CMP1, CMP2, CMP7, and CMP8 for these temperature variations were 1.19”, 1.03”, 1.05”, and 1.06”, respectively. The calculated displacements at

these locations are 1.13", 1.19", 0.94", and 0.84". The calculated displacements match the measured values reasonably well. It appears that the newly installed expansion joints are functioning well.

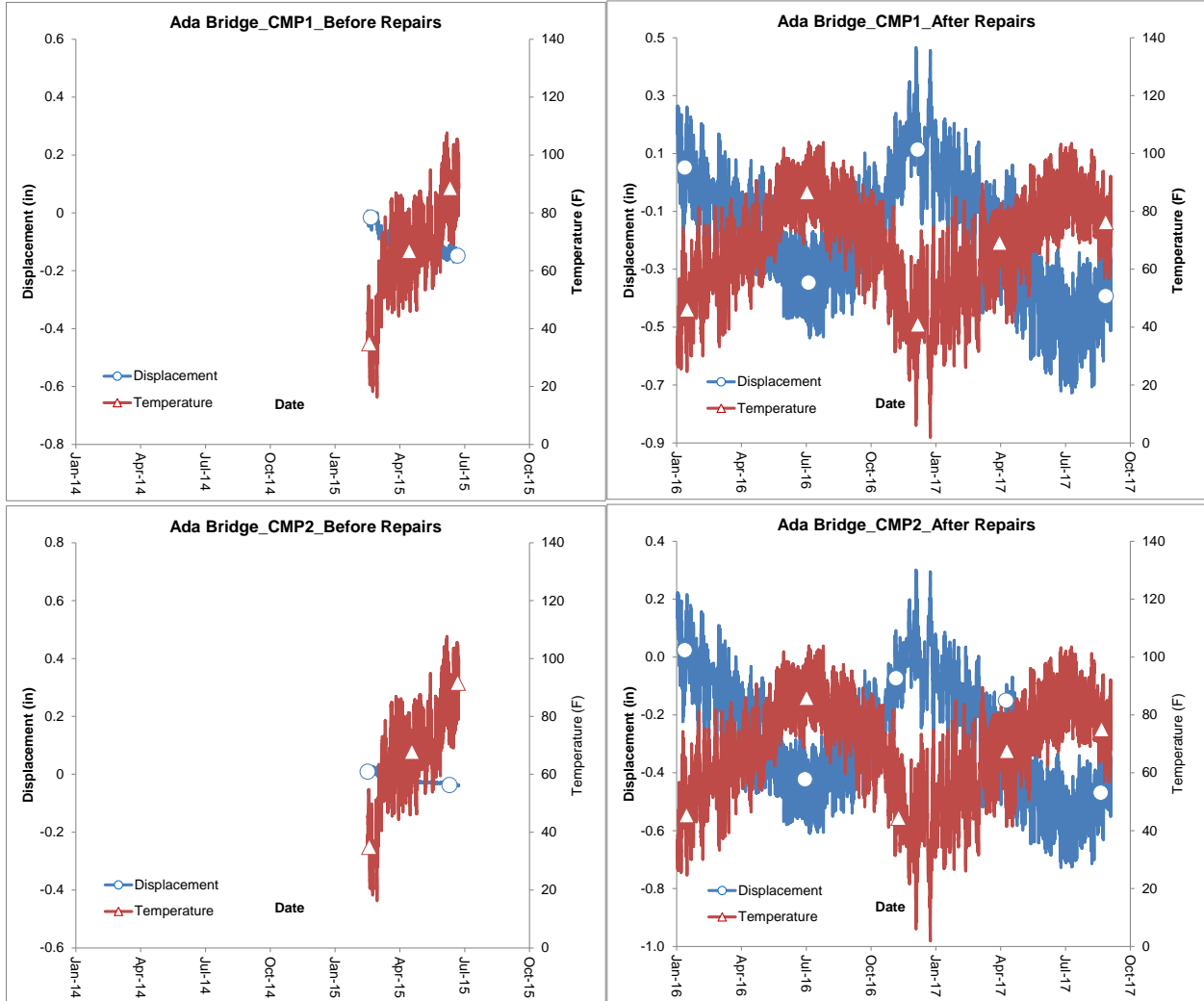


Figure 84. SH-3 north bridge over BNSF railroad – comparisons of crackmeter CMP1 and CMP2 data before and after repairs

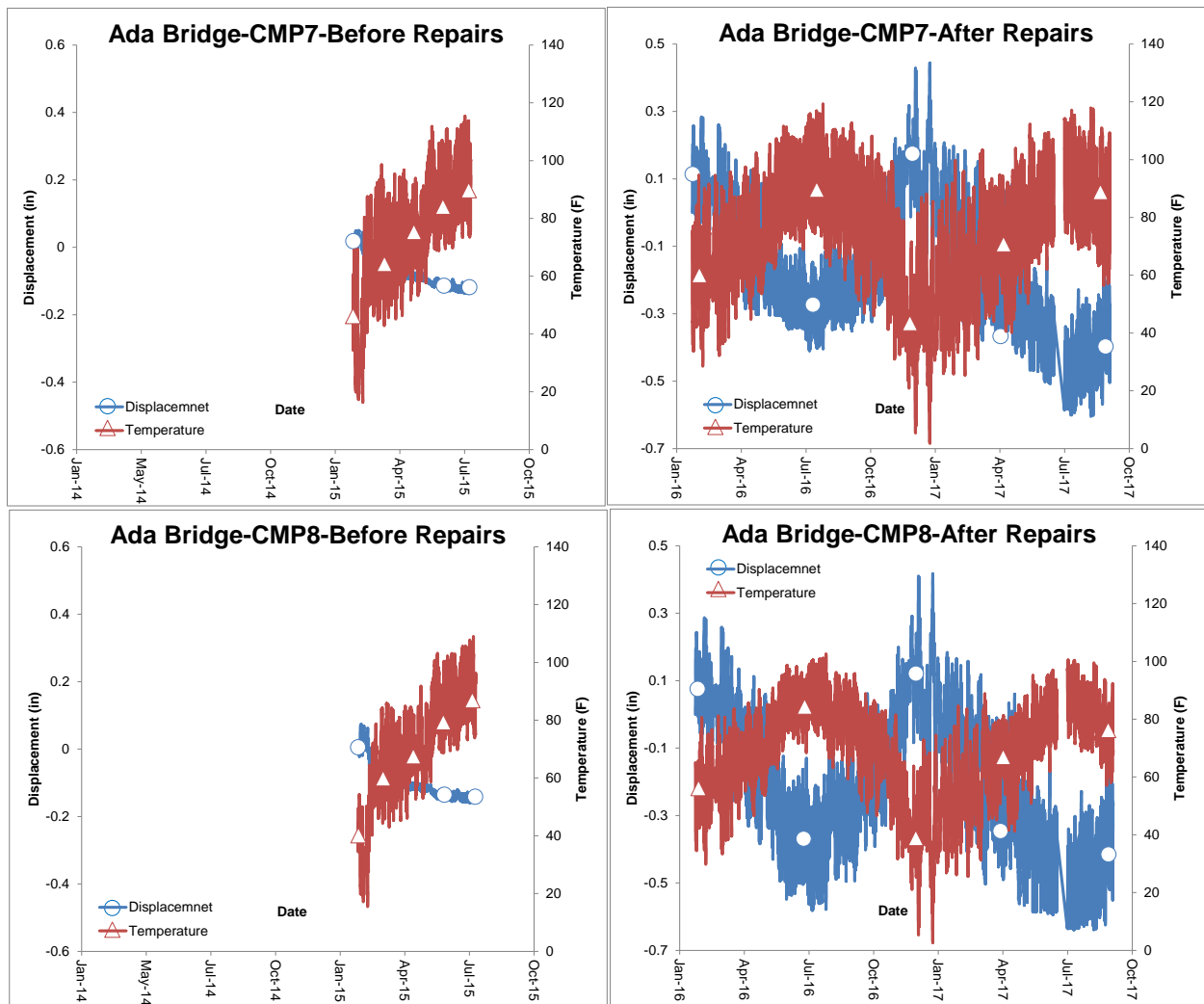


Figure 85. SH-3 north bridge over BNSF railroad – comparisons of crackmeter CMP7 and CMP8 data before and after repairs

2.2.5. The 19th Street/I-35 Bridge before Repairs

The instrumented bridge is located at the intersection of I-35 (under) and 19th Street in Cleveland County, Oklahoma (Figure 86). This particular bridge was chosen for instrumentation primarily because of various issues with the bridge that seem to point to adverse interactions between the bridge and the approach pavement. The bearing pads that support the concrete girders are permanently skewed in the direction of the bridge deck. This may indicate pressure on the bridge deck from the approach slab/pavement. Two pressure relief joints, 4 inches in width, have been cut on the eastern and western sides (see Figure 86) sometime between 2005

and 2009 and filled with asphalt; providing further evidence to the fact that previous problems with pavement pressure have occurred.

Bridge inspections are carried out by ODOT personnel every 2 years to assess the overall health of the bridge superstructure, deck, approach slabs, abutments, and expansion joints. Originally, two separate bridges were built in 2000. Prior to that a single bridge existed on the north side. Therefore during the construction of the bridges in 2000, completely new fill would have been added on the south side. Furthermore, deeper girders would have required grade raise and additional fill on the north side as well. In 2009, a center turning lane was added and the bridges were joined together as a single bridge. There are three inspections reports that exist from 2003, 2005, and 2007 for each bridge. The inspection report in 2009 covers both the bridges as a single structure. Beginning in 2003 the inspection report for the north bridge noted the following:

- The sealed expansion joint in the center of the bridge deck is full of debris and requires cleaning.
- The construction joint between the approach slab and approach pavement were not sealed during construction and needed to be sealed.
- The eastern anchor bolts tied to the elastomeric pad assembly had bent forward toward the bridge deck due to approach slab movement.
- Roadway creep had pushed the eastern approach slab toward the center of the bridge deck and is now hanging over the abutment back wall 1 inch.

The 2003 report for the South Bridge noted the same maintenance issues as the north bridge with the following exceptions:

- The center expansion joint is full of debris, is closed, and requires cleaning.
- There is a 6 inch spall at the top of the north east wing wall due to 1 inch approach slab movement.
- There is a longitudinal crack in the eastern approach slab.

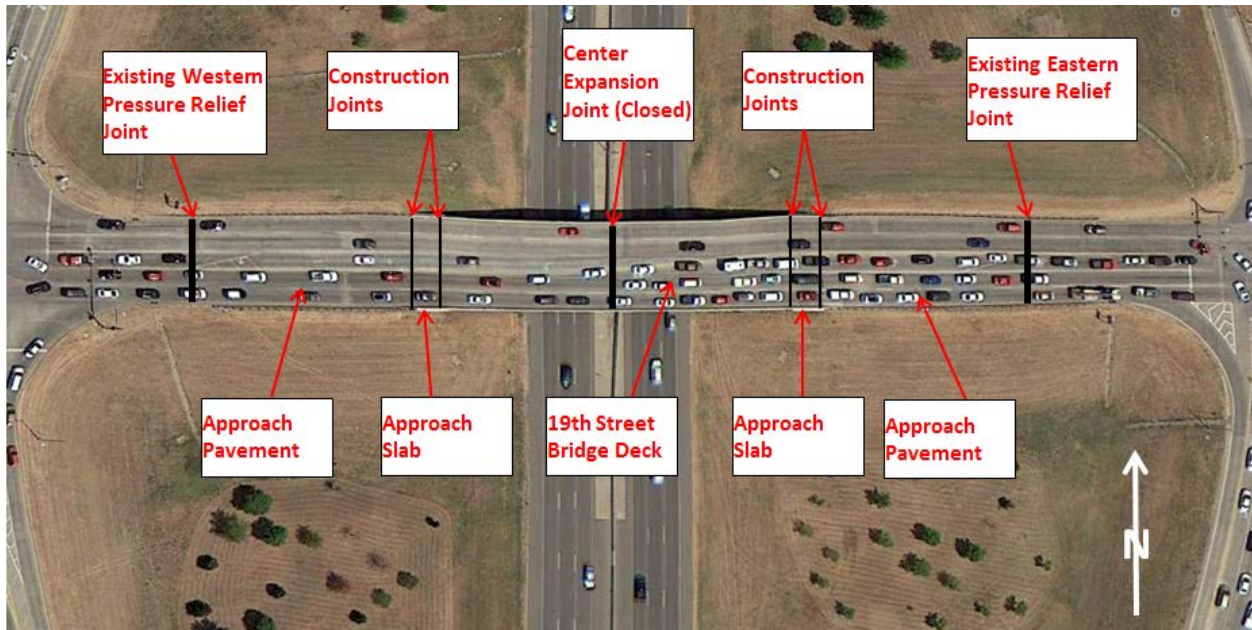


Figure 86. 19th Street/I-35 Bridge

The 2005 report for the north bridge stated all of the maintenance issues in the 2003 and noted that “roadway creep” has pushed the eastern approach slab up to 2 inches toward the bridge deck and that the elastomeric bearing pads had deformed. The “roadway creep” term used by the inspectors may refer to displacements caused by pavement pressure. The 2005 report for the south bridge noted the same issues as the 2003 inspection report for the south bridge with the addition of 2 inches of movement of the approach slab similar to the north bridge. Figure 87 shows photos taken in 2005 and illustrates various maintenance issues discussed. . Figure 88 shows photos of the center expansion joint for the north and south bridge in 2005. Precise locations of where each photo was taken are not available for the figures presented. The inspection in 2007 for the north and south bridges noted the same observations as the previous inspections. The top of the anchor bolts and the elastomeric bearing moving away from the abutment backwall (Figure 87c) is a strong evidence of pavement pressure. In 2009, an additional turning lane was added in the center of the bridge that merged the westbound and eastbound decks together making the entire bridge deck width 70.4 feet. At this time, the center expansion joint was also eliminated. NBI 25441 was dropped as a bridge designation and NBI 25440 was used to name the entire structure. Four additional Bulb-Tee prestressed concrete girders were added to the superstructure to support the middle deck for a total of 20 prestressed concrete girders for the entire bridge. The pier caps were also merged and an additional pier was added in the center of the pier cap. Finally, the eastern and western

abutments were merged. During construction of the center turning lane it was likely discovered that the anchor bolts on the eastern abutment bridge seat had gone from a bent condition to a sheared condition as shown in Figure 89. Figure 90 shows heavy cracking of the south eastern approach slab adjacent to south bridge deck in 2009. In 2009, after the center turning lane construction, a bridge inspection was carried out and noted the same maintenance issues previously discussed. Site visits were carried out jointly by the University of Oklahoma (OU) and ODOT personnel on January 28, 2011 and by OU personnel on June 24, 2011. During these site visits, U-shaped cracks, shown in Figure 91 were discovered on the eastern abutment back wall similar to that shown by Burgueño and Li (2008).

Instrumentation for this bridge consisted of installing various sensors along the approach pavement, approach slabs, and bridge abutments at key locations in order to collect useful data regarding strain, temperature, and movements of the approach slabs, approach pavements, and bridge abutments. The data obtained from these instruments are discussed in the following sections. All the instruments on the eastern side (see Figure 92), except the ones installed on the abutment backwall (NE_TM, NE_TH, SE_TM, and SE_TH), were removed in January – March 2015 during the expansion of the pavement near the bridge as a part of the new Sam's Club construction in Moore.



a) Bent anchor bolts on the eastern abutment bridge seat



b) Approach slab overhang with eastern abutment wing wall spall



c) Bent anchor bolts with deformed elastomeric bearing pads on the eastern abutment bridge seat



d) Large crack in the eastern abutment back wall

Figure 87. 19th Street/I-35 Bridge photos showing distress in 2005



a) Center expansion joint on the North Bridge at 19th Street



b) Center expansion joint on the North Bridge at 19th Street (close up)



c) Center expansion joint on the South Bridge at 19th Street



d) Center expansion joint on the South Bridge at 19th Street (close up)

Figure 88. Center expansion joint on north and south Bridge at 19th Street/I-35 in 2005



Figure 89. 19th Street/I-35 Bridge sheared anchor bolts in 2009



Figure 90. Cracking of the south eastern approach slab adjacent to south bridge deck in 2009



Figure 91. U-shaped cracking at 19th Street/I-35 Bridge eastern abutment back wall in 2011

A total of 44 instruments were installed on the eastern and western sides of this bridge consisting of strain gages, crackmeters, tiltmeters, and thermistors. Figures 92 and 93 show the locations of all the instruments on the bridge. Each end of the bridge, east and west, has a Mirco-1000 data logger installed at the midpoint of the abutment back wall on top of the slope wall for the data collection from 22 instruments per side. Figures 94 and 95 illustrate the locations of the sensors attached to the south side of the eastern approach pavement. Data collected from the sensors before a new pressure relief joint was installed on the eastern approach pavement near the approach slab in April/May 2016 are first presented. Data collected after the installation of the pressure relief joint are then presented and compared to the data collected before the installation to evaluate the effectiveness of the new pressure relief joint.

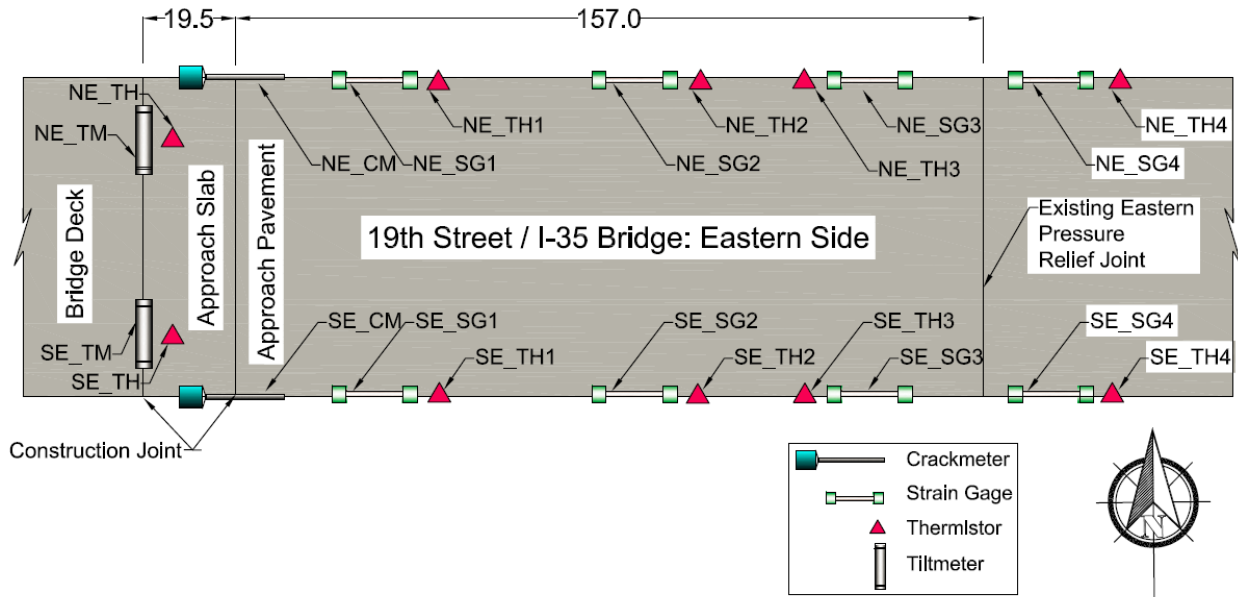


Figure 92. Instrumentation layout for the eastern side of the 19th Street/I-35 Bridge

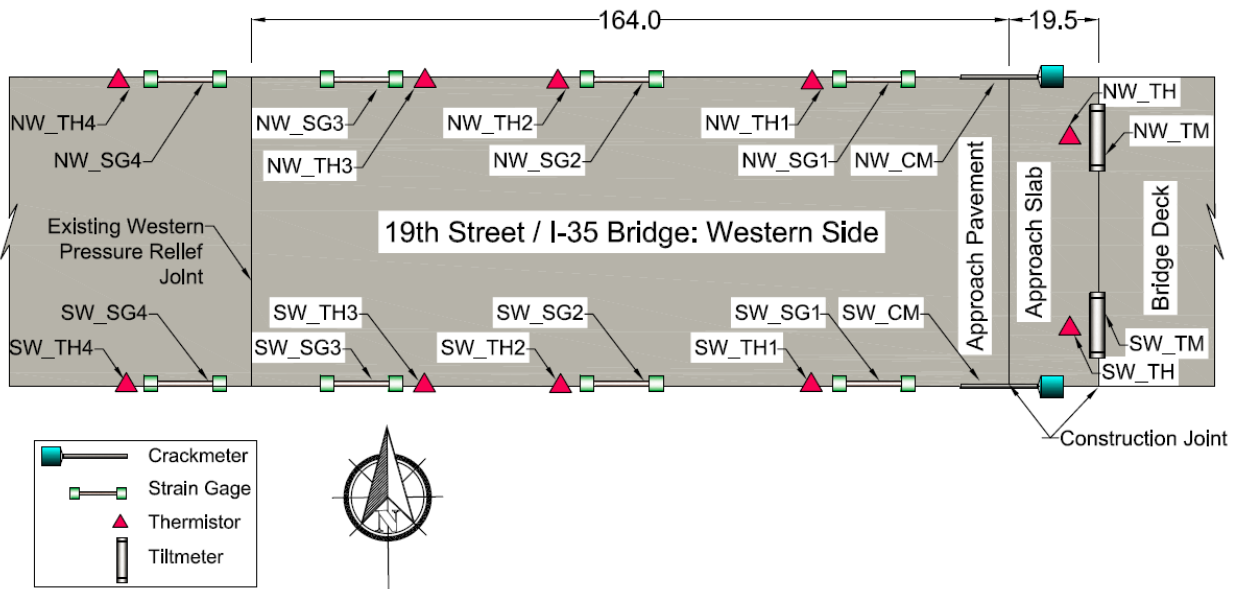


Figure 93. Instrumentation layout for the western side of the 19th Street/I-35 Bridge

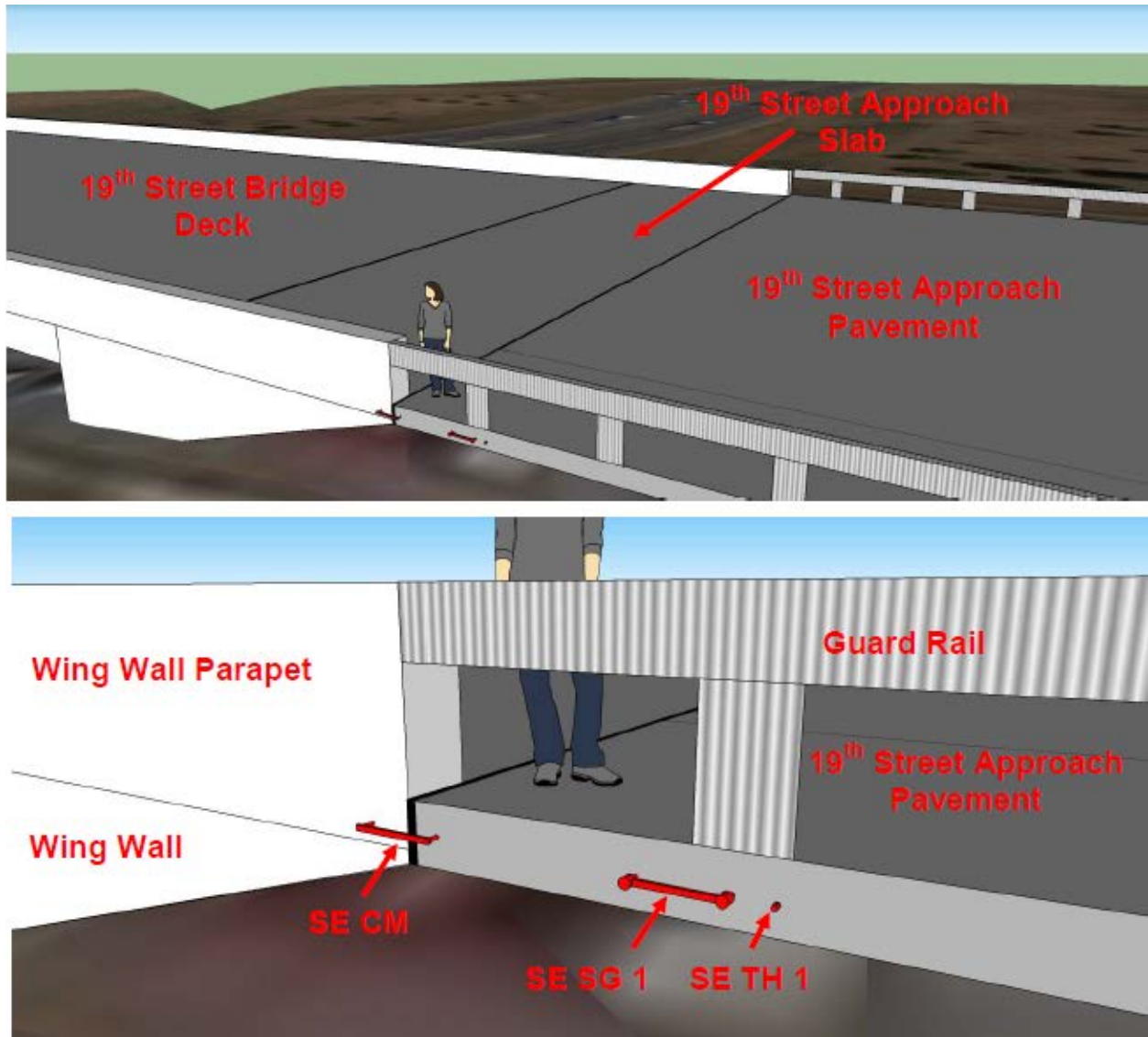


Figure 94. Instruments attached to south side of eastern approach pavement near approach slab (Bright, 2012)

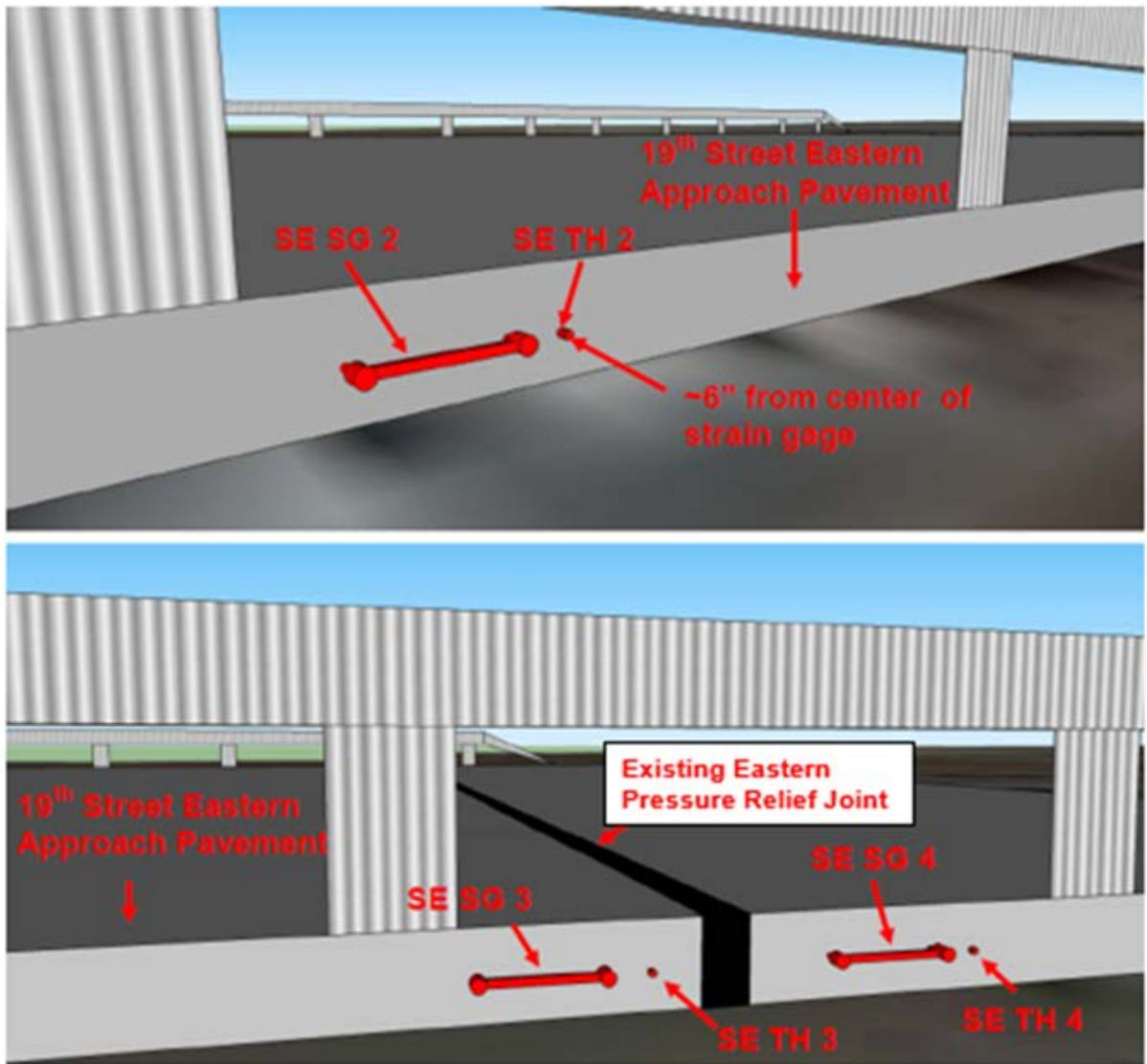


Figure 95. Instruments attached to south side of eastern approach pavement (Bright, 2012)

2.2.5.1 Abutment Backwall Rotation before Repairs

Tiltmeters are located on each corner of the abutment backwalls as shown in Figures 92 and 93. The figures in this section show the data trends for each tiltmeter. A negative trend in the tiltmeter data indicates the abutment is tilting toward the approach pavement and a positive trend indicates that the abutment is tilting toward the bridge deck, as shown in Figure 96. This applies to all of the tiltmeter data presented.

A negative trend in the tiltmeter data indicates that the abutment is tilting toward the approach pavement

A positive trend in the tiltmeter data indicates that the abutment is tilting toward the bridge deck

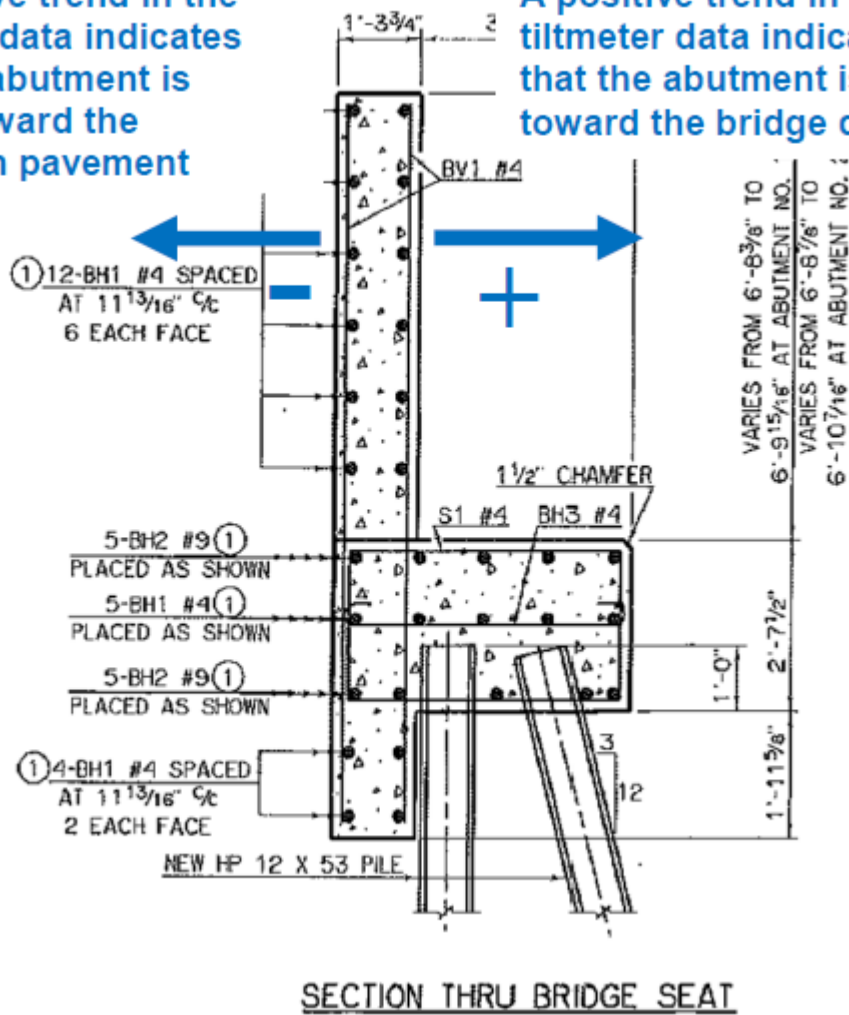


Figure 96. Illustration of the tilt trends for 19th Street/I-35 Bridge abutments (from EST Inc., 2008)

Figure 97 shows the data collected by the northeast tiltmeter. It can be seen that as the temperature increases the tilt decreases and vice versa. This indicates as the temperature rises from winter to summer the abutment tilts toward the approach pavement. Same behavior can also be observed in the southeast tiltmeter (Figure 98) as well as the tiltmeters located on the western abutment (see for example, Figure 99 and 100). The maximum measured tilts are, however, larger for the southeast and southwest tiltmeters than for their northern counterparts.

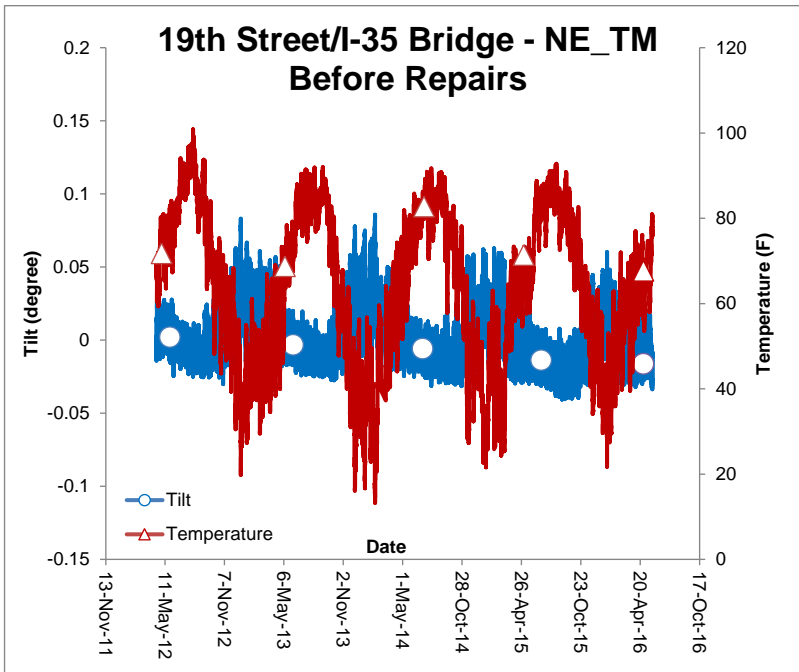


Figure 97. Eastside of the 19th Street/I-35 Bridge – northeast tiltmeter (NE_TM) data before repairs

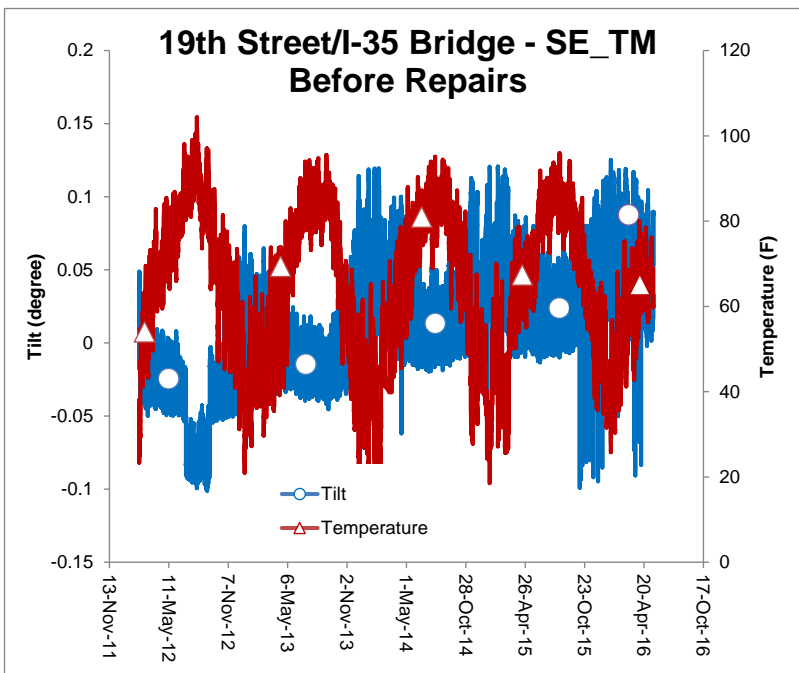


Figure 98. Eastside of the 19th Street/I-35 Bridge – southeast tiltmeter (SE_TM) data before repairs

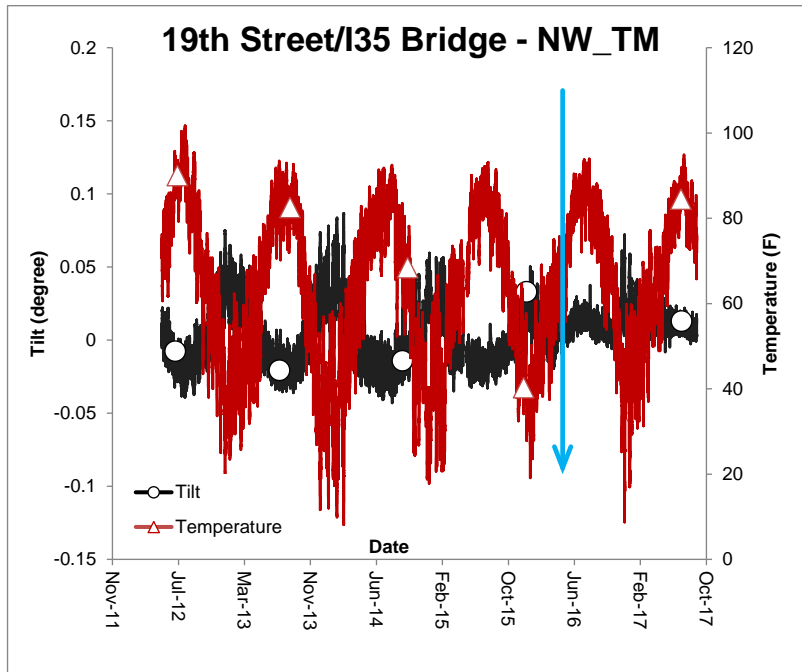


Figure 99. Westside of the 19th Street/I-35 Bridge – northwest tiltmeter (NW_TM) data

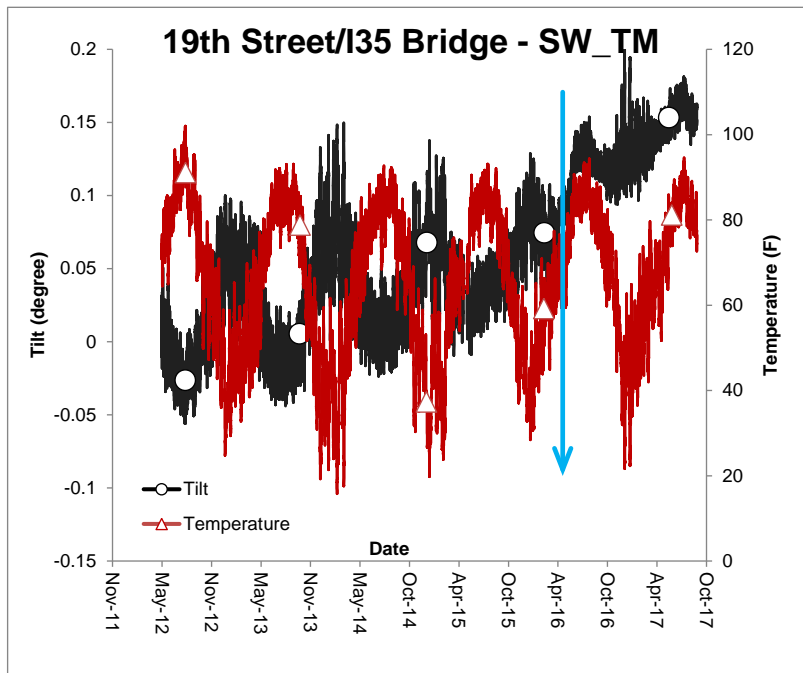


Figure 100. Westside of the 19th Street/I-35 Bridge – southwest tiltmeter (SW_TM) data

It appears from the data presented that thermal expansion of the bridge deck is controlling the behavior of the abutment backwall. It can be assumed that at this point the bridge deck

cannot thermally expand toward the center because of the closed center expansion joint. As a result, as the temperature rises, the bridge deck expands outward and pushes on the both eastern and western approach slabs. The opposite is true when the temperature decreases. As the approach slabs moves toward the approach pavements the friction from the approach slabs and bridge deck “drags” the abutment back walls with the approach slabs. Figure 101 shows a cross-section through the bridge deck, abutment back wall, and approach slab. As seen from this figure, the bridge deck and the approach slab are tied together with reinforcing steel. This means that for all practical purposes the bridge deck and approach slab are acting together as a single structural element.

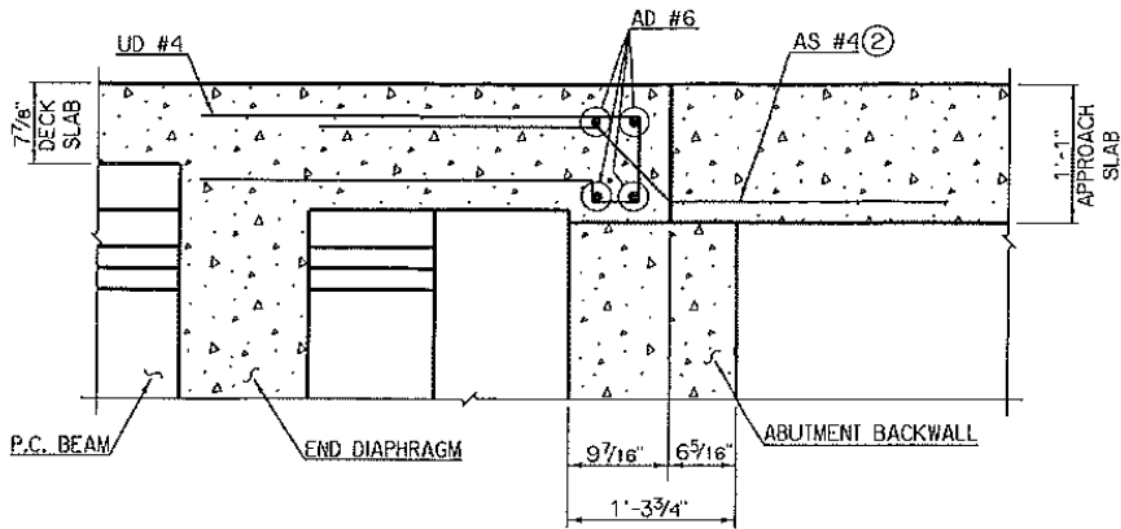


Figure 101. Cross-section through the bridge deck, abutment back wall, and approach slab (EST 2008)

As seen from the eastern tiltmeter data (Figures 97 and 98), the south section of the eastern abutment backwall tilts more than the north section. This is likely because on the south side of the eastern pavement, there is additional space between the approach slab and approach pavement along the construction joint for the bridge deck/approach slab to thermally expand and contract during temperature cycles. An observation that supports this interpretation is that there is far more spalling of concrete/U-shaped cracks on the southern side of the east abutment backwall than the northern side. As the overstressed abutment backwall tilts back and forth, it leads to U-shaped cracks and eventual spalling of concrete. Therefore, more tilting on the south side leads to more cracking and spalling on this side. As mentioned earlier, prior to

2009 the northern and southern abutment backwalls were separate structures and were joined together by the third structure when the center turning lane was added to the center of the bridge. This could further explain the differences in abutment tilt because the abutment was not originally constructed as one structure.

2.2.5.2 Relative Displacement between the Approach Pavement and the Abutment Wing Wall before Repairs

Crackmeters are located in each quadrant, southeast, northeast, southwest and northwest. They are attached to the abutment wing wall parapet and the approach pavement, between the construction joint as seen in Figure 102. It is assumed that the wing wall undergoes only minor displacement compared with the approach pavement because the wing wall is supported on driven piles. Figures 103 and 104 show the data collected by the northeast and southeast crackmeters. It can be seen that as the temperature increases displacements decrease and vice versa. Similar trend can also be observed in the crackmeters located on the western abutment (Figures 105 and 106).

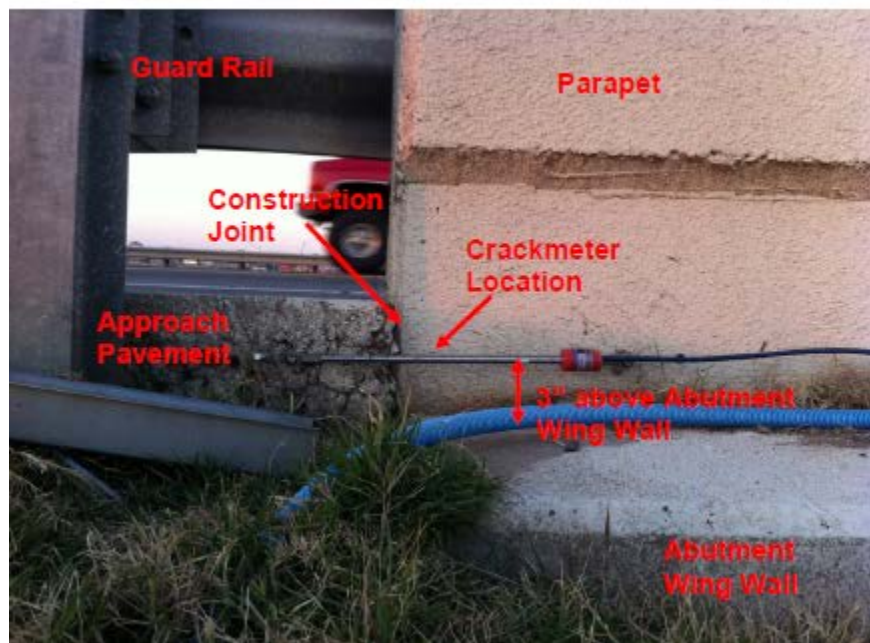


Figure 102. Installed crackmeter attached to approach pavement and parapet above abutment wing wall (Bright, 2012)

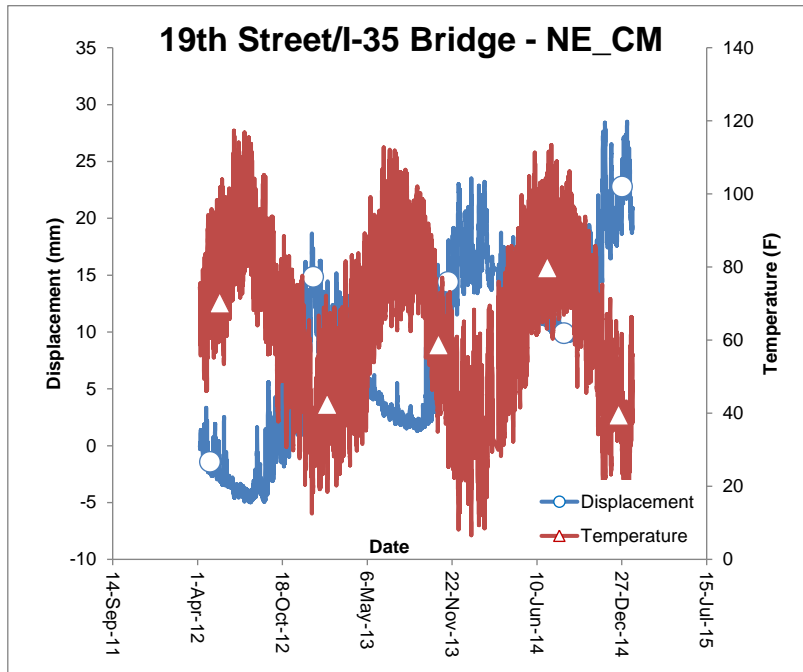


Figure 103. Eastern side of the 19th Street/I-35 Bridge – northeast crackmeter NE_CM data before repairs

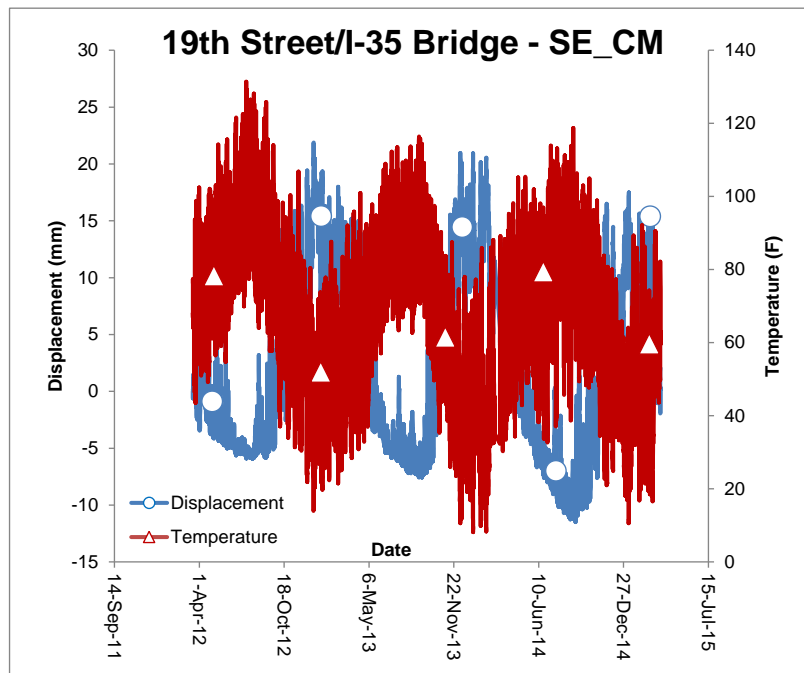


Figure 104. Eastern side of the 19th Street/I-35 Bridge – southeast crackmeter SE_CM data before repairs

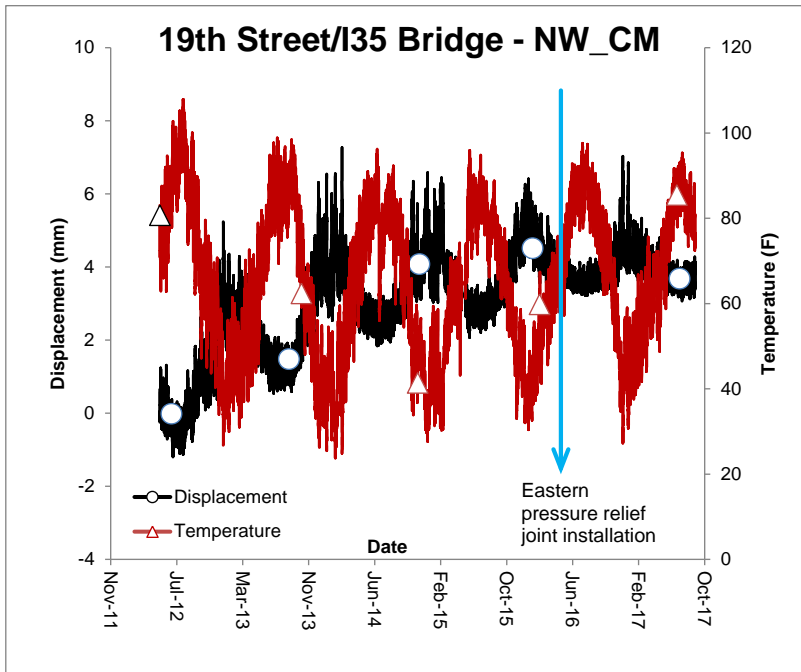


Figure 105. Western side of the 19th Street/I-35 Bridge – northwest crackmeter NW_CM data before and after repairs

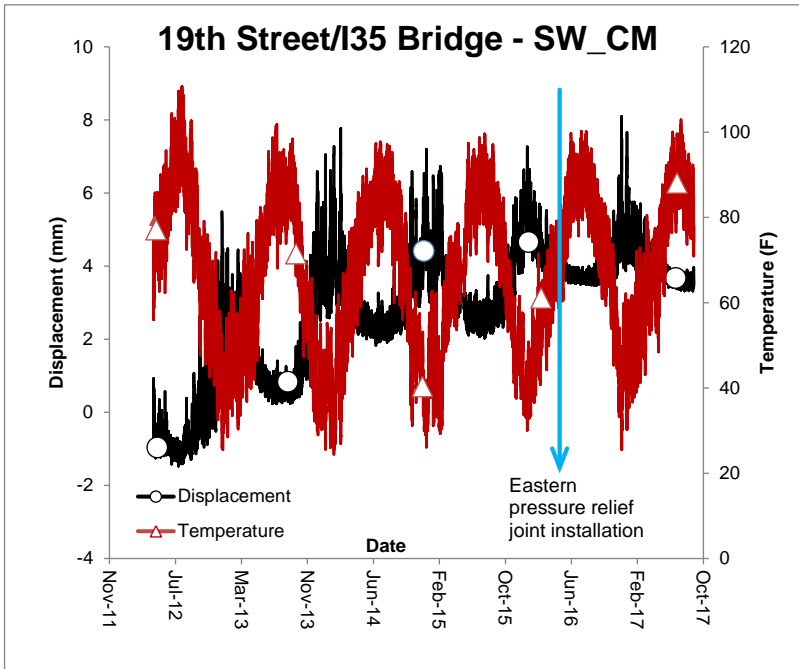


Figure 106. Western side of the 19th Street/I-35 Bridge – southwest crackmeter SW_CM data before and after repairs

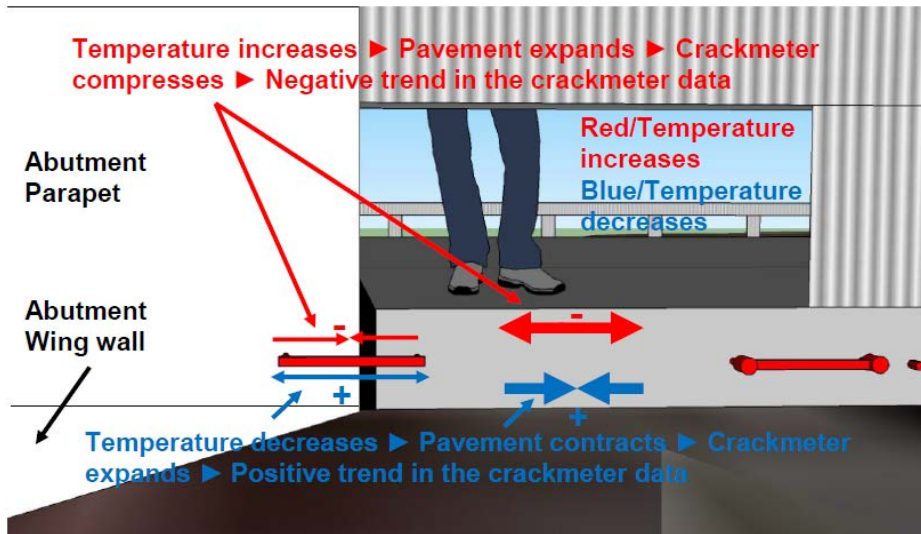


Figure 107. Illustration of crackmeter displacement trends (Bright, 2012)

As the temperature increases, the approach pavement expands toward the approach slab. This causes the crackmeter to contract and a negative trend is registered on the crackmeter. A negative trend indicates that the crackmeter is experiencing compression. When the temperature decreases, the approach pavement relaxes back and moves away from the approach slab and causes the crackmeter to expand. This causes the crackmeter to measure a positive trend. Figure 107 illustrates this mechanism.

If Figure 103 is compared with Figure 104, larger amplitudes can be seen in the southeast crackmeter when compared to the northeast crackmeter. This comparison is similar to that made between the northeast and southeast tiltmeters. This likely means that there is additional room at the construction joint between the east approach slab and the east approach pavement at the south side for expansion and contraction of the approach pavement to occur. The amplitude of expansion or contraction is larger on eastern side than the western one. The reason for this may be that the approach slab and the approach pavement are locked together more on the western side.

2.2.5.3 Axial Strains before Repairs

Strain gages were installed at different locations on both the eastern and western sides of the 19th Street approach pavement. Figures 108 -111 show axial strain variations with

temperature for selected strain gages. Most of the discussion will be focused on the eastern strain gages located close to the bridge deck, southeast strain gage 1 (SE_SG1), and northeast strain gage 1 (NE_SG1). This is because these two strain gages are located close to the approach slab/bridge deck and their data is much more relevant for studying the interactions between the bridge deck, the approach slab, and the approach pavement. An increase in strain (elongation of the gage) typically implies that the surrounding pavement is expanding, and a decrease in strain (shortening of the gage) implies that the surrounding pavement is contracting. Looking at the trends for SE_SG1 and NE_SG1 shown in Figures 108 and 109, it can be seen that when the temperature increases there is an increase in strain for SE_SG1 and vice versa. A trend that is opposite to this can be seen for NE_SG1 data shown in Figure 109. An explanation for why southeast and northeast strain gages at these locations are showing opposite trends is provided below.

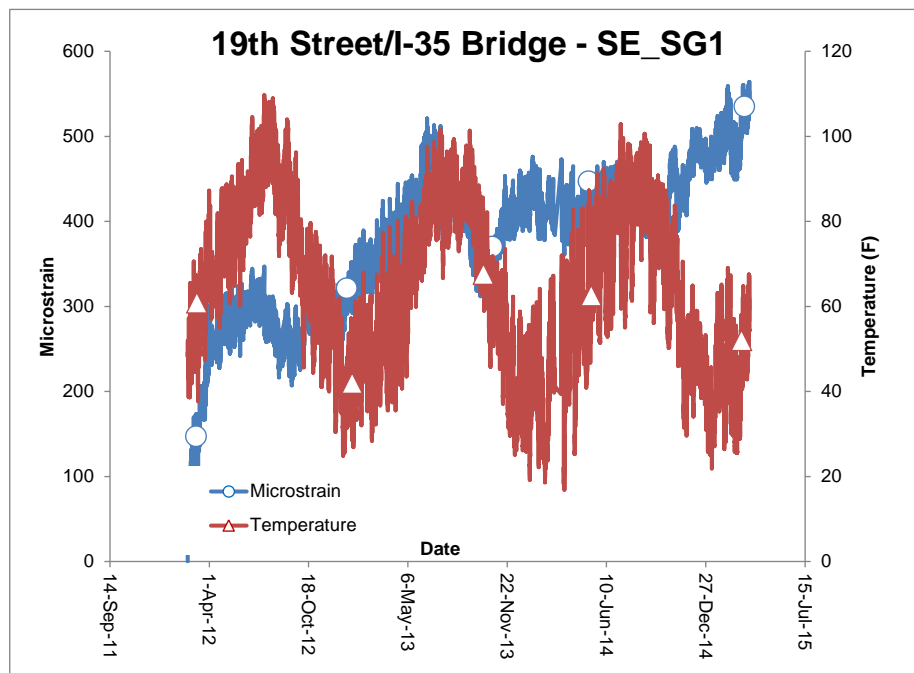


Figure 108. Eastern side of the 19th Street/I-35 Bridge – southeast strain gage SE_SG1 before repairs

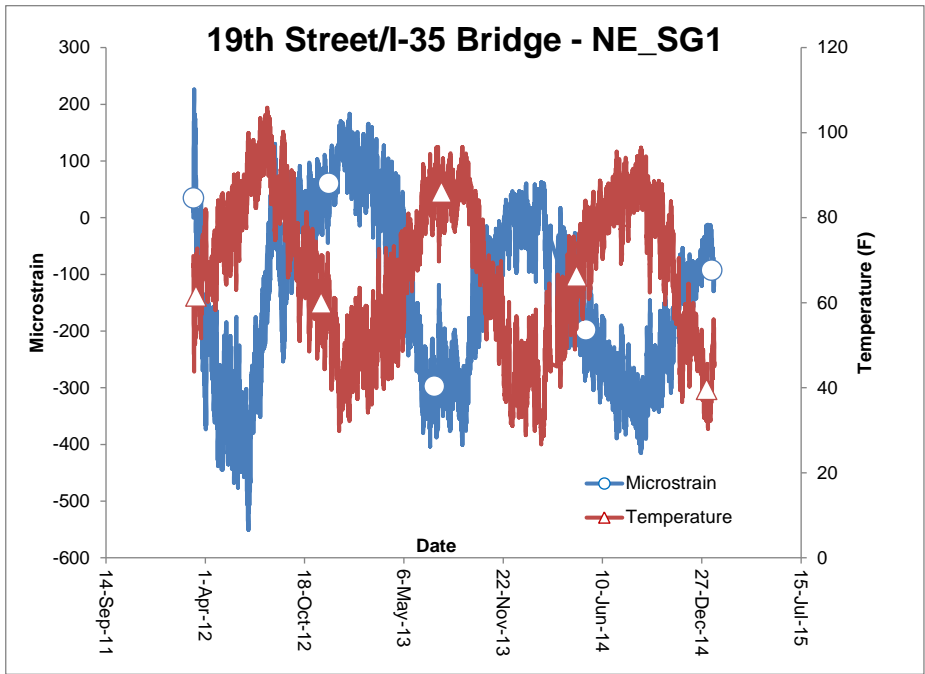


Figure 109. Eastern side of the 19th Street/I-35 Bridge – northeast strain gage NE_SG1 before repairs

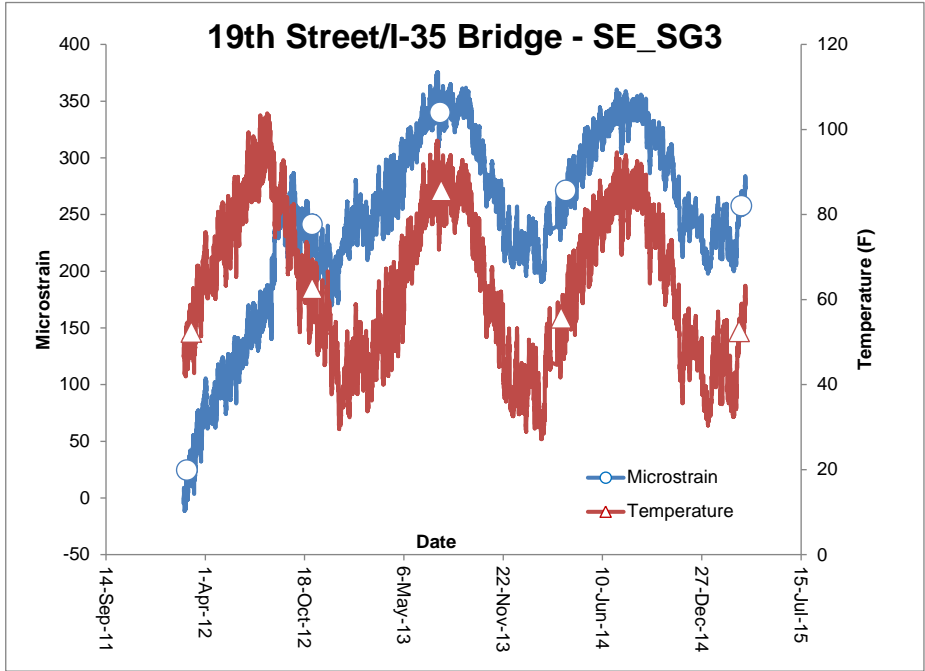


Figure 110. Eastern side of the 19th Street/I-35 Bridge – southeast strain gage SE_SG3 before repairs

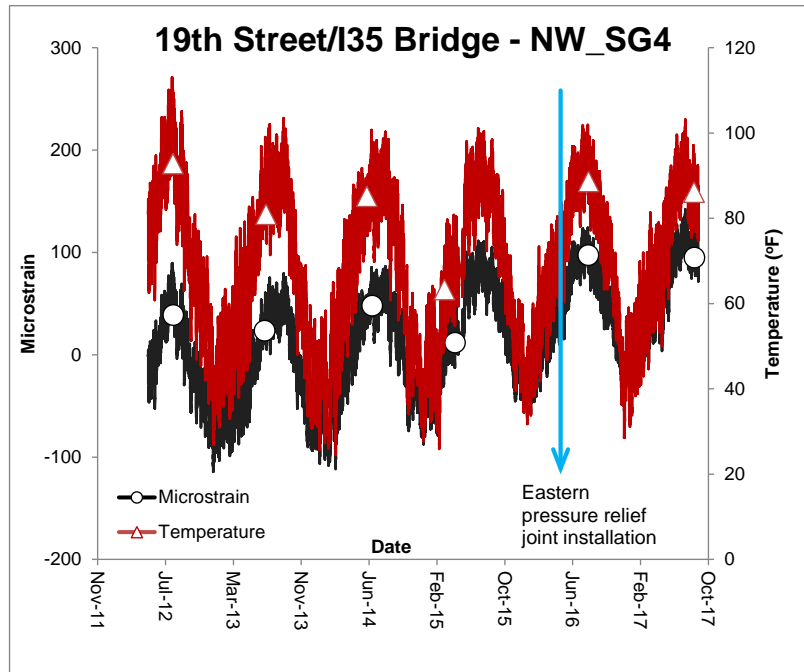
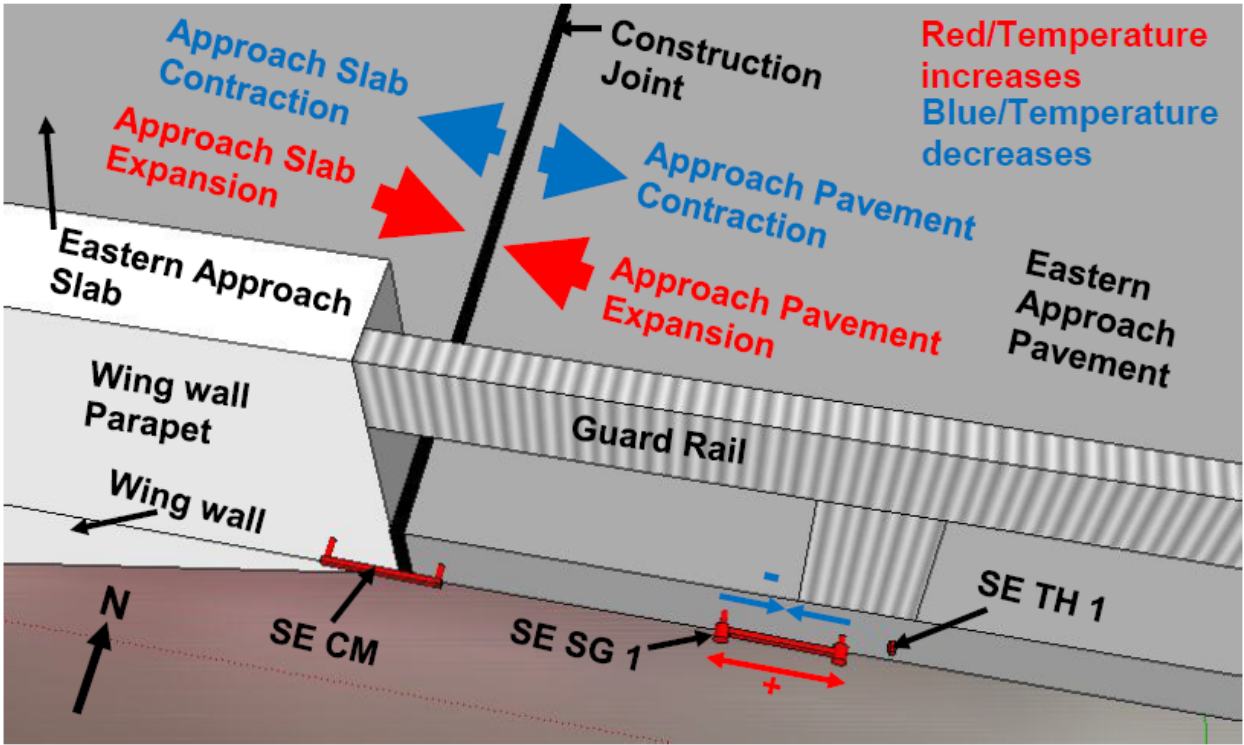


Figure 111. Western side of the 19th Street/I-35 Bridge – northwest strain gage NW_SG4 before and after repairs

Figure 112 and 113 show schematically the behavior seen in Figures 108 and 109. The southeast strain gage SE_SG1 expands as the temperature increases indicating that the surrounding approach pavement is also expanding, when the temperature decreases the approach pavement contracts and the southeast strain gage 1 (SE_SG1) registers a contraction. This behavior is not seen in the northeast strain gage 1 (NE_SG1), when the temperature increases the strain gage contracts indicating that the surrounding pavement also is contracting.

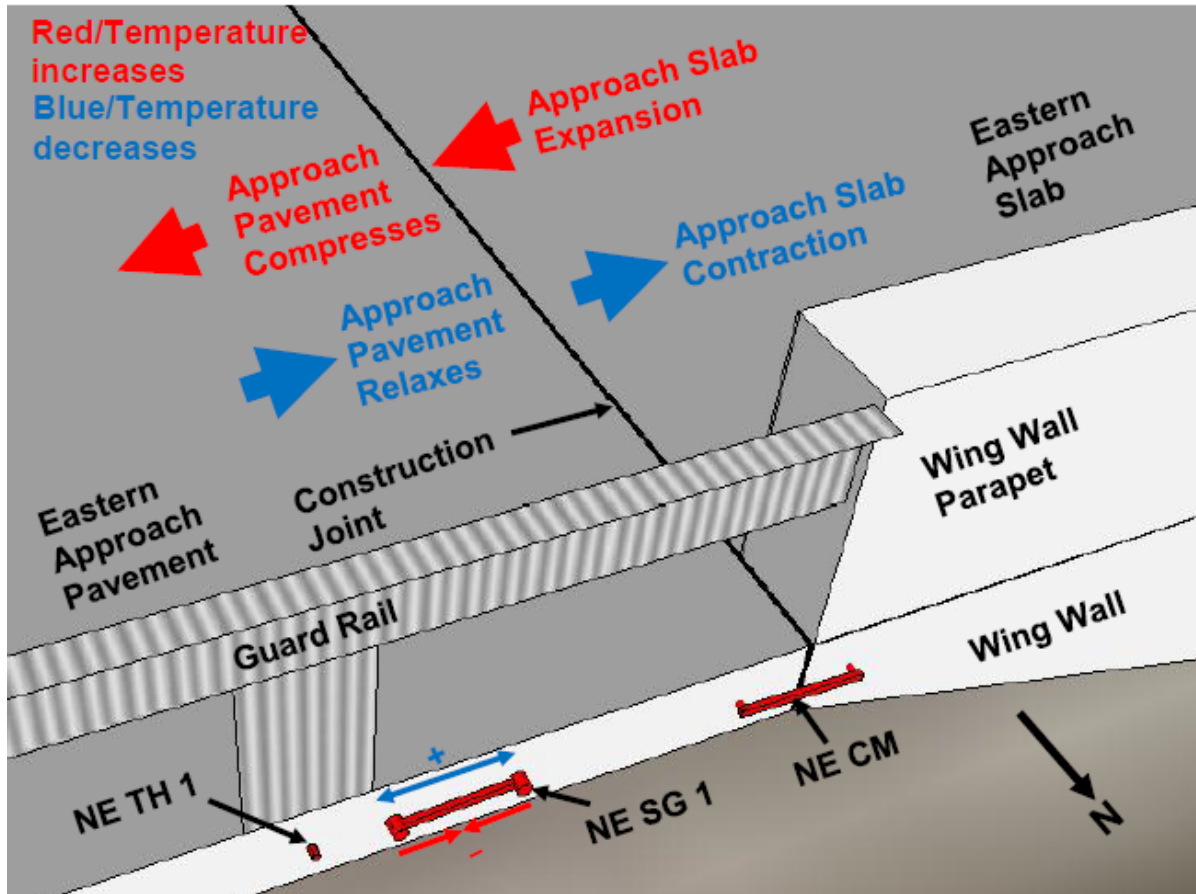
Temperature increases ► Approach Slab Expands ► Approach Pavement Expands ► Strain Gage Expands ► Positive trend in the SE SG 1 data



Temperature decreases ► Approach Slab Contracts ► Approach Pavement Contracts ► Strain Gage Contracts ► Negative trend in the SE SG 1 data

Figure 112. Southeast strain gage SE_SG1 trend illustration (Bright, 2012)

Temperature increases ► Approach Slab and Bridge Deck Expands ► Approach Slab pushes against Approach Pavement ► Approach Pavement Compresses ► Strain Gage Contracts ► Negative trend in the NE SG 1 data



Temperature decreases ► Approach Slab Contracts ► Approach Pavement Relaxes toward Approach Slab ► Strain Gage Expands ► Positive trend in the NE SG 1 data

Figure 113. Northeast strain gage NE_SG1 trend illustration (Bright, 2012)

As the temperature increases, the bridge deck expands outward and pushes on the approach slab. This pressure from the approach slab is then transferred to the approach pavement in the northeast area and compresses the pavement locally likely because there is no room at the construction joint between the approach slab and approach pavement at this location. When the temperature decreases, the bridge deck and the approach slab retract away allowing the approach pavement to “relax” toward the bridge deck. This transfer of compressive forces is not seen in the southeast strain gage possibly because there is additional room across

the construction joint in the eastern area for both the approach pavement and approach slab to expand and contract with temperature change. The above mentioned compression of the approach pavement with a temperature increase is also not seen in the data for the strain gages that are located away from the bridge (Figures 110 and 111).

2.2.5.4 Proposed Remedial Measures

In order to relieve the stresses on the 19th Street Bridge, it was proposed that new pressure relief joints be installed at Locations #2 and #3 shown in Figure 114. It was also recommend that these pressure relief joints be load-transfer joints, if possible. The details of the proposed pressure relief joint with a load-transfer are shown in Figure 115. The details of a pressure relief joint without load-transfer are given in Figure 116. In developing these joint designs, a report by Smith et al. (1987) and the joints used by Kansas, Ohio, Michigan, New Jersey and Florida Departments of Transportations were reviewed. The expected joint movement for a temperature range of -10°F to 130°F at Locations #1 and #4, calculated using the pavement and bridge lengths shown in Figure 115, is about 1.5 in. and this value is about 2.6 in. at Locations #2 and #3. A joint width of 4 in. should accommodate the expected movements and provide additional cushion in case part of the joint is blocked by debris. After the installation of pressure relief joints, proper maintenance of the joints is key to preventing pavement pressures from developing in future.

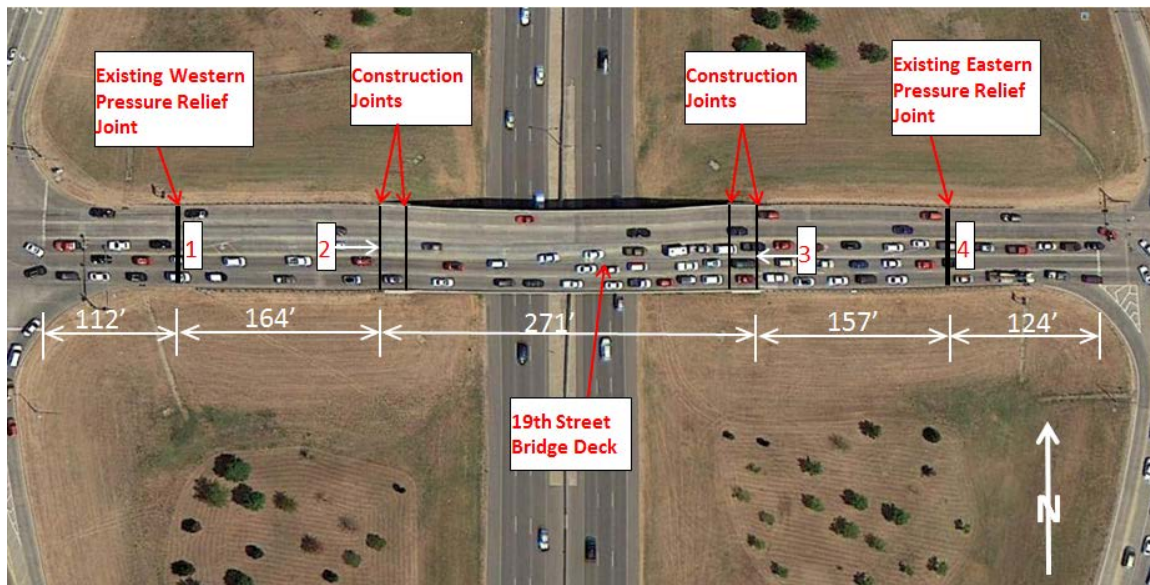
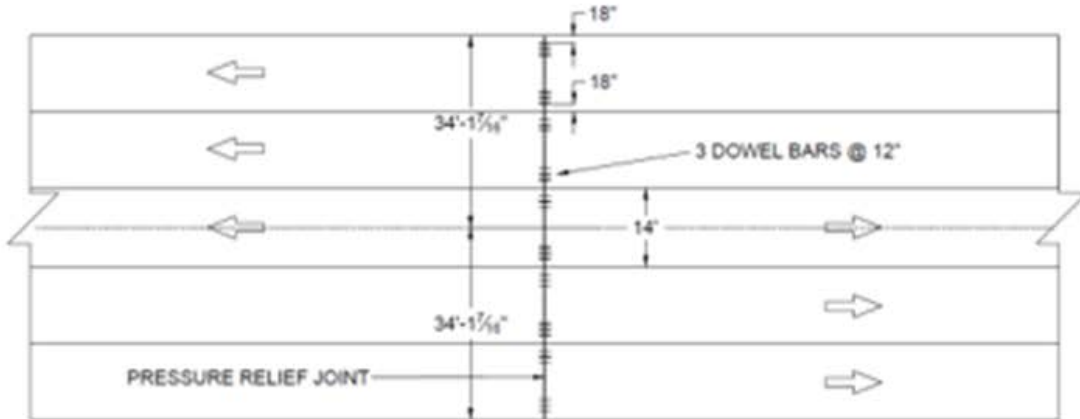
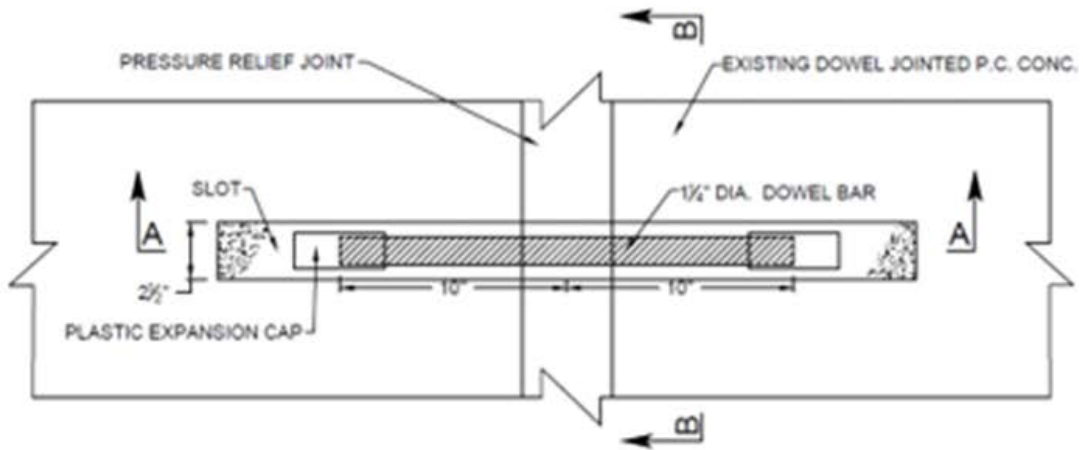


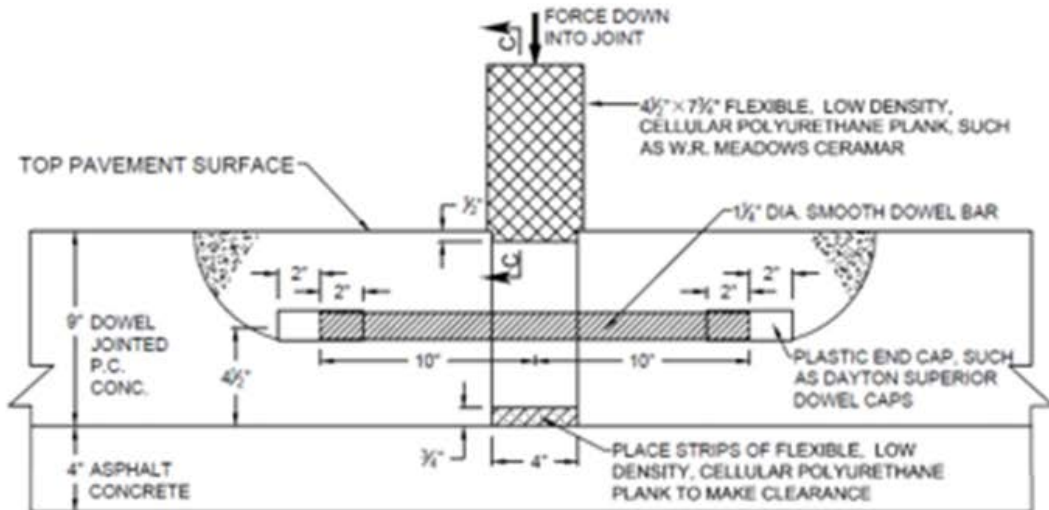
Figure 114. Locations of the proposed pressure relief joints (#2 and #3)



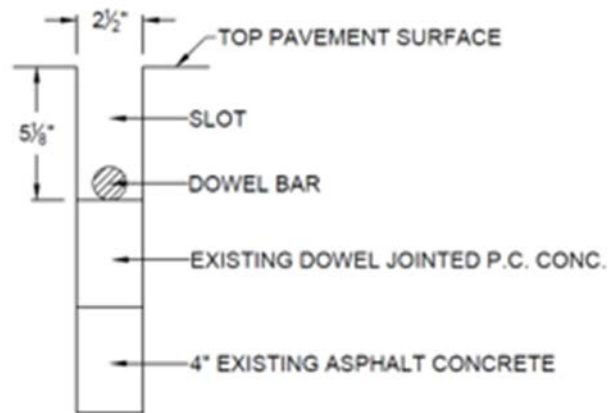
(a) Plan



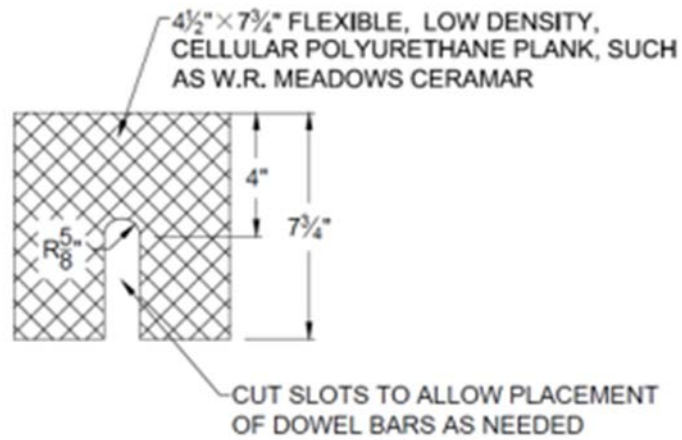
(b) Dowel Bar Placement Details (Plan view)



(c) Section A-A



(d) Section B-B



(e) Section C-C

Figure 115. Proposed pressure relief joint with load transfer

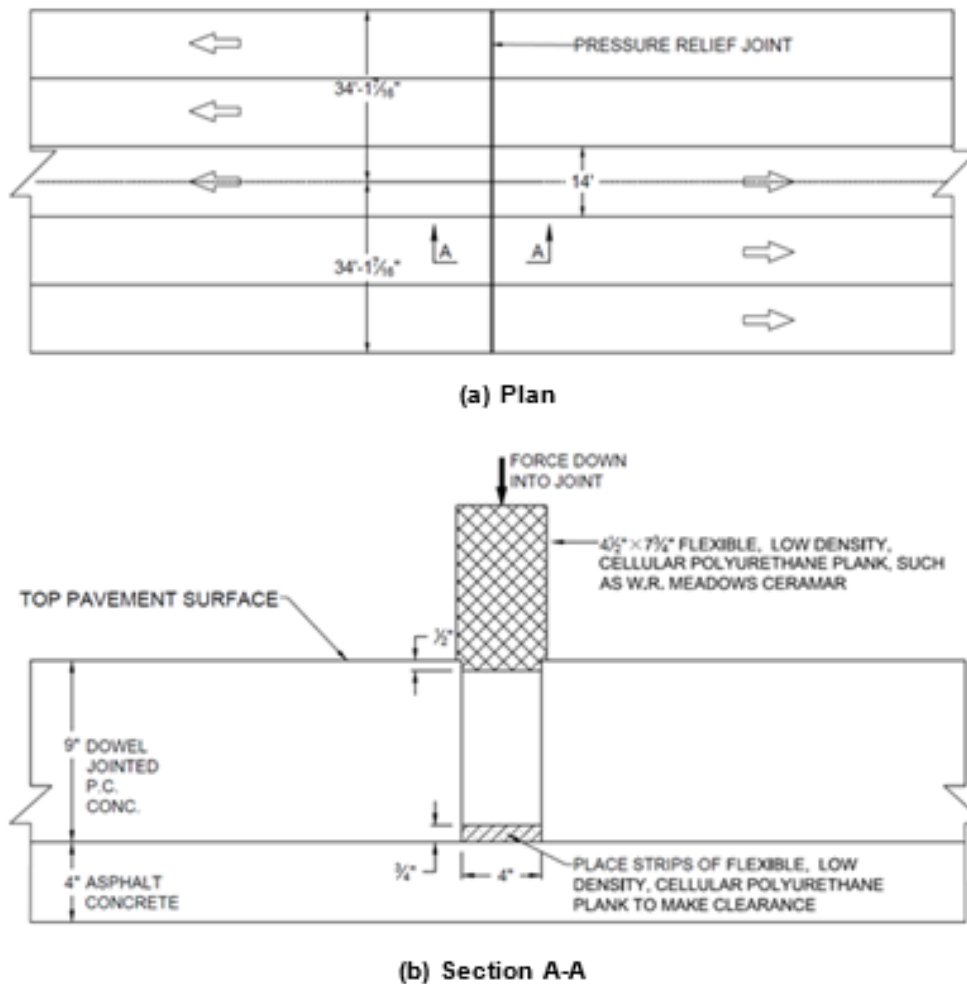


Figure 116. Proposed pressure relief joint without load transfer

2.2.6. The 19th Street/I-35 Bridge after Repairs

Four new strain gages, four new thermistors, and two new crackmeters were installed on the east side of the 19th Street Bridge in March 2016. These instruments were the replacements for the instruments lost or damaged during the expansion of the pavement on the east side due to the new Sam's Club construction.

Due to available material and ease of installation, another pressure relief joint system, BEJS (Bridge Expansion Joint System) by EMSEAL Joint Systems Ltd. (EMSEAL, 2016), than

those described in Section 2.2.5.4 was chosen for the 19th Street/I-35 Bridge. BEJS joint is shown in Figure 117. The system is pre-compressed in its packaging and can expand when released. It is capable of movement of +50% and -50% (total 100%) of nominal material size. Due to limited material available, it was also decided to install a pressure relief joint only at Location #3 (see Figure 114).

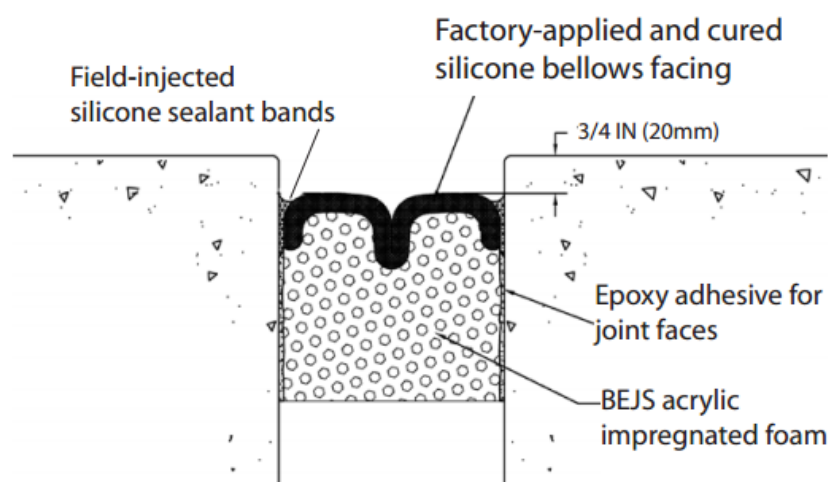


Figure 117. BEJS joint in typical installation — new or retrofit (EMSEAL, 2016)

On April 26, 2016, the City of Moore removed and replaced about 7.5' of approach pavement near the eastern approach slab (see Figure 118). ODOT Division 3 personnel installed the northern part of the 4" BEJS pressure relief joint on May 3 night/May 4 morning and May 4 night/May 5 morning and the southern part of the joint on May 10 night, 2016. The completed pressure relief joint is shown in Figure 118. All the removed instruments were reconnected to the data logger on May 12, 2016. Two new crackmeters, NE_CM3 on the northeast side and SE_CM4 on the southeast side were also installed across the pressure relief joint on May 12, 2016. The crackmeter CM1 on the northeast side of the bridge was damaged during the pressure relief joint installation and removed on May 12, 2016. A new crackmeter was purchased and installed at the previous location of CM1 on May 25, 2016. Instrumentation layout is presented in Figure 119. The data obtained from these instruments are discussed in the following sections.

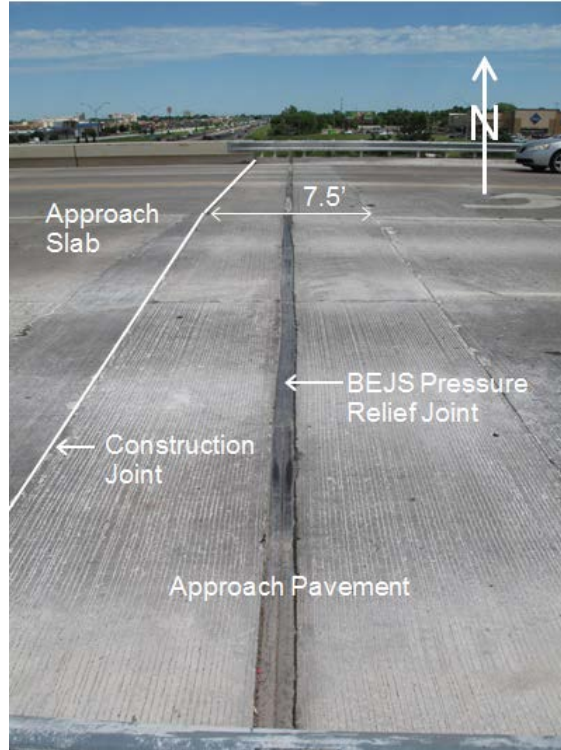


Figure 118. New approach pavement near the approach slab and completed BEJS pressure relief joint on the east side of the 19th Street Bridge

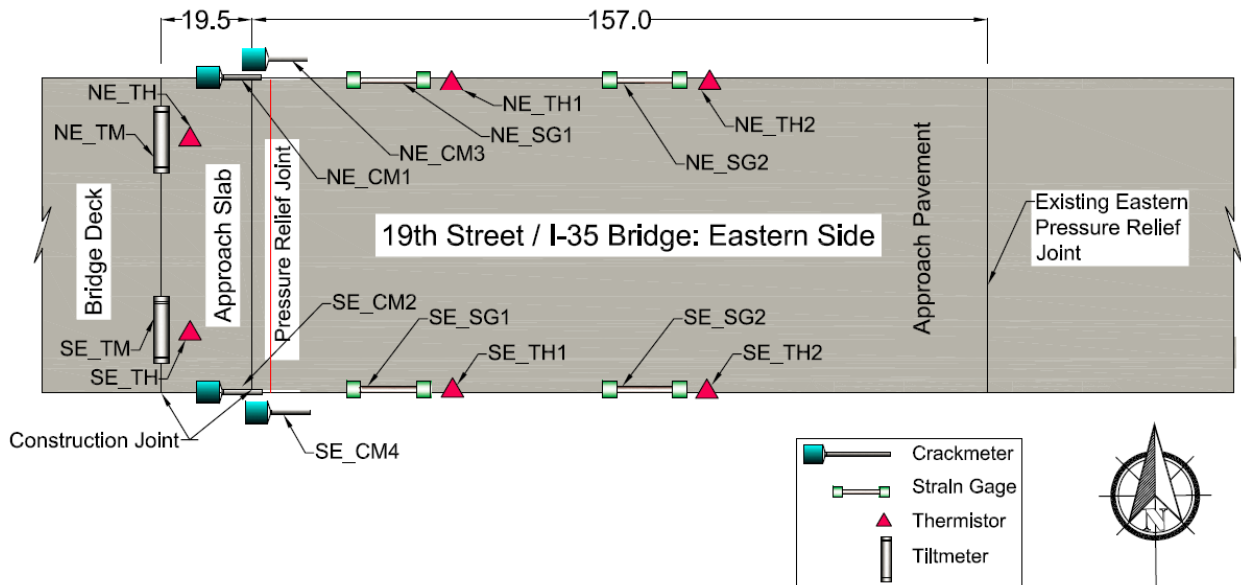


Figure 119. Instrumentation layout for the eastern side of the 19th Street/I-35 Bridge after repairs

2.2.6.1 Displacement of the Pressure Relief Joint after Repairs

Data from new crackmeters installed across the pressure relief joint (northeast crackmeter NE_CM3 and southeast crackmeter SE_CM4) are shown in Figure 120 and 121. It can be seen that the width of the pressure relief joint reduced since its installation in May 2016 until August 2016 as the temperatures increased and the stresses in the bridge were relieved. As the temperatures reduced, starting in Aug 2016, the pressure relief joint rebounded somewhat. It was noticed that the construction joint shown in Figure 118 also began to open as the temperatures reduced. This full-depth construction joint opened as much as 1 in. on Dec. 7, 2016. This explains why that the pressure relief joint only rebounded partially. As the temperatures increased again starting in Jan. 2017, the width of the pressure relief joint began to reduce again, but the construction joint remained opened. The rate of reduction of the width does, however, appear to be smaller than the initial rate of reduction in 2016. This may indicate that the width changes of the pressure relief joint is stabilizing. The construction of the new pressure relief joint provides room for the approach slab to move toward the approach roadway. Since there is additional room across the construction joint in the southeastern area, the displacement of the southeast area is larger than that of northeast area. .

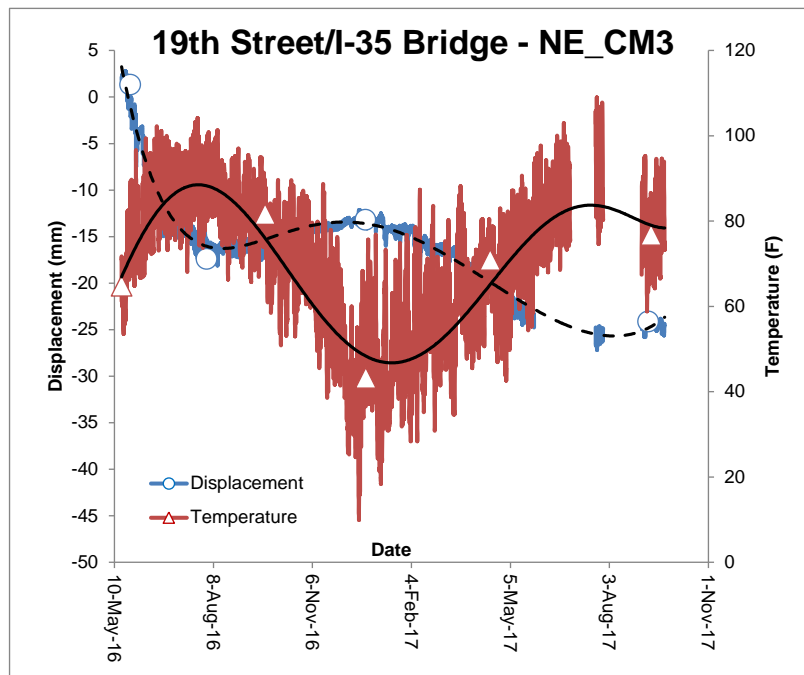


Figure 120. Eastern side of the 19th Street/I-35 Bridge – northeast crackmeter NE_CM3 data after repairs

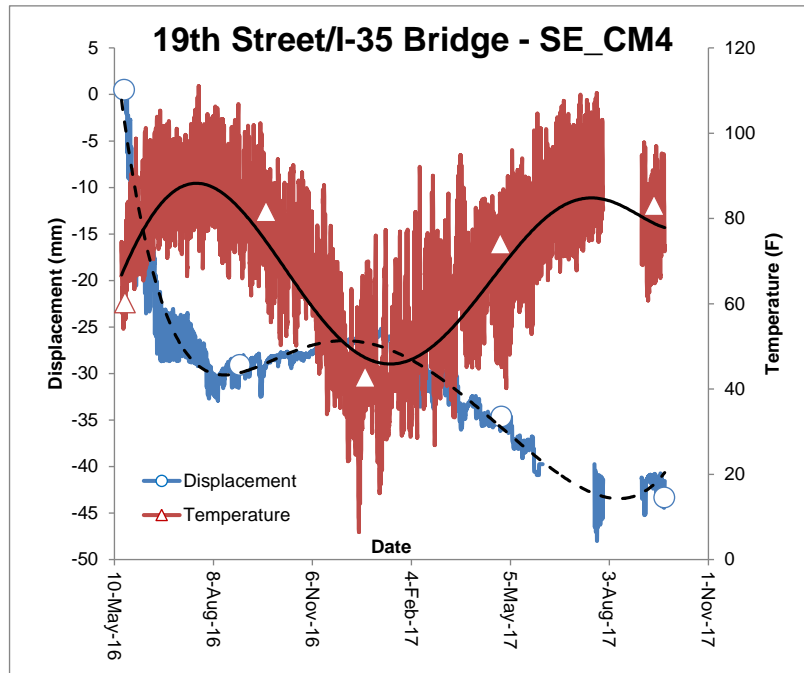


Figure 121. Eastern side of the 19th Street/I-35 Bridge – southeast crackmeter SE_CM4 data after repairs

2.2.6.2 Abutment Backwall Rotation after Repairs

Figures 122 and 123 show the data trends for tiltmeters located on each corner of the eastern abutment backwall before and after repairs. The same time period from 2014 and 2016 is used to compare data from before and after repairs. Same trend in tilt can be observed before and after repairs, i.e., as the temperature increases the tilt decreases and vice versa. Substantially more daily variations in tilt can, however, be seen after the repairs. This is likely because the deck/approach slab has now more space to expand/contract into the pressure relief joint.

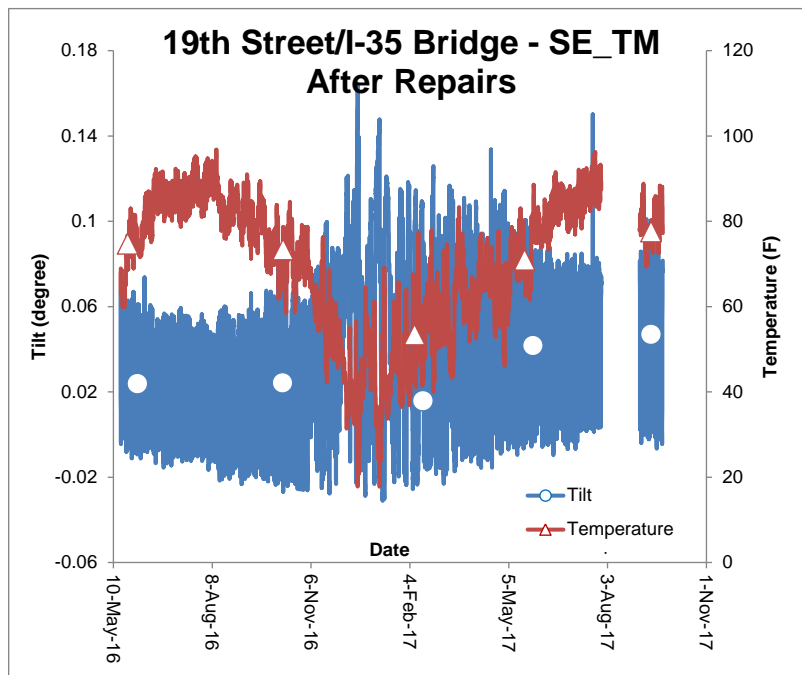
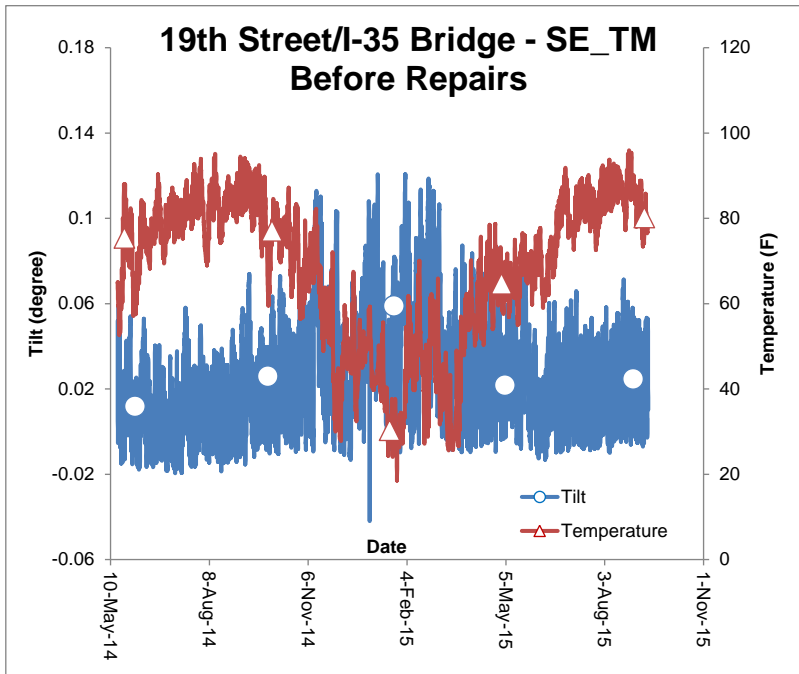


Figure 122. Eastern side of the 19th Street/I-35 Bridge – comparison of southeast tiltmeter SE_TM data before and after repairs

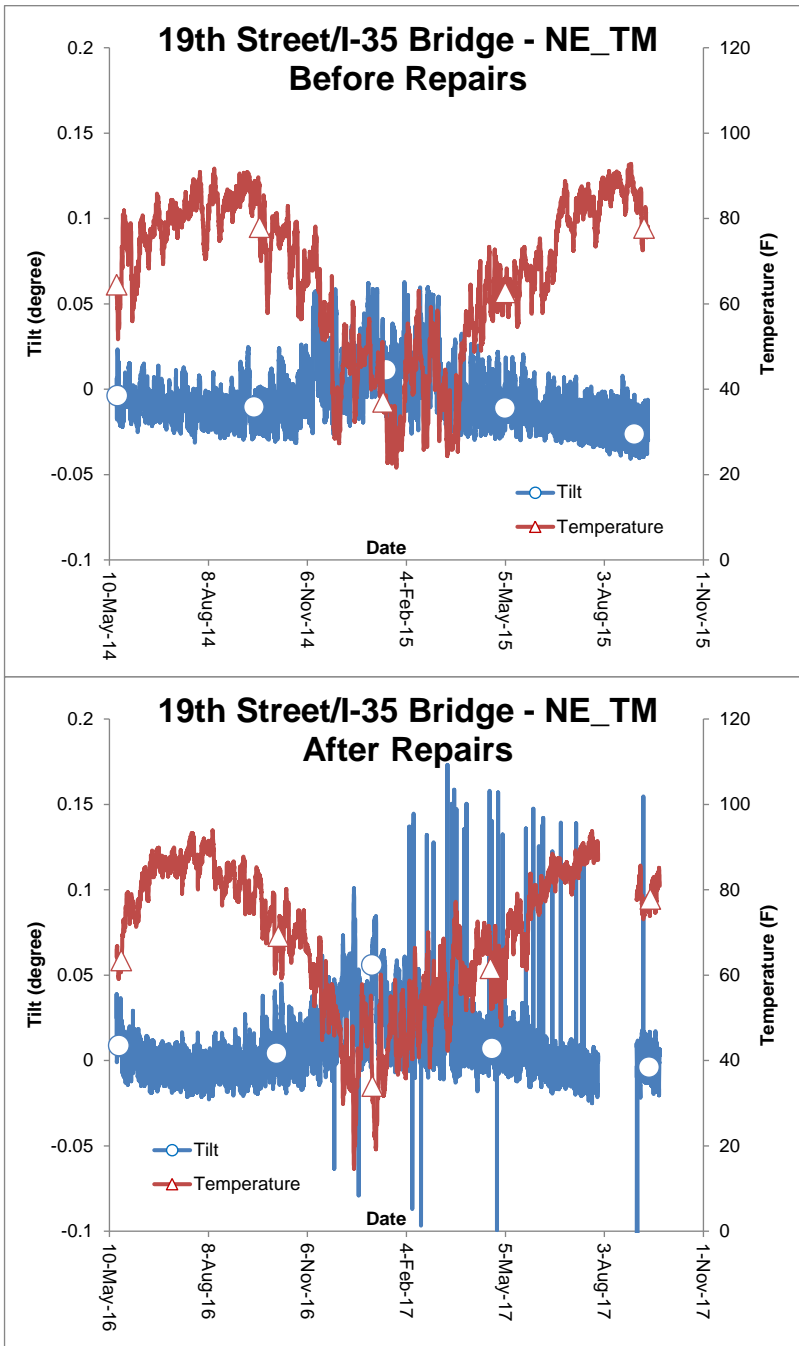


Figure 123. Eastern side of the 19th Street/I-35 Bridge – comparison of northeast tiltmeter NE_TM data before and after repairs

2.2.6.3 Relative Displacement between the Approach Pavement and the Abutment Wing Wall after Repairs

Figures 124 and 125 show the data collected by the northeast and southeast crackmeters before and after repairs. While the trends are similar, substantially more daily variations in displacements can be seen after the repairs. These results indicate that the new expansion joint is performing as intended.

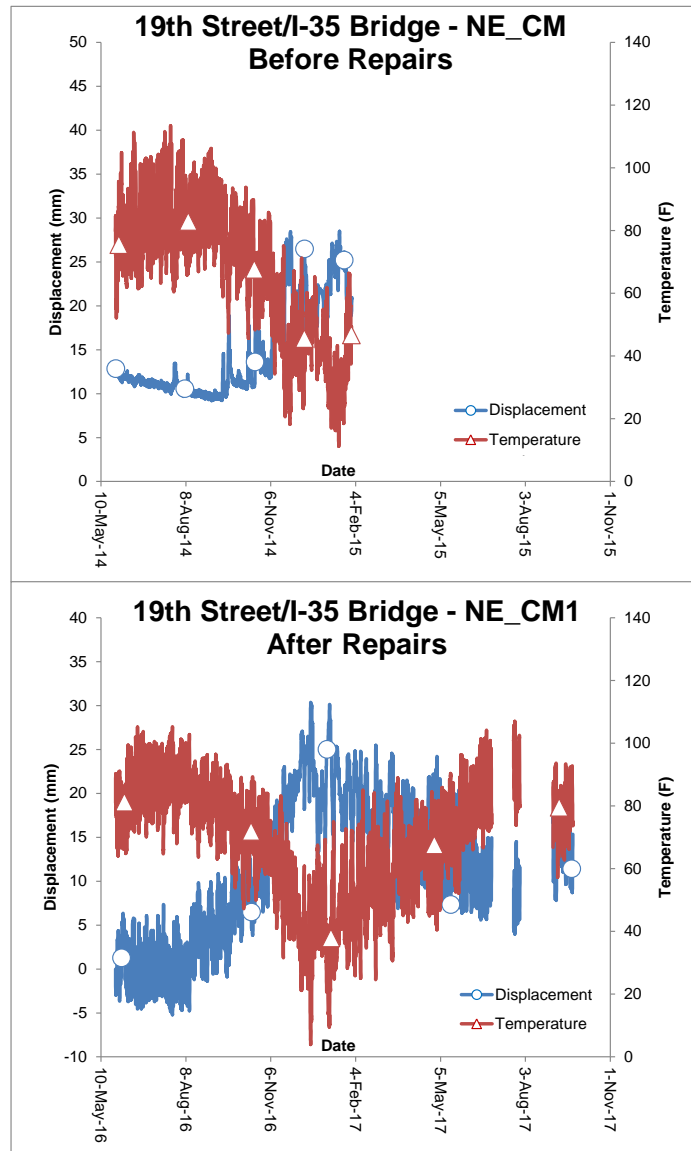


Figure 124. Eastern Side of the 19th Street/I-35 Bridge – comparison of northeast crackmeter data before and after repairs

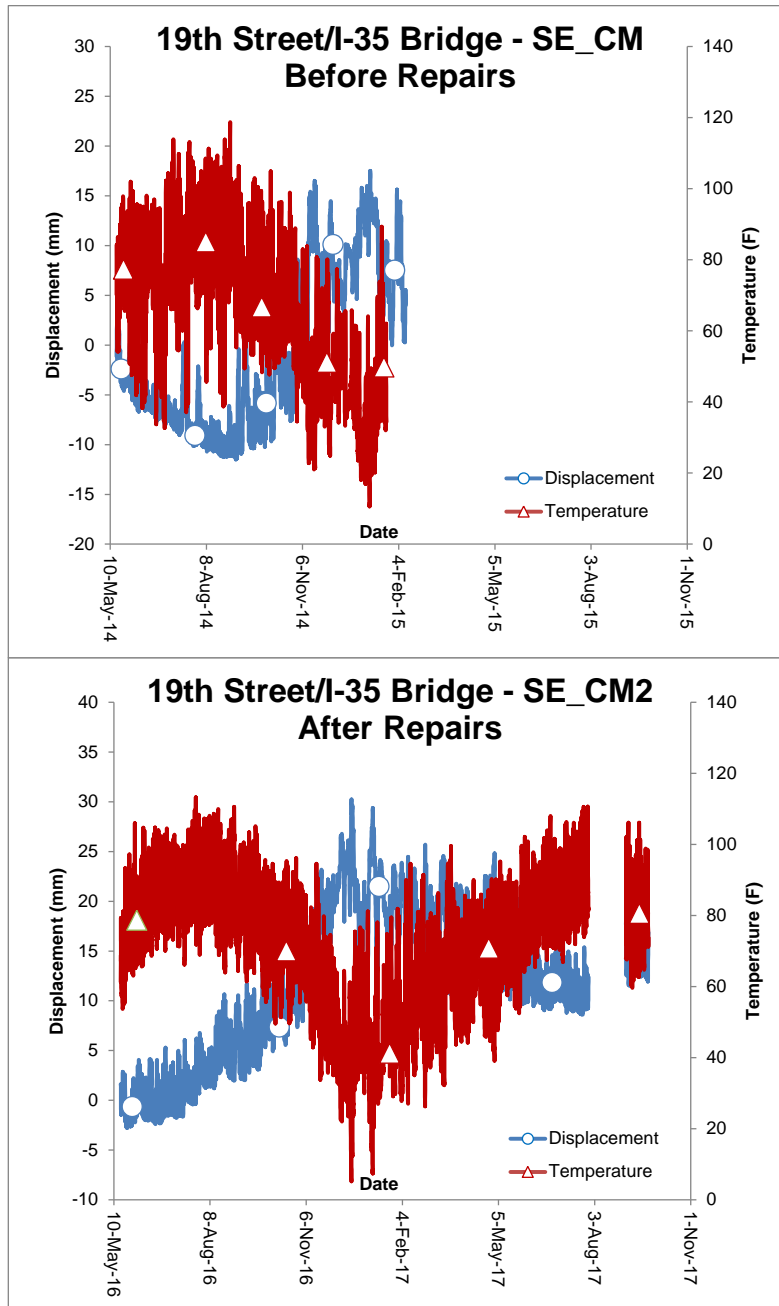


Figure 125. Eastern side of the 19th Street/I-35 Bridge – southeast crackmeter data before and after repairs

2.2.6.4 Axial Strains after Repairs

Figures 126 -129 show axial strain variations with temperature for selected strain gages before and after repairs. It can be seen that when the temperature increases there is an

increase in strain and vice versa for all the strain gages after repairs. This means that the approach pavement is expanding when the temperature increases and vice versa after repairs. The opposite trend was observed at NE_SG1 before the repairs. As described earlier, pavement pressure at the northeast corner was the reason for this opposite trend. This pressure is now seemed to have been relieved.

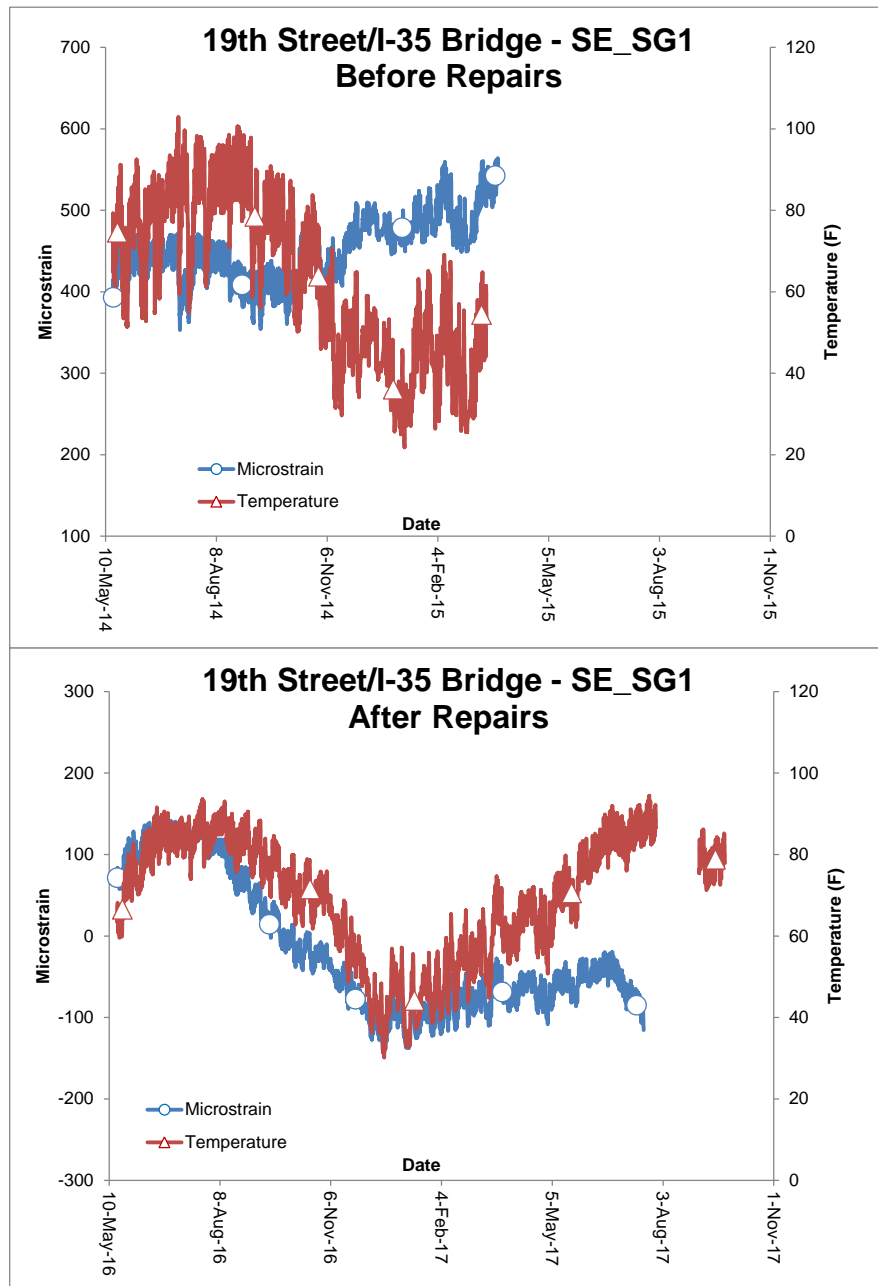


Figure 126. Eastern Side of the 19th Street/I-35 Bridge – Southeast Strain Gage 1 (SE_SG1) before and after Repairs

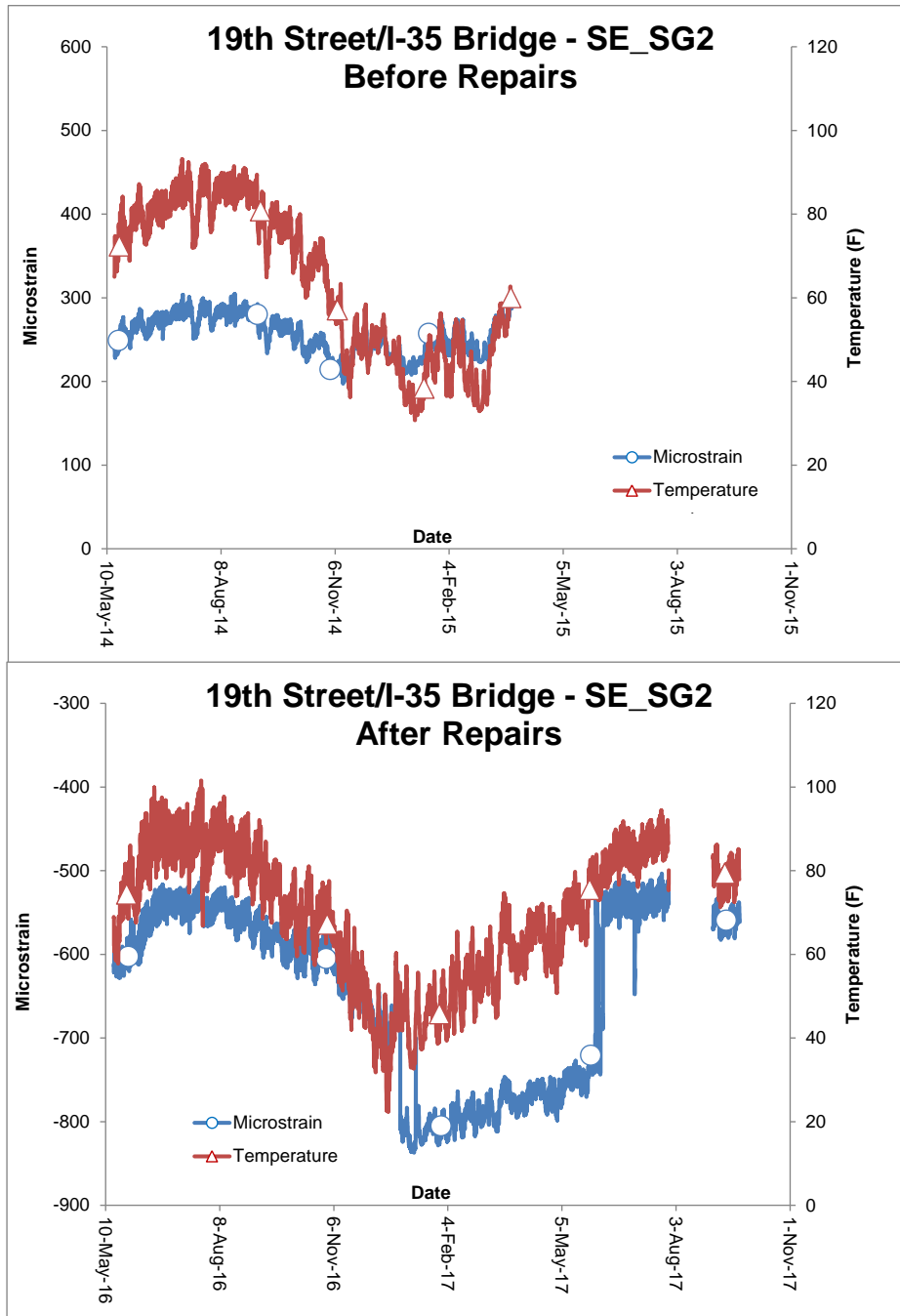


Figure 127. Eastern Side of the 19th Street/I-35 Bridge – Southeast Strain Gage 2 (SE_SG2) before and after Repairs

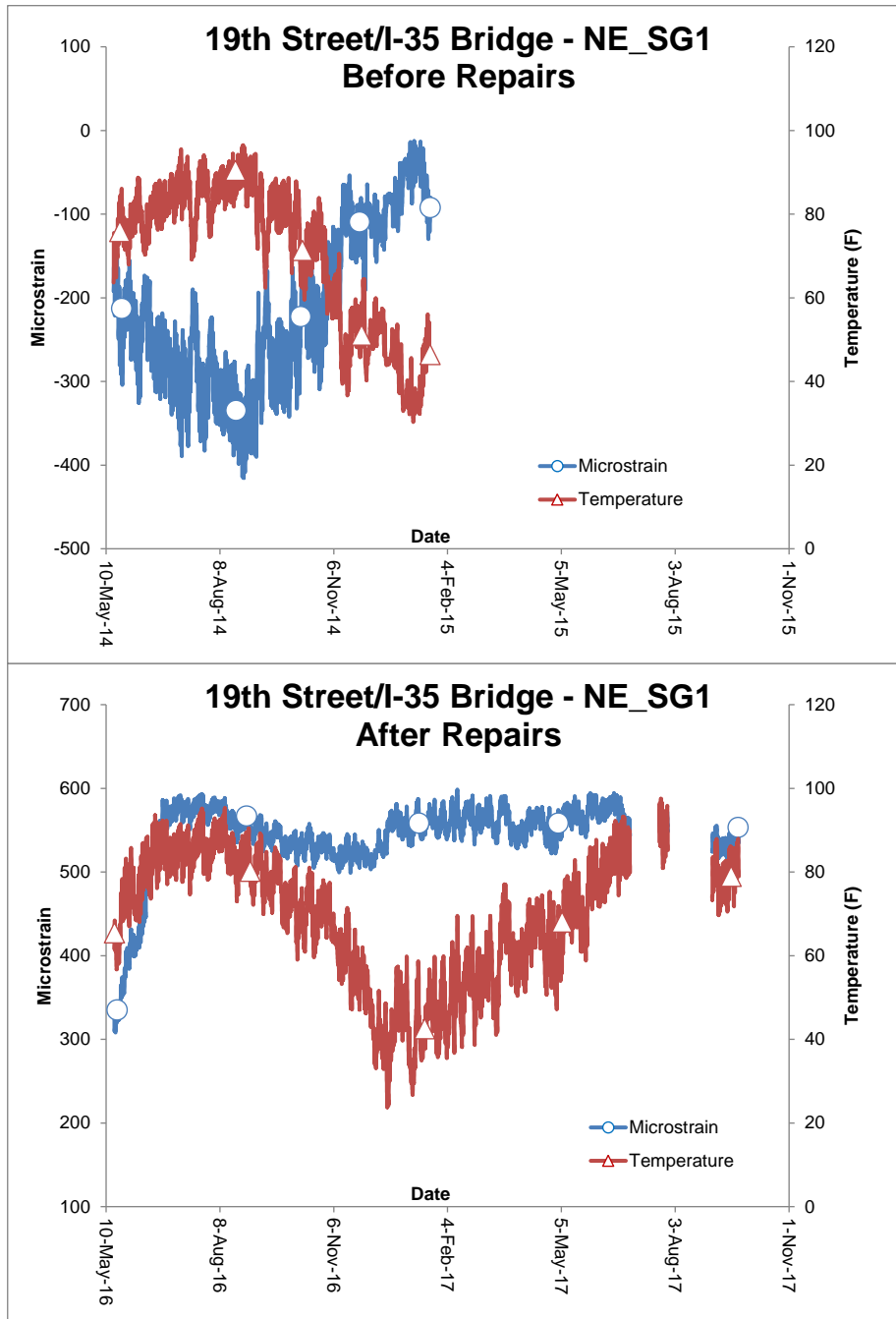


Figure 128. Eastern Side of the 19th Street/I-35 Bridge – Northeast Strain Gage 1 (NE_SG1) before and after Repairs

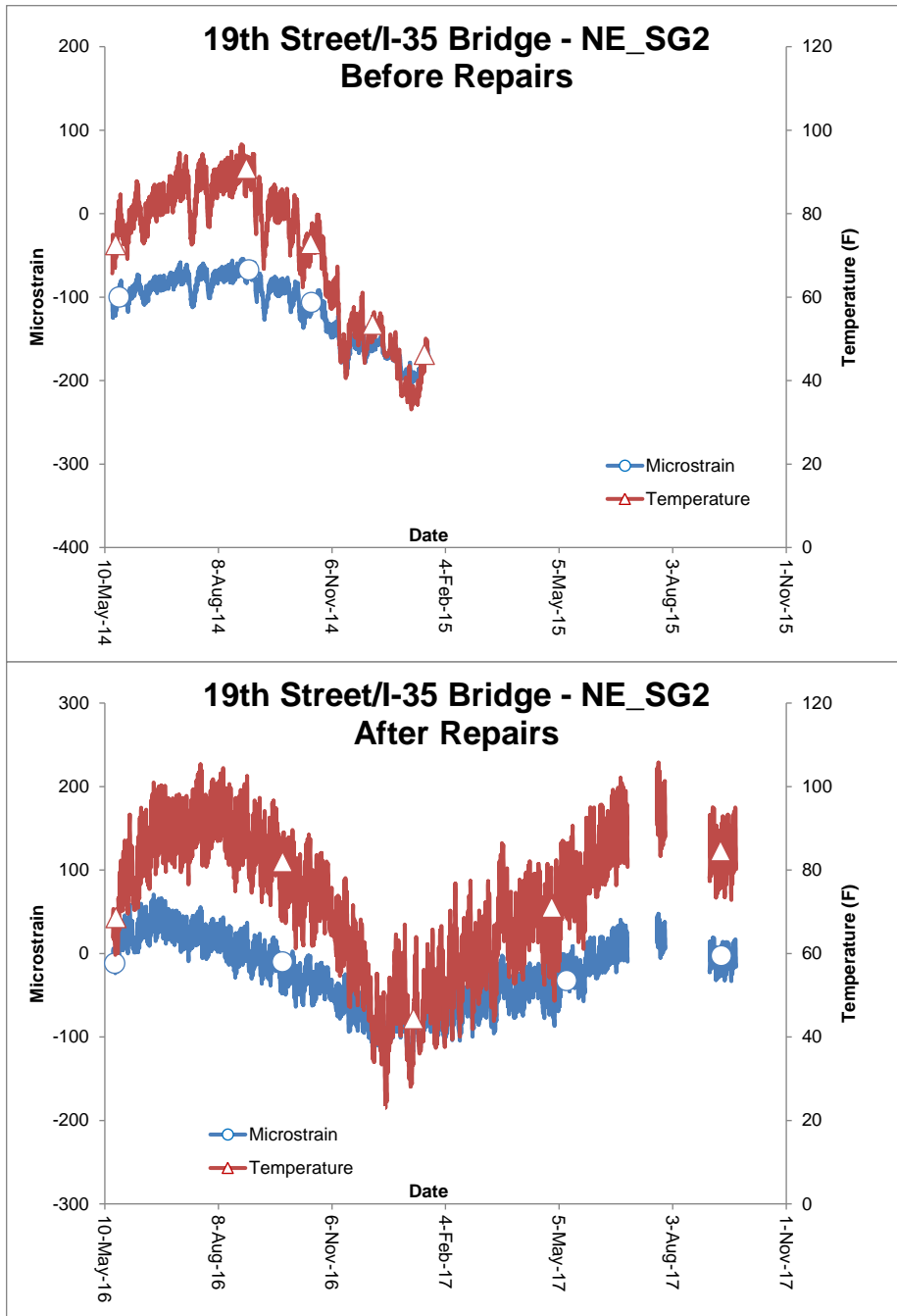


Figure 129. Eastern Side of the 19th Street/I-35 Bridge – Northeast Strain Gage 2 (NE_SG2) before and after Repairs

3.0 Analyses

A possible scenario for the distresses observed on the SH-3 Bridges is lateral deformation of the soft clay layer the embankments are founded on early in the life of the bridges. Below the existing embankment is a layer of soft clay, as denoted on the plans from ODOT (circa 1976), that extends to a depth of approximately 15 feet below the preconstruction grade. Stiff clay, denoted as shale on the plans, extends beyond the soft clay layer, see Figure 40 for a generalized soil profile. It is believed that once the embankment was constructed the soft clay layer began to deform vertically and horizontally resulting in the embankment moving or being dragged along with the soft clay layer.

One indicator for determining lateral movement of the embankment as the cause for distress can be found in the inspection reports for the bridge. According to the inspection reports, lateral movement of the embankments was noted within three years after construction and slowly progressed from there. The lateral movement is characterized by the cracking and then buckling of the slope walls and cracking of the abutment backwalls. Spalling was noted in the concrete surrounding the expansion joints in 1997 suggesting by this time the joints were no longer contracting enough to allow for the expansion caused by thermal movement. The thermal movement is further restrained by the joints on the end of the bridge being closed and covered with asphalt from repairs to deal with settlement of the approach slabs noted in the 1993 inspection report. If the movement at the bridge was only the result of pavement movement or pavement induced stress on the bridge it is believed that the result of the movement would not have been noticed so quickly following construction and that the expansion joints, as designed, would have provided enough room for anticipated thermal movement of the deck and approaches.

The bridge was originally designed with four – 2-inch (nominal) expansion joints that were intended to carry the thermal expansion and contraction of the bridge and approach pavement with changes in temperature. However, it is believed that the lateral deformation of the soft clay layer caused the expansion joints to close up soon after construction requiring the thermal movement of the bridge and pavement to buildup stress in the bridge. The buildup of stress in the bridge led to the distresses observed.

To test the hypothesis that the lateral deformation in the soft clay layer caused the movement of the bridge, the finite element computer program SAC-2 (Herrmann and Kaliakin 1987) was employed. SAC-2 is a two-dimensional, nonlinear, time dependent, finite element code that includes both linear elastic and bounding surface constitutive models for soil. The use

of SAC-2 allowed the horizontal displacement at the top of the embankment to be verified. The finite element model required an extensive list of input parameters to define the bounding surface for the soft clay layer. To assist in narrowing down the values of the parameters the slope stability software GStabl7© with STEDwin© (Gregory Geotechnical) was utilized. By entering the embankment and soil layers into GStabl7, the soil cohesion can be varied to narrow down the soil parameters. In the GStabl7 software the soil parameters were varied while the factor of safety was monitored. A factor of safety of 1.0 would mean failure in the traditional sense. However, since it is believed that the embankment already moved and slightly failed, a factor of safety of slightly less than 1 was sought in the GStabl7 software. The soil parameters used in SAC-2 was then calibrated using the expected cohesion found from the GStabl7 analysis.

Within SAC-2 the east embankment soil was modeled as linear elastic and the underlying soft clay was modeled with the bounding surface model for isotropic soils. The embankment was modeled as linear elastic since it is anticipated that minimal deformation will occur in a correctly built embankment. The bounding surface model was used for the soft clay because it is assumed that the increased loading from the embankment will increase the pressure in soft clay beyond the linear elastic zone and into a zone of plastic deformation. Boundary conditions were also specified within the program. The base of the model which corresponds to the interface of the soft clay and stiff clay/shale layer below was fixed, meaning no vertical or horizontal movement was allowed. Water flow was also restricted at this boundary. The vertical boundaries of the model were approximately 200 feet on either side of the abutment of the bridge. At the vertical boundaries horizontal deformation was restricted but vertical deformation along with water flow were permitted. See Figure 130 below for the finite element mesh with boundary conditions displayed.

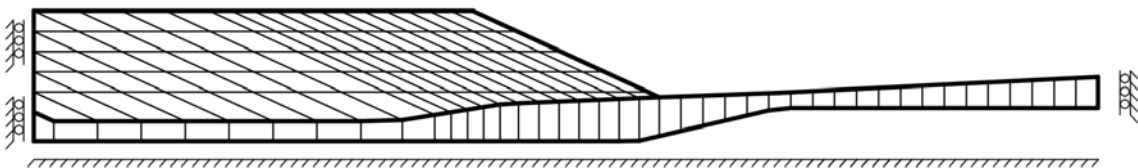


Figure 130. Finite element mesh with boundary conditions

During the analysis the embankment load was added over a period of 7 days. The model was then allowed to calculate deformations within the soil mesh until a steady state was

reached. The analysis was conducted for saturated and unsaturated conditions. The saturated condition took approximately 4 years to come to a steady state while the unsaturated condition took approximately 2 years to reach a steady state.

Since it is believed that the lateral deformation is the cause of the initial movement and the locking up of the expansion joints the lateral movement would need to be around 8 inches for all four expansion joints to close up. The soft clay present under the west embankment would have also provided some of the movement. The west embankment is not as tall as the east embankment and is not founded on as thick of a soft clay layer as the east embankment. Since the east embankment is more problematic based on site conditions it is assumed that most of the movement occurred on the east side.

The results for the unsaturated analysis showed a horizontal displacement at the crest of the embankment of 0.415 feet or 5 inches. The vertical displacement calculated was around 2.31 feet. This vertical and horizontal displacement of the embankment near the crest can be seen in Figure 131 below. In the figure the original mesh is shown by dash lines and is slightly taller than the deformed mesh which is shown by solid lines.

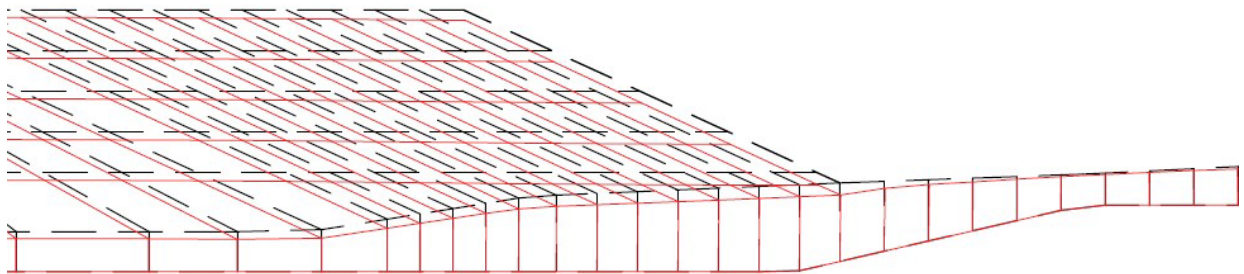


Figure 131. Unsaturated finite element analysis deformed mesh

While the bridge does have some asphalt patch and apparent filling at the east abutment, it is not believed that the embankment actually settled 2.31 feet. The horizontal movement of 5 inches at the crest of the embankment on the east side with about 3 inches coming from the west side would have completely closed all the expansion joints on the bridge.

The results of the saturated analysis showed a horizontal displacement at the crest of the embankment of 0.512 feet or 6 inches. The vertical displacement for the saturated analysis was calculated at 2.25 feet. As mentioned previously it is not believed the embankment settled this

entire amount. This vertical and horizontal displacement of the embankment near the crest can be seen in Figure 132 below. In the figure the original mesh is shown by dash lines and is slightly taller than the deformed mesh which is shown by solid lines.

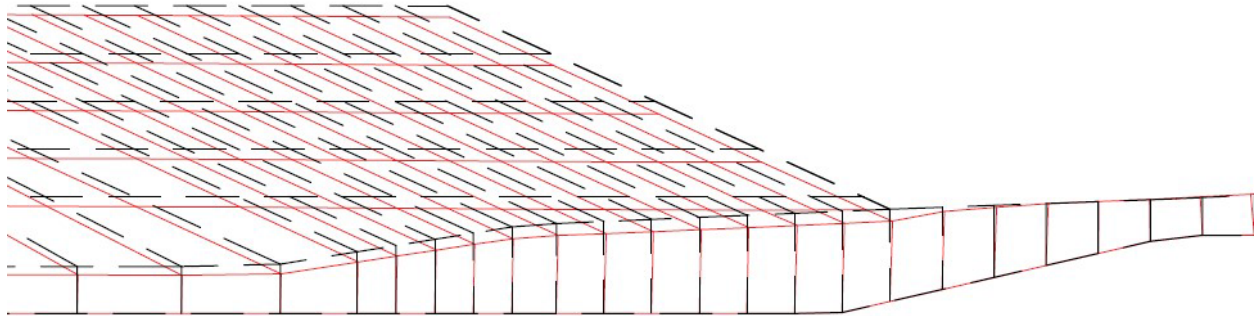


Figure 132. Saturated finite element analysis deformed mesh

In conclusion, saturated and unsaturated finite element analysis were completed for the east embankment of SH-3 North Bridge. The analyses were completed using the finite element model SAC-2. SAC-2 provided reasonable results for the horizontal deformation of the embankment to support the hypothesis that the lateral deformation of the embankments is the cause of the movement at the SH 3 Bridge. The analyses did, however, overestimate the vertical deformation in both the saturated and unsaturated analysis. At this time it is not fully known why the vertical deformation is overestimated. To perform the analysis at optimum accuracy extensive field testing would be needed to be carried out to properly characterize the soft clay layer under the embankment prior to embankment construction. This analysis was completed to present lateral deformation of the approach embankments as a mechanism of initiating stress buildup in bridges. It is believed that for the SH 3 Bridges, lateral deformation was responsible for closing the expansion joints. Once the expansion joints locked up, it is likely that thermal expansion of the pavement induced additional stress on the bridge causing the damage that was observed.

4.0 Summary

4.1 The Shell Creek Bridge

The Shell Creek Bridge is experiencing number of problems related to the interactions between bridge abutments and adjacent roadways, including expansion joints closing, roller support bearings tilting, and beams pushing against abutment backwalls. It is likely that these problems are related to both pavement pressure and lateral displacements of the approach embankments. The tilting of the bearings (Figure 14) indicate that the major contributing factor for the distresses observed is the pavement pressure.

4.2 I-244 Bridges and SH 76 Bridge over Rush Creek

The measurements across expansion joints at I-244 bridges and SH 76 Bridge over Rush Creek were obtained using demountable mechanical strain gage (DEMEC). These data are compared with the calculated joint widths obtained by starting from a width of 2 in. at 60° F and adjusting for temperature changes by Equation (1). Based on the observations, it appears that these expansion joints are performing as expected at this time.

4.3 The SH-3 Bridges over the BNSF Railway

It is believed that the distresses caused to these bridges are due to the lateral movement of the embankments, soon after construction, likely through the soft clay layer shown in Figures 35 and 40. The data from the instruments before the repairs indicated that all the expansion joints on top of the piers were essentially closed and as the bridge heated the deck was pushing against the approach slab which in turn was transmitting the forces into the abutment and the approach embankment. As the bridge cooled, the deck, abutment, and the embankment were all relaxing. The repairs carried out to the SH-3 north bridge between August 2015 and January 2016 involved installing two new sealed expansion joints at Pier Nos. 1 and 4, converting the expansion joints at Pier Nos. 2 and 3 to construction joints, and rehabilitating the construction joints at the abutments. The data from the instruments after the repairs reveal that the new expansion joints at Pier Nos. 1 and 4 are functioning as intended.

4.4 The 19th Street/I-35 Bridge

When the 19th Street Bridge was constructed in 2009 a single expansion joint was placed in the center of the bridge deck. As the bridge deck, approach slabs, and approach pavements expanded and contracted with daily and seasonal changes in temperature, expansion occurred in the direction of least resistance towards the expansion joint in the middle of the deck. Some of these movements toward the middle of the deck were not recovered and eventually the expansion joint at the middle of the bridge deck closed. Following the closure of this expansion joint, further temperature increases and expansion of the deck, approach slabs and approach pavements resulted in compressive forces being transmitted to the bridge distorting the bearing pads, shearing the anchor bolts, and causing damage to the abutment back wall. Sometime between 2005 and 2009, simple pressure relief joints were placed 157 feet and 164 feet from the eastern and western approach slabs, respectively. These joints are approximately 4 inch-wide sections cut in the pavement and filled with asphalt. These joints were likely not effective in preventing compressive stresses being transmitted to the bridge deck because of their distances from the bridge deck. New pressure relief joints near the bridge were recommended. ODOT installed a pressure relief joint on the eastern side of the bridge in April/May 2016. The data from the instruments after the installation of this pressure relief joint reveal that this pressure relief joint is functioning as intended and has substantially reduced the pavement pressure on the eastern side of the bridge. It is highly recommended that a similar pressure relief joint be installed on the western side of the bridge as well.

5.0 Recommendations

Based on this research project, some recommendations for design, construction, repair, and maintenance to alleviate adverse effects of interactions between bridge abutments (non-integral), bridge decks, and adjacent roadways are given below.

(1) Recommendations for design and construction of new bridges:

- (i) Long rigid approach pavements for bridges should be avoided since these pavements can exert significant pressures on the bridges. Expansion joints should be provided on rigid approach pavements at regular intervals.
- (ii) Superior methods for reducing friction between approach slabs and abutments are needed to minimize the effects of pavement pressures on the abutment backwalls.
- (iii) For tall bridge approach embankments on soft clayey soils, proper geotechnical analyses should be carried out to investigate the possibility of large lateral deformations.
- (iv) If calculated lateral deformations are large and expected to close the expansion joints on the bridge, ground improvement techniques such as surcharge loading should be considered to strengthen the soft clayey soils.
- (v) For skewed bridges, such as the SH-3 bridges, analyses of the bridge and adjacent roadways, including approach embankments, as a system may be required to fully understand the forces transmitted to the bridge.

(2) Recommendations for repair and maintenance:

- (i) It is critical that all expansion joints on bridges and rigid approach pavements should be properly maintained and kept free of debris. Debris in expansion joints will eventually result in pavement pressures on the bridges. Since debris in sealed expansion joints results from worn out seals, all worn out seals should be replaced as soon as possible.
- (ii) Pressure relief joints should be installed and maintained on approach pavements closer to the bridges where distress due to pavement pressure is observed. These joints should be at least 4" in. width to accommodate expected bridge movements into the joint during pressure relief.
- (iii) For bridges where expansion joints have closed due to lateral movement of approach embankments, new expansion joints can be installed on the bridge. Since the lateral movement of the embankments are expected to occur early in the life of a

bridge, new expansion joints are expected to last longer, provided they are properly maintained.

6.0 Acknowledgements

ODOT's Assistant Bridge Engineer for Maintenance, Mr. Walt Peters, provided valuable input during all the phases of this project and was highly instrumental in the project's success. His support is gratefully acknowledged.

7.0 References

- Bright, Z.P. (2012), "Bridge Instrumentation to Study Horizontal Forces from Adjacent Roadways," M.S. Thesis, University of Oklahoma, Norman, Oklahoma.
- Burgueno, R., and Li, Z., (2008), "Identification of the Causes and Development of Strategies for Reliving Structural Distress in Bridge Abutments," RC-1508, Michigan Department of Transportation.
- EST, Inc., (2008), "Plan of Proposed City Bridge," State Job Piece No. 15392(07), Cleveland County, OK.
- EMSEAL Joint Systems Ltd., (2016), "BEJS SYSTEM -- Bridge Expansion Joint System", Westborough, MA.
- Geokon, Inc., (2013a), "Instruction Manual for Model 4000 Vibrating Wire Strain Gage," Lebanon, New Hampshire.
- Geokon, Inc., (2013b), "Instruction Manual for Model 3800 Thermistors & Thermistor Strings," Lebanon New Hampshire.
- Geokon, Inc., (2013c), "Instruction Manual for Model 6350 Vibrating Wire Tiltmeter," Lebanon, New Hampshire.
- Geokon, Inc., (2013d), "Instruction Manual for Model 4420 VW Crackmeter," Lebanon, New Hampshire.
- Geokon, Inc. (2013e), "Instruction Manual for Model 8021-1 Micro-1000 Data logger," Lebanon, New Hampshire.
- Geokon, Inc. (2013f), "Instruction Manual for Model 8032 Terminal Board and 16/32 Channel Multiplexer," Lebanon, New Hampshire.
- Gregory Geotechnical, "GSTABL7 with STEDwin Slope Stability Analysis System Version 2.005.2," GREGORY GEOTECHNICAL SOFTWARE (A Division of Gregory Geotechnical), Stillwater, Oklahoma offices.
- Herrmann, L.R. and Kaliakin, V.N. (1987). "User's Manual for SAC-2, a Two Dimensional Nonlinear, Time Dependent, Soil Analysis Code using the Bounding Surface Elastoplasticity-viscoplasticity Model." *Dept. of Civ. Engrg. Report, I-II*, Univ. of California, Davis, Calif.
- Smith, K.D., Snyder, M.B., Darter, M.I., Reiter, M.J., and Hall, K.T. (1987), "Pressure Relief and Other Joint Rehabilitation Techniques," Federal Highway Administration. Washington D.C.